LPS-induced modifications in spontaneous network activity causes neuronal apoptosis in neonatal cerebral cortex

Dissertation

Zur Erlangung des Grades
Doktor der Naturwissenschaften

am Fachbereich Biologie
der Johannes Gutenberg-Universität Mainz

vorgelegt von

Birgit Nimmervoll

geb. am 12.04.1984 in Linz

Mainz 2011

Dekan:

    1. Berichterstatter:

    2. Berichterstatter:

Tag der mündlichen Prüfung: 10.Juni 2011

"If the human brain were so simple that we could understand it, we
would be so simple that we could not"

Emerson M.

Table of contents

Abbreviations

%	percentage
°C	grad celsius
µ	micro

A

a-caspase-3	cleaved caspase-3 (activated)
ACSF	artificial cerebrospinal fluid
AMPA	α-amino-3-hydroxy-5-methyl-4-isoxazolepropionic acid
AMPA-R	AMPA-receptor
ANOVA	analysis of variance
AraC	Arabinofuranoside Cytidine
Asp175	antibody against a-caspase-3

B

BDNF	brain derived neurotrophic factor
BI	burst index
BME	basal medium eagle
BSA	bovine serum albumin

C

Casp-3	caspase-3
CCD-camera	charge coupled device camera
CCL5 (RANTES)	chemokine (C-C motif) ligand 5
CD-14	cluster of differentiation 14
cDNA	complementary DNA
CNS	central nervous system
CO_2	carbon dioxide
CP	cerebral palsy

D

Da	Dalton
DCFH	3´7 dichlorodihydrofluorescein
DEPC-water	diethylpyrocarbonate treated water
DIV	days *in vitro*
DMSO	dimethylsulfoxide

DNA	desoxyribonucleic acid
E	
E	embryonic age
E. coli	escherichia coli
Et al.	et alii
F	
FCS	fetal calf serum
G	
g	gram
GABA	γ-aminobutyric acid
$GABA_A$-R	$GABA_A$-Rezeptor
G-CSF	granulocyte-colony stimulating factor
GFAP	glial fibrillary acidic protein
GM-CSF	granulocyte macrophage colony stimulating factor
H	
h	hour
HBSS	hanks buffered salt solution
HEPES	N-(2-hydroxyethyl)-1-piperazin-N´-2-ethansulfonacid
HS	horse serum
Hz	hertz
I	
IFNγ	interferonγ
IL	interleukin
IL-ra	IL-receptor antagonist
J	
JE/MCP1	monocyte chemoattractant protein-1
K	
KC/CXCL1/3	chemokine interleukin1/3
L	
LPS	lipopolysaccharide
M	
M	Molar
MEA	multi electrode array
MEM	minimal essential medium
mg	milligram

min	minute
MIP2	macrophage-inflammatory protein-2
ml	milliliter
mM	milliMolar
MPBS (-/-)	modified phosphate buffered saline (without Mg^{2+}, Ca^{2+})
mRNA	messenger ribonucleidacid

N

NB	neurobasal medium
NeuN	neuronal-nuclei
NFκB	nuclear factor κB
NO	nitric oxide
NS	nervous system

P

P	postnatal day
[P]	passage
PBS	phosphate buffered saline
PCR	polymerase chain reaction
PEST	Penicillin-Streptomycin
PFA	paraformaldehyde
pH	power of hydrogen
PI3K	phosphatidylinositol-3-kinase
PVLM	periventricular leucomalacia

R

rpm	rounds per minute
RPMI-medium	roswell park memorial institute-medium
ROS	reactive oxygen species

S

s	seconds
SEM	standard error of mean

T

TNFα	tumor necrosis factorα

V

V	volt

W

WM	white matter

<u>List of figures</u>

1. Introduction

1.1. The central nervous system

1.1.1. Anatomical remarks

Anatomically the mouse brain can be separated into forebrain (prosencephalon), midbrain (mesencephalon) and hindbrain (rhombencephalon). Collectively, the forebrain functions to control cognitive, sensory and motor function, and regulate temperature, reproductive functions, eating, sleeping and the display of emotions. The midbrain is responsible for controlling the visual and auditory systems as well as eye movement and control of body movement and the hindbrain functions collectively to support vital body processes (Def. from www.brainexplorer.org).

The forebrain is further subdivided into telencephalon and diencephalon while the midbrain divides into the metencepahlon and myelencephalon. These subregions give rise to the rudiments of the major functional subdivisions of the brain, while the spaces they enclose eventually form the ventricles of the mature brain (Purves et al., 1997). The telencephalon divides into right and left vesicle and the dorsal part of this vesicle generates the cerebral cortex (Gotz and Sommer, 2005).

1.1.2. Formation of the cerebral neocortex

The cerebral neocortex is characterized by six major, radially organized layers. Each of them contains a heterogeneous population of neurons that are morphologically, connectionally, genetically and functionally distinct from those of other layers (O'Leary et al., 2007). In mouse brains neurons proliferate in the ventricular zone (VZ). The first postmitotic neurons built the preplate (PP). Subsequently-born neurons migrate into the preplate to form a new series of layers, known as the cortical plate, which will split the preplate into marginal zone (MZ) and subplate (SP). Additional arriving migrating neurons bypass earlier-generated neurons and form six horizontal cellular layers in an inside-out pattern (Angevine and Sidman, 1961) (**Figure 1**).
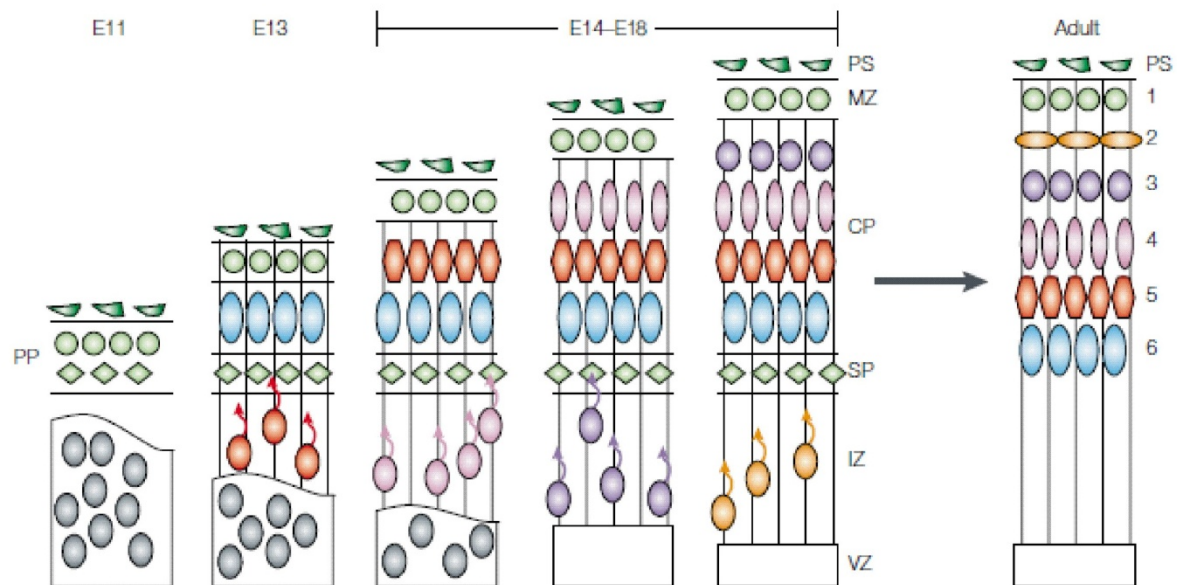
Figure 1. Developmental stages of neocortical-layer formation of the mouse are shown, which occurs mainly by migration along the radial glia. At embryonic stage (E)11 some early born neurons, which have migrated from the ventricular zone to the pial surface build the preplate (PP). By E13 the cortical plate is created through splitting of the PP into the marginal zone and subplate. That occurs through a second postmitotic neuronal wave that migrates through the intermediate zone. During E14-18 subsequent arriving migrating neurons expand the CP in an inside-out fashion, as neurons bypass earlier-generated neurons and settle underneath the MZ. In adulthood, the SP degenerates leaving behind six horizontal cellular layers in the neocortex. Picture adapted from Gupta et al., (Gupta et al., 2002)

1.2. Cell types of the central nervous system

The main cell types of the central nervous system are neurons and glial cells. The characteristic of a neuron is thereby its ability to transmit rapid electrical signals in the form of action potentials. All other cells are called glial cells and can be distinguished into macroglia (astrocytes and oligodendrocytes) and microglia. Glia make up most of the cells in the human brain (90%) while neurons make up only 10%. The proportion of the glia seems to correlate with the size of animals. While nematode worms have only a few glia, the mouse brain already has 65% of these cells (Allen and Barres, 2009). All cells of the central nervous system form a complex system to fulfill its duties (**Figure 2**).
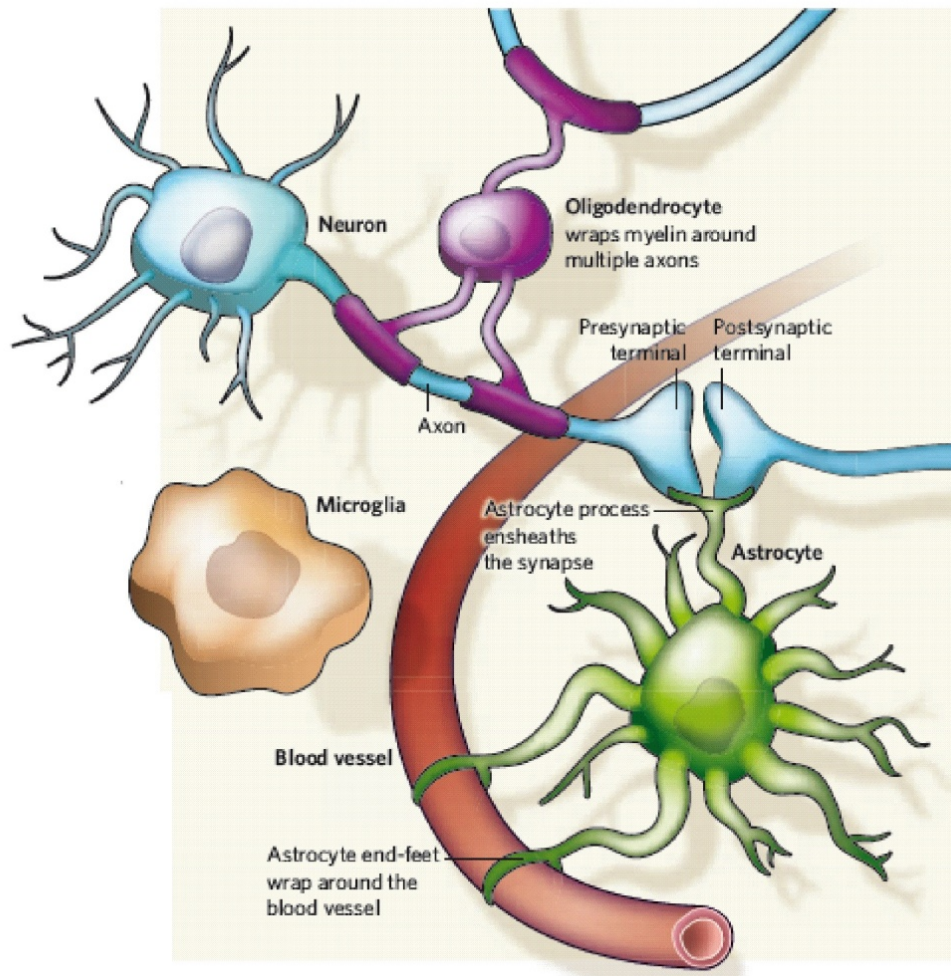
Figure 2. Neurons, astrocytes, microglia and oligodendrocytes are the main cells of the central nervous system and stay in close contact with each other. Microglial cells scan their surrounding and get activated through infection or brain damage. Astrocytes extend their processes and keep in close contact to blood vessels and neurons. Oligodendrocytes wrap myelin sheets around axons and therefore accelerate neuronal transmission. Picture adapted from Allen N.J. & B.A. Barres (Allen and Barres, 2009).

1.2.1. Neurons

The human brain contains about 10^{11} neurons while mouse brains consist of about 5.5 million neurons (Johnson and Erner, 1972). Neuronal precursor cells derive from embryonic germ layer, known as ectoderm (Allen and Barres, 2009). Neurons are highly specialized for intercellular communication and are arranged in networks. This fact is reflected in their morphology, in the molecular specialization of their membranes and in the functional intricacies of the synaptic contacts in between. Signaling of neurons involves the propagation of an action potential down a neuronal axon to a presynaptic terminal. Axons are specialized for signaling conduction and

can be a few hundred micrometers long or much further. At the presynaptic terminal the signal leads to depolarization of membrane and release of neurotransmitters to receptors on the postsynaptic membrane of another neuron. This step is followed by a depolarization of this second neurons, and further propagation of the signal (Allen and Barres, 2009). Also important are the neuronal dendrites that arise from the neuronal cell body. They provide sites for the synaptic contacts made by the terminals of other neurons and can thus be regarded as specialized for receiving information. In the cortex one can find two principal types of neurons: interneurons and pyramidal neurons.The pyramidal neurons which are glutamatergic projection neurons are excitatory and are produced locally by cortical progenitors in the VZ and migrate vertically to invade the cortical plate (CP) along radial glia (Kriegstein and Noctor, 2004;Nguyen et al., 2006). They represent about 75% of cortical neurons, and typically have triangularly-shaped cell bodies (Lewis, 2004). A basal dendritic tree branches out from the base of the soma, while a single apical dendrite can extend upwards from the cell body for hundreds of micrometers (Berens et al., 2008). The GABAergic interneurons are inhibitory and born outside the cortex in the ganglionic eminences and migrate from the ventral telencephalon to the cortex [(Nguyen et al., 2006) for review see (Kriegstein and Noctor, 2004;Wonders and Anderson, 2006)]. Interneurons have dendrites without spines and their axons arborize locally and innervate other neurons in the same area of the prefrontal cortex (Berens et al., 2008;Lewis, 2004;Lewis, 2004).

1.2.2. Microglia

Microglia are the resident immune cells of the central nervous system and enter the brain from the blood circulation early in an organism´s development (Allen and Barres, 2009). Some brain areas consist of up to 15% of microglial cells which are a stabile cell population that is only little replaced by bone marrow precursors (Hauwel et al., 2005). Microglial cells monitor the brain for damage and infection and respond to every pathological event in the CNS, with a program of supportive and protective activities. Activated microglia have the ability to destroy invading microorganisms, as well as to engulf dead cells and debris (Kreutzberg, 1996). They have also been implicated in synaptic remodeling during the development of the nervous system, when they are proposed to remove inappropriate synaptic connections through the process of phagocytosis (Allen and Barres, 2009). Moreover they are activated in

many neurodegenerative diseases, but whether they are helpful or harmful in these disease conditions is a matter of debate. Microglia cells present a compromise between harmful energy of the immune system and the vulnerability of the central nervous system after injury and disease (Streit, 2002).

<u>Description of microglia</u>

Ramified phase

Microglia of healthy adult brain tissue reveal a unique ramified morphology (Hanisch, 2002). Ramified morphology is associated with a low expression of surface antigens, which are normally associated with activated function in microglia (Garden and Moller, 2006;Hanisch and Kettenmann, 2007). However it was found that ramified microglia are not dormant, their processes are highly mobile (Nimmerjahn et al., 2005). So it is suggested that ramified microglia scan their environment without disturbing the fine-wired neuronal structure. As soon as an injury or an infection occurs the random scanning changes to targeted movement towards the injury or infection. Depending on the severity of the damage microglia cells become activated or stay in an alerted stage (Hanisch and Kettenmann, 2007) (**Figure 3**).

Amoeboid phase

Microglia can be activated by various molecules and conditions and transform into an amoeboid or activated phase (**Figure 3**). These two conditions have one thing in common: a threat to the structural and functional integrity of the CNS. This could be a factor, usually not seen in the brain environment, like microbial structures or factors that rise over a critical concentration (Hanisch and Kettenmann, 2007). These differences are detected by an array of cell surface and nuclear receptors that play a critical role in initiating and/or modulating microglial immune response (van Rossum and Hanisch, 2004). Like for example the Toll-like receptors (TLRs), which are able to detect viral and bacterial structures (Olson and Miller, 2004). After bacterial activation of microglia, they start to release inflammatory mediators, like ROS, NO or proinflammatory cytokines like $TNF\alpha$ which can lead to neuronal or oligodendroglial damage (Hanisch and Kettenmann, 2007), additional phagocytosis occurs (Hausler et al., 2002).
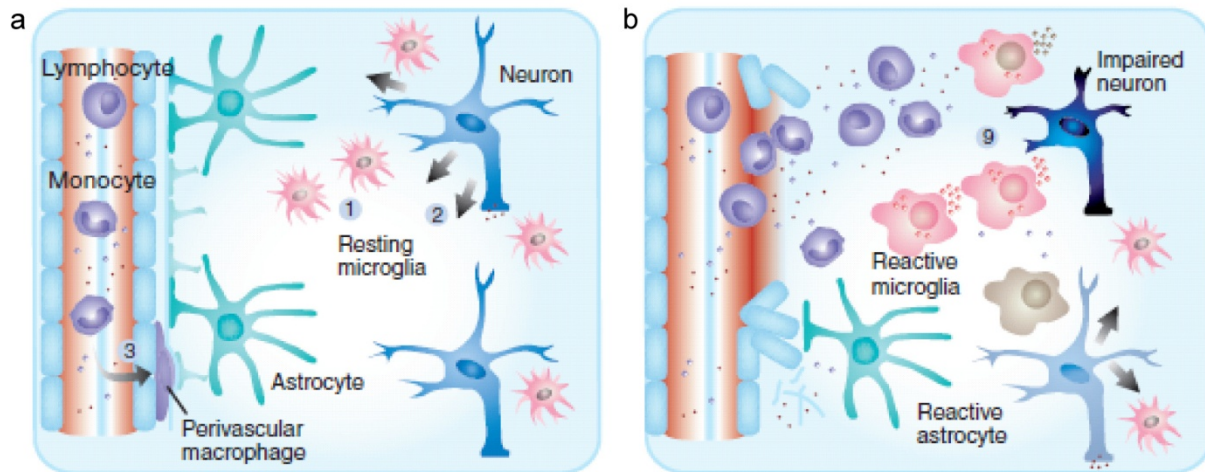
Figure 3. From ramified to amoeboid – activity states of microglia. (**a**) (1) resting microglia in a normal tissue. They screen their environment constantly for intruders or damage, which they can sense with different receptors on their membrane. Therefore the name resting is not fitting perfect, better would be the term "surveying" microglia. They constitutively rearrange their processes to scan the environment properly. 2) Neurons can emit signals indicating a healthy state, keeping microglial cells inactivated. In addition to parenchymal microglia, there are also perivascular macrophages which are traveling through the blood vessels and can enter the brain (3). (**b**) Stronger insult to the CNS, like infection or tissue damage triggers changes in the functional phenotype of microglia. They become activated and therefore amoeboid. In this amoeboid stage they can become over reactive and contribute to pathological scenarios, by impairing neurons and other glia (9).
Picture adapted from Hanisch & Kettenmann (Hanisch and Kettenmann, 2007).

Microglia activation upon lipopolysaccharide

The activation of microglia cells by lipopolysaccharide (LPS), a cell wall component of gram-negative bacteria which induces a massive immune response, was one of the first to be described in the literature (Hetier et al., 1988). It´s effects are mediated through the TLR-4/CD14 complex (Lehnardt et al., 2002;Lehnardt et al., 2003), which is by far the best described activation pathway in microglia (Rivest, 2003), and can be only found on microglia. Therefore microglial cells are the only cells which can bind LPS directly and are activated upon treatment. Astrocytes and oligodendrocytes are only activated and also damaged secondarily (Lehnardt et al., 2002;Lehnardt et al., 2003). Furhter neurons are able to inform microglia about their state of health by a chemokine called fractaline (Zujovic et al., 2000) (**Figure 4**). One of the earliest responses of microglia upon LPS activation is migration to the site of injury or inflammation and production of nitrite oxide, ROS and phagocytosis. To generate an adaptive immune response, microglia present antigens (MHCII) to invading T-cells,

even though they might need some additional signals from circulating dendritic cells to generate a complete response. In addition one of the major functions is to send signals to other cells of the immune system. They communicate over cytokines, chemokines, trophic factors, ATP and small molecule mediators of inflammation such as prostaglandins. LPS-induced inflammatory mechansims lead to release of chemokines and proinflammatory cytokines from microglia, which tend to have toxic effects on surrounding cells (Garden and Moller, 2006), especially neurons (Hanisch, 2002) (see **Table 1**).

Table 1

Abbreviation	Full name
IL-1-α /IL-1-β	Interleukin-1α/1-β
IL-1ra	Interleukin-1 receptor antagonist
IL-6	Interleukin-6
IL-8	Interleukin-8
IL-10	Interleukin-10
IP-10	Gamma interferon inducible protein-10
MCP-1	Monocyte chemoattractant protein-1
M-CSF	Macrophage colony stimulating factor
MIP-1α/1β	Macrophage inflammatory protein-1α/1β
MIP-2	Macrophage inflammatory protein 2
MIP-3 β	Macrophage inflammatory protein 3 β
TGFβ	Transforming growth factor β
TNFα	Tumor necrosis factor α
RANTES	Regulated on activation, normal T cell expressed and secreted

Table 1. Cytokines and chemokines released from microglia. Table adapted from (Hanisch, 2002;Rock et al., 2004).

LPS activated microglia further recruit astrocytes and neighboring immune cells leading to an amplification of the inflammatory response, like increased glutamate release which can further damage neuronal cells (Hanisch, 2002).

Microglial cell line, BV-2

For all experiments with microglia, the immortalized murine microglia cell line BV-2 was used, which was created by V. Bocchini (Universtiy of Perguia, Perguia, Italy). It was derived by infecting primary mouse microglia cultures with a v-raf/v-myc

oncogene carrying retrovirus (J2) (Blasi et al., 1990). BV-2 cells are semi-attached cells with most of the the morphological, phenotypical and functional properties of activated primary microglial cells. Morphologically they resemble activated primary microglia cells, with short, thick processes. In general the model can be used for studies where activation of microglia is under investigation. Upon LPS treatment BV-2 cells show similar behavior than primary microglia, in producing NO and proinflammatory cytokines (Horvath et al., 2008). There are two different forms, the round BV-2 cells, which simulate the active form of primary microglia, and the more adherent cells, which resemble the inactive form. Through serum-free medium the cells undergo phenotypic changes and stay in an inactivated state (Laurenzi et al., 2001).
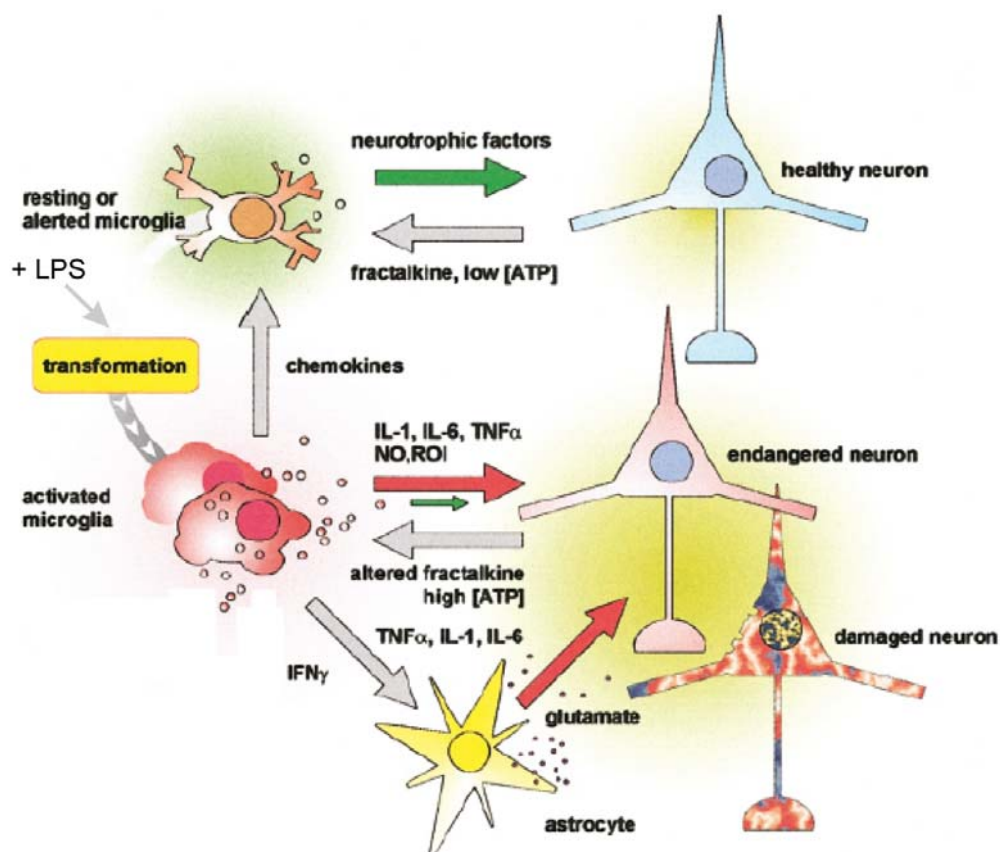
Figure 4. Communication between microglia and other cells of the CNS in health and disease. Healthy neurons communicate with microglia over fractaline and low ATP levels to inform them about their state of health. Microglia under physiological conditions release neurotrophic factors to support neuronal function and survival. After inflammatory stimulus, like LPS, microglia become activated and produce cytokines (e.g. TNFα, IL-1, IL-6) and other harmful factors like NO and ROS, with potential toxicity for neurons. Further microglia can recruit astrocytes, amplifying their inflammatory response, which can lead to further neuronal damage through for example glutamate. Picture adapted from Hanisch U.K. (Hanisch, 2002).

1.2.3. Oligodendrocytes

Oligodendrocytes are also restricted to the central nervous system. They are the glial cells that produce the myelin sheets of axons in the brain (Lipton, 2006). Myelin, a lipid-rich membrane has important effects on the action potential conduction, by accelerating the conduction of electrical impulses. In the peripheral nervous system, the cells that elaborate myelin are called Schwann cells (Allen and Barres, 2009). Demyelination leads to various diseases including multiple sclerosis (Lipton, 2006) and happens most often due to damage of oligodendrocytes.

Survival and proliferation of oligodendrocytes is highly dependent on neuronal contact and neuronal soluble factors, secreted by axons. Both cell types communicate to make sure that the number of free axons does not exceed that of oligodendrocytes, therefore neurons and oligodendrocytes cross talks is highly important during development of the brain (Gomes et al., 2001). During inflammatory processes in the brain oligodendrocytes are vulnerable to insults especially through released cytokines (Schmitz and Chew, 2008).

1.2.4. Astrocytes

Astrocytes are derived from ependymoglia of the developing neuronal tube (Abbott et al., 2006), they are restricted to the brain and spinal cord and elaborate local processes that give these cells a star like appearance, and therefore their name. In the adult brain astrocytes don´t overlay each other (Allen and Barres, 2009) but are linked together via gap junctions (Abbott et al., 2006). They act as physical barriers between synaptic connections of neighboring neurons. They provide energy and substrates to neurons for neurotransmission, control blood vessel flow through their fine processes (Allen and Barres, 2009) and they take part in the blood-brain-barrier build up (Abbott et al., 2006). By removing exorbitance neurotransmitters from the extracellular space, they allow discrete and precise encoding of neurotransmission and synaptic signals. Recently identified roles for astrocytes showed that they also seem to be involved in modulating synaptic function and the formation of synapses (Allen and Barres, 2009).

Astrocytes and lipopolysaccharide

In pure astrocyte cultures, LPS failed to stimulate mRNA or protein expression for IL-1β, TNFα and IL-6 (Lee et al., 1993). This is not surprising as Lehnardt et al. (Lehnardt et al., 2002) showed that microglia but not astrocytes express TLR-4 receptor, which is necessary to bind and respond to LPS. But astrocytes are getting activated by IL-1β or other cytokines released by microglia. Therefore microglia may be the key regulators of astrocytes response (Lee et al., 1993). Upon treatment of microglia with LPS microglia release various factors that lead to hypertrophic shape of astrocytes compared to control conditions, but not to a decrease of cell number (Lehnardt et al., 2003). Most likely candidates for this astrocytic trophy are proinflammatory cytokines. This phenomenon is known as astrogliosis, which is a characteristic response of astrocytes to inflammation and trauma of the CNS (Balasingam et al., 1994).

1.3. LPS-induced inflammation is linked to disease models of newborns

During the perinatal period the developing brain is most vulnerable to inflammation (Hagberg and Mallard, 2005). Prenatal infection or exposure to inflammatory factors can have a profound impact on fetal neurodevelopment with long-term neurological deficits, such as cognitive impairment, learning deficits, perinatal brain damage and cerebral palsy, a spastic motor deficit (Folkerth, 2005;Volpe, 2001;Volpe, 2003;Deverman and Patterson, 2009). There is a lot of evidence that maternal infection causes neurodevelopmental abnormalities and increases the risk factors for cerebral palsy, schizophrenia, periventricular leukomalacia (PVL) and autism in the offspring. PVL is one of the leading causes for perinatal brain as well as for cognitive or attention deficits in low birth weight infants (Deverman and Patterson, 2009;Folkerth, 2005). The possible link between maternal/fetal infection and PVL might be the cytokine release. Cytokines reach the fetus over the placenta or the fetus generates its own immune response and the cytokine induction might affect neurodevelopment. The cytokine induction can also occur as a result of exposure of the brain to circulating bacterial agents, for example LPS (Folkerth, 2005). Inflammation-induced release of cytokines may subsequently have a critical impact on the survival of immature neurons and lead to apoptosis.

Apoptosis is one of the most important and best controlled forms of cell death, which occurs under different physiological and pathophysiological conditions and leads to stereotypic morphological and biochemical changes. Apoptosis is a relatively ordered process of energy-dependent programmed cell death, in contrast to necrosis (Taylor et al., 2008). During apoptosis a cell undergoes characteristic morphological alterations like cell shrinkage, "blebbing" on the membrane, deletion of the chromosomal DNA by nucleases, formation of many membrane bound fragments and compacting of cytoplasmic organelles (Kerr et al., 1972;Raffray and Cohen, 1997;Zierler et al., 2006). Morphological and biochemical changes during this apoptotic process are activated through effector caspases. All pathways lead to activation of the major effector caspases, caspase-3 (casp-3), caspase-6 and caspase-7 (Taylor et al., 2008). For example the activation of casp-3 represents a valuable marker of apoptosis. Caspases are considered to be one of the most highly conserved families of pro-apoptotic families, involved in programmed cell death (Marin-Teva et al., 2004;Oppenheim et al., 2001). Apoptosis is especially important for embryonic development, to control cell population, tissues homeostasis and neuronal degeneration.

1.4. The early cortical neuronal networks

During embryonic development, cortical neurons form connections to establish cortical networks. The immature neuronal circuits are established first on genetic information, followed by spontaneous and sensory-driven activity, which is equally important for the set up of the highly organized functional cortical networks (Khazipov and Luhmann, 2006) (**Figure 5**).

An increasing body of evidence suggests that neuronal activity is important in the regulation of neuronal survival during early development (Mennerick and Zorumski, 2000), e.g. programmed cell death (apoptosis) is augmented when neuronal activity is blocked (Heck et al., 2008;Voigt et al., 1997). Electrical activity also controls other mechanisms, like neuronal differentiation, migration, synaptogenesis and synaptic plasticity (Katz and Crowley, 2002;Rakic and Komuro, 1995;Spitzer et al., 2004;Zhou and Poo, 2004).

Studies in neonatal rodents have shown that early patterns of synchronized cortical activity share many features with special electrical pattern in newborn human babies. They are classified as spontaneous activity transients (Tolonen et al., 2007) or delta-

brush oscillations (Colonnese et al., 2010;Yang et al., 2009) with a frequency up to 25-30 Hz and might therefore be a good model to study electrical changes under experimental conditions (Khazipov and Luhmann, 2006).
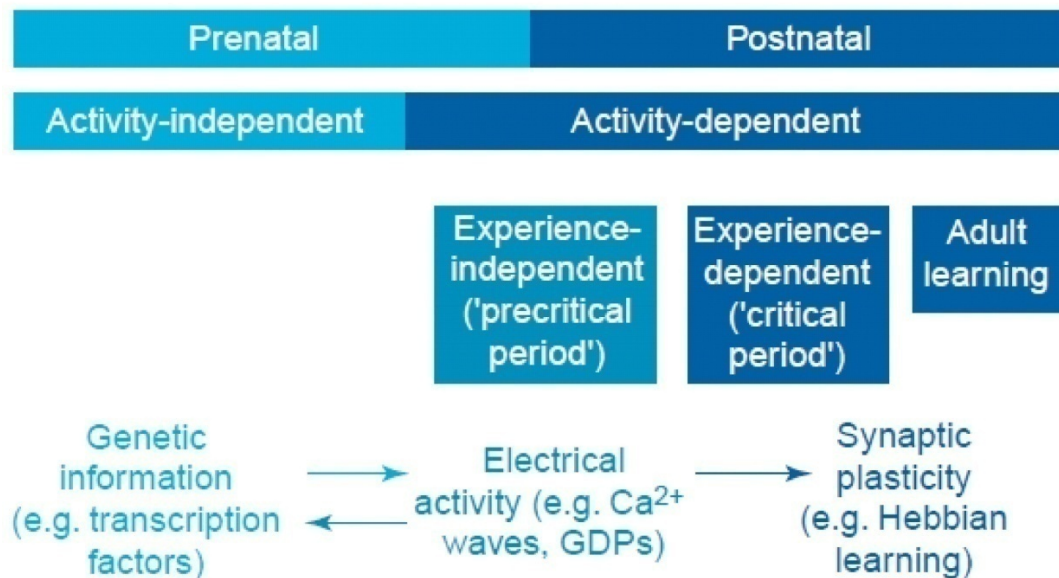
Figure 5. Formation of early neuronal networks depends on genetic information as well as electrical activity. During early embryonic development, genetic information plays the most important role in setting up neuronal circuits and topographic connections. Afterwards certain electrical activity patterns play a determining role for tuning the development of neuronal networks. During critical periods of development, the network is formed in an experience-dependent manner. Picture adapted from Khazipov and Luhmann (Khazipov and Luhmann, 2006)

1.4.1. Network oscillations and their formation in the brain

Slow potentials (EEG waves) are recorded directly from the scalp while neuronal activity is measured via local field potential (LFP). To measure LFP the electrodes must be near specific layers of the cortex or near nuclei of neurons. The signal is generated by various neuronal processes in the cell ensemble and reflects the synchronization among the neuronal activity. EEG and local field potential are integrated excitatory postsynaptic potentials (EPSPs) and inhibitory postsynaptic potentials (IPSPs) of neuronal membranes (Berens et al., 2008;John, 2002). In cortex and hippocampus neurons have parallel orientation. When these orientated neurons receive synaptic inputs at once, the extra-cellular signals do not average out, but rather add up to give a signal, that can be recorded as LFP. Already at earliest developmental stages rhythmic network activity can be observed in various neuronal structures, like hippocampus (Ben-Ari et al., 2007), visual cortex (Hanganu

et al., 2006) and cerebral cortex (Khazipov and Luhmann, 2006). In the developing neocortical networks *in vivo* three patterns of oscillatory activity can be seen. Spindle burst, with a duration of 1-2 sec and a frequency of 10 Hz, which occur every 10 seconds. Gamma oscillations with a frequency of 30-40 Hz, a duration of 150-300 milliseconds and occurrence of 10-30 seconds. And propagating long oscillations that synchronized in the 10-20 frequency range and were lasting up to 83 seconds (Yang et al., 2009). Disturbance of the neuronal network activity during early development may lead to changes in the developmental programs and may cause long-term alteration in cortical microcircuits, and further changes in organization of the affected structures, which might lead to cognitive dysfunction (Le Van Quyen M. et al., 2006;Levitt et al., 2004).

1.4.2. Early developmental formation of neuronal network activity

Developing neurons and neuronal networks show primitive patterns of synchronized activity during defined developing stages. When synapses start to be established, or even before, a primitive form of network-driven activity provides most of the synaptic activity. These patterns need a high degree of synchrony in immature neurons, because the functional synapses are small in number. This formation of neuronal circuits is conserved in a wide range of structures and species which suggests that there is a developmental program that has been conserved throughout evolution (Ben Ari, 2001). During a brief developmental period (postnatal days [P] P0 to P7 in mice) the cortical network switches from a subplate-driven, gap junction coupled syncytium to a synaptic network, acting through NMDA receptors to generate synchronized oscillatory activity. This may function as an early functional template for the development of the cortical columnar architecture (Dupont et al., 2006). These patterns of activity lead to release of Ca^{2+} and seem to lead to adaptive changes in for example cAMP-responsive element binding protein (CREB)-mediated gene expression of Ca^{2+}/CaM-dependent protein (CaMKII) in neurons (Dolmetsch et al., 2001). Thereby the temporal dynamics seem more important than the concentration. Frequency, duration and interval in between of action potential firing leads to effects on different intracellular signaling pathways and transcription of genes for example the IEG *nur77* is induced by patterns that failed to induce *c-fos* (Sheng et al., 1993), indicating that different genes are activated by different patterns of neuronal firing (Fields et al., 2005). This genes, regulated by oscillatory activity are important for

various processes during the development of the cerebral cortex, for example apoptosis (Hara and Snyder, 2007), neuronal differentiation (Spitzer et al., 2004) and neuronal migration (Ben-Ari et al., 2007). This early synchronized network activity observed in rodents seems to be comparable to delta brushes described in human premature cortex. Evidence therefore is: They both occur at similar ontogenetic time points and their activity is in a similar frequency range (5-25 Hz) (Khazipov and Luhmann, 2006).

1.4.3. In vitro *and* in vivo *recordings of spontaneous oscillations in the cortex*

A hallmark of the developing central nervous system are coordinated patterns of spontaneous neuronal activity (Katz and Shatz, 1996). In the cortex, these spontaneous oscillations communicate through gap junctions and Ca^{2+} release from intracellular Ca^{2+} stores (Yuste et al., 1992;Yuste et al., 1995).

Spontaneous electrical activity patterns recorded in organotypic neocortical slice cultures, with the help of the multi electrode array system (MEA) resemble in many aspects the spontaneous activity patterns observed *in vivo* (Dupont et al., 2006;Heck et al., 2008;Khazipov et al., 2004). The MEA system consists of 60 electrodes and one can record field potentials from surrounding neurons in organotypic slice cultures as well as from dissociated neuronal cultures.

As in neonatal cerebral cortex, synchronized rhythmic activity also develops spontaneously in slice cultures and neuronal networks. Neuronal cultures formed by embryonic neurons in cell culture grown on multi-electrode arrays have been used in many studies of network physiology. They resemble hallmark features of *in vivo* models, in terms of electrical recordings, imaging and pharmacological intervention (Wagenaar et al., 2006) and also resemble features of spontaneous correlated activity recorded in cortical slices. Already after two days *in vitro* synchronous oscillatory activity can be found in slice culture. Dissociated cultures *in vitro* start firing after 4 days in culture (Golbs et al., 2010) and at the end of the first week synchronization patterns can be found, simultaneously with the development of synapses in the culture (Opitz et al., 2002;Voigt et al., 1997). Unlike *in vivo*, where bursting only occurs during development, lasting for maximal one week, to establish appropriate connections (Ben Ari, 2001), neuronal ensembles in culture maintain activity patterns dominated by global bursts for the lifetime of the culture. This might be caused by a lack of input from other brain areas (Wagenaar et al., 2005).

In organotypic slice cultures and *in vivo* field potentials are recorded, which show certain frequency bands of oscillations and can be divided into five groups:

- delta   0.5 – 4 Hz   associated with slow-wave sleep
- theta   4 – 8 Hz   associated with REM sleep
- alpha   8-13 Hz   associated with relaxed wakefulness
- beta   13-30 Hz   associated with relaxed arousal
- gamma   30-80 Hz   associated with arousal state

(Engel et al., 2001;Hughes et al., 2004;Sejnowski and Destexhe, 2000). *In vivo* electrical recordings can be performed by using Michigan electrodes, positioned in the cortex of young mammalians. Three distinct patterns of synchronized oscillatory activity were found so far *in vivo*. First spindle bursts, second gamma oscillations and third long oscillations (Yang et al., 2009).

Many of the patterns which have been found *in vitro* and *in vivo* share common features and probably reflect the same phenomena (Khazipov and Luhmann, 2006).

1.5. Proinflammatory cytokines and how they are related to electrical activity and apoptosis

Cytokines are immunomodulatory peptides which serve for cellular communication (Hanisch, 2002). They are released after microglia activation and tend to have both toxic effects on surrounding cells as well as effects on the CNS that are separate from their role in stimulating the immune response. Chemokines are a family of peptide chemoattractant molecules that interact with a specific family of G-protein-coupled receptors (Garden and Moller, 2006).

Glial cells are capable to release a bunch of pro-inflammatory cytokines and chemokines (**Table 1**) among them G-CSF, KC, GM-CSF, IL-6, JE, IL-1ra TNFα, MIP-2, IL-6 and RANTES. G-CSF is hypothesized to increase the activation of resident microglia and mobilization of bone-marrow-derived microglia (Sanchez-Ramos et al., 2009). KC, also called CXCL1, and RANTES are chemoattractants for a variety of inflammatory immune cells like neutrophils (van Rossum et al., 2008). GM-CSF induces proliferation and activates microglia (Reddy et al., 2009) and IL-1ra inhibits IL-1 activity (Sims, 2002). TNFα, MIP-2 and IL-6 are important cytokines primarily involved in inflammation. It has been demonstrated that IL-6 causes reactive astrogliosis but no neuronal damage (Fattori et al., 1995;Raivich et al.,

1999). Especially activated microglia participate in the pathogenesis of neurological disorders by secreting these various cytokines (Hanisch, 2002).

The focus of my work was on TNFα and MIP-2 as the most likely downstream candidates of LPS which seem to induce neuronal desynchronization and cell death. The release of the pro-inflammatory TNFα, enhances excitatory synaptic function by increasing the surface expression of AMPA receptors (Beattie et al., 2002). Thus constitutively released TNFα homeostatically regulates, in an activity-dependent manner, the balance between neuronal excitation and inhibition (Stellwagen and Malenka, 2006). Since TNFα has direct toxic effects on neuronal structures and myelin (Hanisch, 2002) and is also involved in neuronal death (Chaparro-Huerta et al., 2008;Harry et al., 2008), the interplay between neuronal activity and TNFα may control the process of cell death and cell survival in developing neuronal networks.

Another likely candidate participating in electrical activity and cell survival is MIP-2. This chemokine is triggered by TNFα release (Matejuk et al., 2002;Otto et al., 2001;Sakai et al., 1997) and MIP-2 injection into the hippocampus leads to apoptotic cell death of neurons (De Paola et al., 2008;Kalehua et al., 2004).

1.6. Questions that arise

In my study I was interested on the impact of inflammation on neuronal activity and cell survival during early cortical development. To address this question, we used *in vivo* approaches with newborn rats as well as organotypic slice cultures and dissociated neuronal cultures of the somatosensory cortex from newborn mice and analyzed inflammation-induced modifications in neuronal activity and apoptotic cell death. Inflammation was experimentally induced by application of the endotoxin lipopolysaccharide, which initiates a rapid and well-characterized immune response (Hagberg and Mallard, 2005). I studied the consequences of inflammation on spontaneous neuronal network activity and cell death by combining electrophysiological recordings with multi-electrode arrays and quantitative analyses of apoptosis. In addition, the use of a cytokine array and antibodies directed against specific cytokines allowed us the identification of the pro-inflammatory factors, which are critically involved in these processes. To get a link to the *in vivo* situation we treated (cooperation with Jen-Wei Yang and Shuming An) P3-4 rats with LPS cortical injection while recording simultaneously electrical field potentials.

In detail I addressed the following questions: (i) What is the effect of LPS-induced inflammation on apoptotic cell death and spontaneous neuronal network activity in organotypic slice cultures? (ii) Which factors are released from LPS treated microglia influencing neuronal survival and network activity in dissociated neuronal cultures? (iii) What is the time course of these actions of the pro-inflammatory factor(s)? (iv) Does neutralization of the identified cytokines lead to re-establishment of synchronized burst activity and cell survival? (v) What are the consequences of LPS-induced inflammation on spontaneous network activity and apoptotic cell death in the neonatal cerebral cortex *in vivo*?

2. Material

2.1. Chemicals

Alamar Blue (Resazurin Natrium Salt)	Sigma, Deisenhofen
AraC	Sigma, Steinheim
B27	Gibco, Karlsruhe
BME	Sigma, Steinheim
BSA	Sigma, Steinheim
Calcium chloride	Merck, Darmstadt
Calcein red-orange	Invitrogen, Karlsruhe
DCFH (2´7´dichlorodihydrofluorescein)	Sigma, Steinheim
D(+)-Glucose	Merck, Darmstadt
DEPC water	Invitrogen, Karlsruhe
DMSO	Sigma, Steinheim
Donor Horse Serum (10%)	Biochrom AG, Berlin
Ethanol	Carl Roth, Karlsruhe
FCS	Biochrom, Berlin
Fluoromount-G (embedding media)	SouthernBiotech, Birmingham, USA
Gentamycin	Gibco, Karlsruhe
Glutamax	Invitrogen, Karlsruhe
Glycerin	Sigma, Steinheim
Glycin	Carl Roth, Karlsruhe
HBSS	Gibco, Karlsruhe
HEPES	Carl Roth, Karlsruhe
Magnesium chloride	Merck, Darmstadt
L-Glutamin	Sigma, Steinheim
Lipopolysaccharide (LPS) from *E.coli.* 055:B5	Sigma, Steinheim
MEM	Gibco, Karlsruhe
Neurobasalmedia	Invitrogen, Karlsruhe
Paraformaldehyd	Carl Roth, Karlsruhe
PBS (10x)	Gibco, Karlsruhe
Penicillin/Streptomycin	Invitrogen, Karlsruhe
Phenolred	Sigma, Steinheim

Poly-L Ornithinhydrobromid	Sigma, Steinheim
Potassiumchlorid	Merck, Darmstadt
RPMI medium	Gibco, Karlsruhe
Sampling buffer 6x (Loading dye 6x)	NEB, Ipswich, MA, USA
Triton X 100	Serva, Heidelberg
Trypsin 0.05% / EDTA	Invitrogen, Karlsruhe
Trypsin 0.25%	Invitrogen, Karlsruhe

2.2. Equipment

-80 freezer (Hera freeze)	Heraeus, Hanau
Air objective (4x/340)	Olympus, Tokyo, Japan
Analysis chamber	Luigs and Neuman
Analytical balance (JL-200)	Chyo Balance Corp., Tokyo, Japan
Anti-vibration table	Institute of Physiology, Mainz
Autoclave (Systech 65)	Systech, Wettenberg
Balance	Kern und Sohn GmbH, Ballingen
Binocular	Zeiss, Jena
CCD-camera	Roper Scientific, Trenton, USA
Centrifuge (5415C)	Eppendorf, Hamburg
Centrifuge (Sorvall SS34)	Kendro, Vienna, Austria
CO_2 incubator (HeraCell 240)	Kendro, Vienna, Austria
Confocal microscope (BX51WI)	Olympus, Tokyo, Japan
Drying oven	Kendro, Vienna, Austria
Freezer (Herafreeze)	Kendro, Vienna, Austria
Ice maschine (AF 20)	Scotsman, Milan, Italy
Infinite F200 microplate reader	Tecan, Crailsheim
Inverted microscope	Optica microscopes, Bergamo, Italy
Lamp for binocular (KL1500 electronic)	Schott, Bad Gandersheim
Laser	Laser Physics, West Jordan, USA
Light Cycler	Roche, Mannheim

3-D MEA Chips	Ayanda Biosystems, Lausanne Switzerland
Planar MEA-Chips	Multi Channel System, Reutlingen, Germany
MEA1060-INV-BC interface	Multi Channel System, Reutlingen, Germany
Microscop CK40	Olympus, Tokyo, Japan
Microscope	Zeiss, Jena
Millipore (Synergy)	Millipore, Schwalbach
Neubauer-chamber (cell counting)	Brand GmbH, Wertheim
Nikon coolpix 4500	Nicon, Tokyo, Japan
Osmometer	Knauer, Berlin
pH Meter	InoLab, Weinheim
Object 4x (air object)	Olympus, Tokyo, Japan
Object 20x, 60x (water immersion object)	Olympus, Tokyo, Japan
PCR maschine (mastercycler personal)	Eppendorf, Hamburg
Piezo	Piezosystem, Jena
Pipet (Pipetman)	Gilson, Bad Camberg
Pipet (*research*)	Eppendorf, Hamburg
Pipettierhilfe (Easypet)	Eppendorf, Hamburg
Refrigerator (Liebherr *profiline*)	Liebherr, Lindau
Scalpel (Microscalpel)	Medicon, eG, Tuttlingen
Scissor (mikro 2000)	Medicon, eG, Tuttlingen
Table centrifuge (Minispin plus)	Eppendorf, Hamburg
Table wobbler	Cneco Instruments, Breda, Netherlands
Temperature control system	Luigs and Neuman
Temperature control unit (TC02)	Multi Channel Systems, Reutlingen
Tissue chopper (McIlwain TC752)	Vibratom, St. Luis, USA
Tissue ruptor	Quiagen, Hilden
Tweezers (#5)	Neolab, Heidelberg
Urethane injection	Sigma-Aldrich, Taufkirchen, Germany)

Vakuum pump   KNF Lab, Trenton, USA

Water bath   Memmert, Schwabach

Water objective (20x/0,5, 60x/0,9)   Olympus, Tokyo, Japan

Wobbler (Titramax 1000)   Heidolph Instruments,
                                              Schwabach

Work bench (Herasafe HS15, Heraguard)   Kendro, Vienna, Austria

2.3. Consumption items

96 well plates   Greiner, Frickenhausen

24 well plates   Greiner, Frickenhausen

6 well plates   Greiner, Frickenhausen

Cover slips   Roth, Karlsruhe

Culture flasks (T25)   Sarstedt, Nümbrecht

Culture flasks (T75)   Sarstedt, Nümbrecht

Cuvettes (UV-cuvette, Micro)   Brand, Wertheim

Eppendorf tubes   Biozym, Hessich Oldendorf

Falcon tubes (15 und 50 mL)   Sarstedt, Nümbrecht

Gloves (rotiprotect Latex)   Carl Roth, Karlsruhe

Millicell-CM membranes   Millipore, Bedford, MA, USA

Object holder   Carl Roth, Karlsruhe

Petri dishes   Nunc, Langenselbold

Pipet tips (0.1-2 µl)   Biozym, Hessich Oldendorf

Pipet tips (100-1000 ml)   Plastibrand, Wertheim

Pipet tips (2-200 µl)   Plastibrand, Wertheim

Pipets (5, 10 und 25 mL)   Sarstedt, Nümbrecht

Polyamidfilter (80 µm pore size)   VWR, Bruchsal

Steril filter (Filtropur S 0.2 µm)   Fluka, Steinheim

2.4. Antibodies and co.

anti-GFAP   Dako, Hamburg

anti-MAP-2 (HM-2)   Sigma, Steinheim

anti-NeuN   Chemicon now Millipore,
                                              Bedford, MA, USA

Anti-MIP2	Sigma, Aldrich, St. Louis, MO, USA
Anti-TNFα	antibody online.de Aachen, Germany
Anti-TNFα (for Westernblot)	Chemicon now Millipore, Bedford, MA, USA
CD14 (M-20) antibody	Santa Cruz Biotechnology, Inc., California, USA
Cleaved caspase-3 antibody (Asp175)	Cell Signaling Technology, San Diego, USA
DNase I	Roche, Mannheim
Fluorescent conjugates of lipopolysaccharides (LPS)	Molecular Probes, Karlsruhe
Goat-anti-mouse-Alexa Fluor568/red	Molecular Probes, Karlsruhe
Goat-anti-rabbit (biotinylated)	Vector Laboratories, Burlingame, USA
Goat-anti-rabbit Cy-2	Dianova, Hamburg
Propidium iodid (PI)	Sigma, Steinheim
Streptavidin-Alexa488	Molecular Probes, Karlsruhe
Streptavidin-Cy3	Jackson ImmunoResearch, Suffolk, UK

2.5. Kits

Cytokine array panel A array kit	R&D System, Minneapolis, USA
Griess reagent (modified)	Sigma, Saint Louis, MO, USA
Light Cycler Taqman Master Kit	Roche Applied Science, Mannheim
RNeasy Mini Kit	Qiagen, Hilden
Transcriptor High Fidelity cDNA synthesis kit	Roche Applied Science, Mannheim

2.6. Laboratory animals

Cage type	Makrolon type III A
Floor measure	383 x 221 mm

Floorage	810 cm^2
Fodder	Altromin 1314 – Panacur with fenbendazol
High	150 mm
Litter	rough chipped wood
Mice	C57BL/6
Wall thickness	3 mm
Water	pH neutral, no add on

2.7. Software

Adobe imaging version 7	Adobe Systems Inc., Munich
Adobe Photoshop CS2	Adobe Systems Inc., Muni ch
CorelDraw version 12	Corel Corporation, Unterschleißheim
Excel MS Office 2007	Microsoft, Redmond, USA
GraphPad Prism 3.02	Graphpad Software, Inc, San Diego, USA
ImageJ	http://rsbweb.nih,gov/ij/
Matlab version 7 and 7.7	The Math Works Inc., Natick, USA
MC_Rack	Multi Channel Systems, Reutlingen, Germany
Metamorph	Universal Imaging Corporation, Sunnyvale, USA
Office 2007	Microsoft Corporation, Redmond, USA
Reference Manager Pro 10	OSO ResearchSoft, Philadelphia, USA
Universal Probe library assay design center	https://www.roche-applied-science.com
Word MS Office 2007	Microsoft, Redmond, USA

2.8. Media and buffer solutions

ACSF	1.8	mM	$CaCl_2$
	25	mM	Glucose
	10	mM	HEPES
	5.3	mM	KCl
	0.812	mM	$MgCl_2 . 6 H_2O$
	51.3	mM	NaCl
	26	mM	$NaHCO_3$
	0.9	mM	$NaH_2PO_4 . 1 H_2O$
ACSF special	1.8	mM	$CaCl_2$
	25	mM	Glucose
	10	mM	HEPES
	5.3	mM	KCl
	0.812	mM	$MgCl_2 . 6 H_2O$
	51.3	mM	NaCl
	26	mM	$NaHCO_3$
	0.9	mM	$NaH_2PO_4 . 1 H_2O$
	0.23	mM	sodium pyruvat
	0.5	mM	L-glutamine
	0.4	mM	glycine
	0.4	mM	L-serine
	0.02	mM	L-alanine
	0.028	mM	choline chloride
	0.2	µM	$Fe(NO_3)_3 H_2O$

Equilibrated with 95 % O_2; 5 % CO_2 (pH 7.4; osmolarity 205 mOsm).

BME/10 % FCS	1	times	BME
	10	%	FCS
DNaseI	0.05	%	DNaseI in HBSS$^{-/-}$
MEM+	1	times	MEM
	200	µM	Glutamin
MPBS (-/-)	1	mg/mL	BSA
	6	µg/mL	DNaseI
	10	mM	Glucose

	1	mM	Glutamax
	4	mM	NaOH
	1	times	PEST
	5	mg/mL	Phenolred
	1	mM	Pyruvat in PBS
NB/B27	2	%	B27
	2	mM	Glutamax
	10	µg/mL	PEST
HBSS^{+++}	2	mM	CaCl$_2$
	10	mM	glucose
	1	mM	MgCl$_2$
PBS (0.01M)	0.01	M	phosphate
pH 7.4	0.138	M	NaCl
	0.0027	M	KCl
MEM+10% HS	500	ml	MEM
	2	mM	L-glutamin
	10	%	Horse serum
	5	µg/ml	Gentamycin
RPMI + 10% FCS	10	%	FCS
	10	µg/ml	PEST
	2	mM	L-glutamin

3. Methods

3.1. Cell culture

3.1.1. Prearrangement of the Millicell-CM membranes

Millicell-CM membranes were transferred under sterile conditions into 6-well plates and pre-incubated with 1ml NB/B27 media over night for equilibration before use.

3.1.2. Preparation of organotypic neocortical slice cultures of the mouse

All experiments were conducted in accordance with the national laws for the use of animals in research and approved by the local ethical committee (Landesuntersuchungsamt Rheind-Pfalz 23.177-07/G 10-1-010).

Organotypic neocortical slices were prepared from newborn (postnatal days [P] P0 and P1) C57Bl/6 mice and cultivated according to the method described by Stoppini et al (Stoppini et al., 1991). Previous studies have demonstrated that organotypic slice cultures are well suited to investigate the molecular and cellular mechanisms underlying apoptosis during early cortical development (Haydar et al., 1999). Animals were killed by decapitation and the brains were quickly removed. All subsequent procedures were performed in Minimal Essential Medium (MEM; Invitrogen GmbH, Darmstadt, Germany) supplemented with 2 mM glutamine, pH 7.4 at 4° C. Neocortical hemispheres were isolated from the hippocampus, thalamus and striatum and 350 μm thick coronal slices containing the parietal cortex were cut with a tissue chopper (McIlwain, Mickle Laboratory Engineering, Surrey, United Kingdom). The meninges were carefully removed and the dorsolateral part of the cerebral cortex was dissected with a microscalpel. The isolated cortical slices were transferred onto Millicell-CM membranes (Millipore, Bedford, MA) placed into 35 mm petri dish. Slices were kept at 37° C, 5% CO_2 in medium containing neurobasal medium supplemented with 2% B27 (Invitrogen), 2 mM glutamax (Invitrogen) and 10 μg/ml penicilline/streptomycine (NB/B27 medium). After 24 h, 1 μM Arabinofuranoside Cytidine (AraC, Sigma-Aldrich, Steinheim, Germany) was added to the medium. Thereafter, culture medium with AraC (added every second time) was renewed every two days.

3.1.3. Prearrangement of cover slips

Round steril cover slips were transferred into 24-well-plates. Every cover slip was covered with at least 300 µL poly-ornithin (10 µg/ml, diluted in aqua dest.) and incubated over night. 1 h before starting with the preparation, the cover slips were put into the incubator. Shortly before the transfer of the cells the cover slips were washed 3 times with HBSS$^{-/-}$ and once with NB/B27.

3.1.4. Prearrangement of the MEA-chips

As they were reused cleaning procedure was very strict. Planar MEA-chips with 59 recording electrodes and one reference electrode (**Figure 6 a**) were incubated with 500 µl trypsin (2.5%) over night to remove leftover cells and debris. Subsequent MEA-chips were washed at least 3 times with Millipore water and sterilized for 2.5 h at 120°C in the drying oven. One day before use they were pre incubated with 1 mg/ml poly-ornithin at room temperature. Shortly before the transfer of the cells the MEA-chips were washed 3 times with HBSS$^{-/-}$ and once with NB/B27 before dissociated neuronal cultures were cultivated on MEA-chip (**Figure 6 b**).
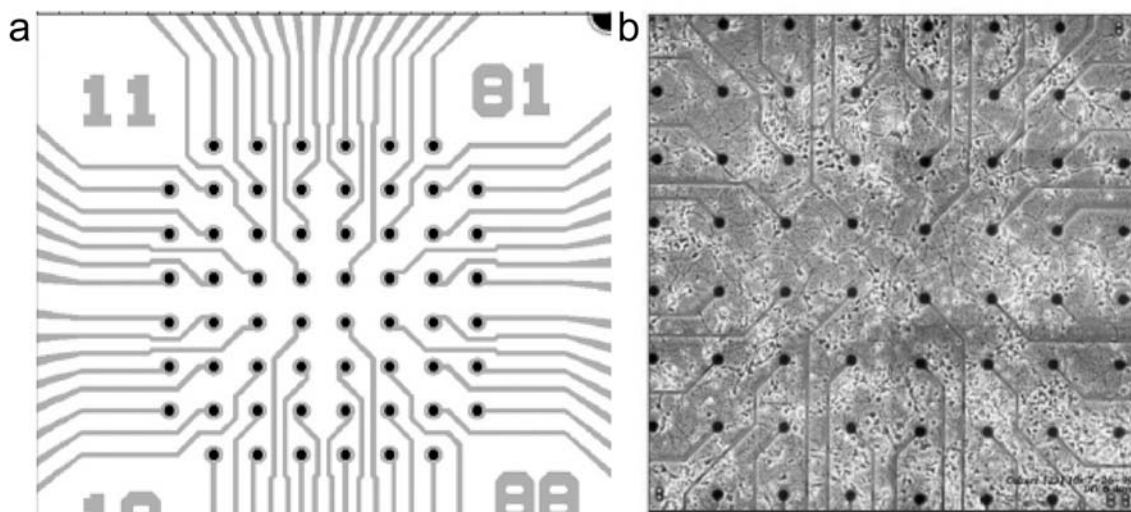
Figure 6. Planar MEA chip. (**a**) MEA chip, 59 electrodes and one reference electrode. (**b**) Dissociated neuronal cultures cultivated on MEA chip.

3.1.5. Preparation of dissociated neuronal cultures of the neocortex

Cultures of neocortical neurons were prepared from P0–P1 newborn C57Bl/6 mice. The mice were decapitated and the cerebral hemispheres were placed in ice-cold MEM supplemented with 200 µM glutamine. Both hemispheres were isolated and the meninges were removed. The cortices were separated from the hippocampus,

striatum and thalamic nuclei. The dissociation of the cerebral cortex was achieved by incubation in modified phosphate buffered saline without Ca^{2+} and Mg^{2+} containing 0.25% trypsin (Invitrogen) at a temperature of 37° C for 12 min. Trypsinization was finally blocked by addition of basal medium eagle (Invitrogen) containing 10% fetal calf serum (BME/10% FCS). Cortices were further dissociated in 0.05% DNase (diluted in $HBSS^{-/-}$) by sequentially repeated passages through a pipette blue tip cut to obtain a wider opening (3 mm) followed by a fire-polished Pasteur pipette. The number of cells was estimated by cell counting with a Neubauer chamber. Three million cells were preplated in a 3 cm Petri dish in BME/10% FCS at 37° C, 5% CO_2 for 45 min. This treatment allowed astrocytes to attach to the bottom of the Petri dish whereas neurons remained in the medium. For electrophysiological recordings, the resulting cell suspension, which was enriched in neurons compared to glial cells, was plated at a density of 1,000,000 cells per ml on poly-ornithin (Sigma) coated multi-electrode arrays (MEAs; Multi Channel Systems, Reutlingen, Germany). For analyses of the neuronal survival rate, cells were plated on 96-well plates at a density of 500,000 cells per ml. For immunostaining they were plated on 24 well plates on poly-ornithin coated cover slips at a density of 200,000 cells per well. Neurons were cultured in NB/B27 medium at 37° C, 5% CO_2. After 1 day *in vitro* (DIV) the medium was completely changed and after 7 days 33% of medium was exchanged. Neurons where kept 14 days in culture, where they showed a clear neuronal morphology and a lot of fine processes (**Figure 7 a, b**).
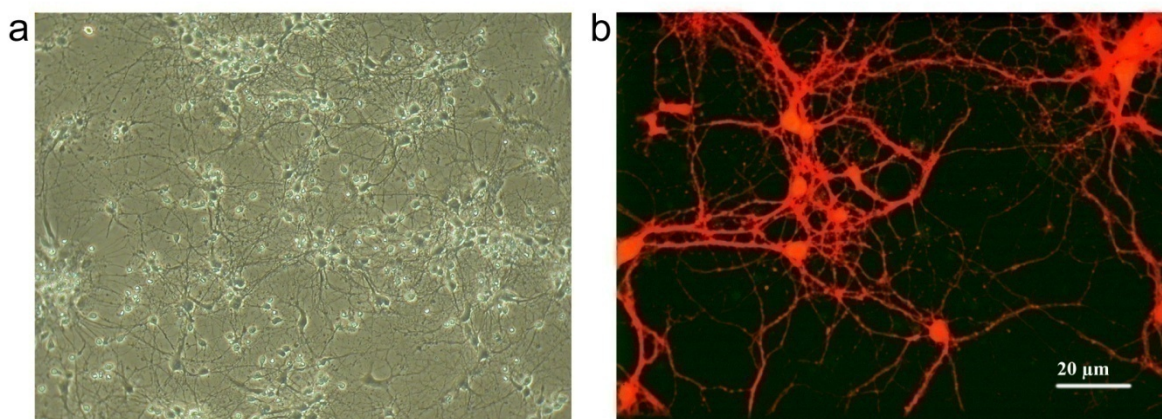
Figure 7. Dissociated neuronal cultures of the neocortex. (**a**) DIV 7 light microscopic picture of dissociated neuronal cells. (**b**) 14 DIV dissociated neuronal cultures, stained with Calcein-red orange.

3.1.6. BV-2 microglial cell culture

Cells of the murine microglial cell line BV-2 cells made by V. Bocchini (University of Perguia, Perguia, Italy) were used (**Figure 8 a**). The BV-2 cell line was created by infecting primary mouse microglia cultures with a v-raf/v.Myc oncogene carrying retrovirus (J2) (Blasi et al., 1990). They reveal comparable attitudes as primary microglia (Horvath et al., 2008) and were maintained in 25 cm^2 culture flasks in RPMI + L-Glutamine + 10 µg/ml PEST supplemented with 10% FCS (Invitrogen) at 37° C in a humified atmosphere of 5% CO_2. Cells were passed two to three times per week by trypsinization (trypsin/EDTA for 2 min). Cells were used till passage 20. The culture medium was changed to NB medium before each experiment. BV-2 cells were seeded into 25 cm^2 culture flasks splitting them 1:6 after 75% confluence and let them grow for 2 days in RPMI-media. For the conditioned medium BV-2 microglial cells were divided into 6 groups and each was treated with various factors for 6 h (**Table 2**). For analyses of the cell survival rate, cells were plated on 24-well plates at a density of 40,000 cells per well in RPMI+L-Glutamine supplemented with 10% FCS (Invitrogen) medium at 37°C, 5% CO_2 for 2 days prior to experiments.

Table 2

Abbreviation	Full name	Conditioning	Antibodies
C-CM	Control conditioned Medium	6 h in NB-Medium	
LPS-CM	LPS conditioned Medium	6 h in NB-Medium containing 10 µg/ml LPS	
C-CM + LPS	Control conditioned Medium + LPS	6 h in NB-Medium + applying 10 µg/ml LPS to supernatant	
LPS-CM heat	LPS conditioned Medium heat inactivated	6 h in NB-Medium containing 10 µg/ml LPS thereafter supernatant is heated for 10 min at 60°C	
LPS-CM + antiTNFα	LPS conditioned Medium + antiTNFα	6 h in NB-Medium containing 10 µg/ml LPS	Addition of anti-TNFα (4 µg/ml) for last 4 h

LPS-CM + antiMIP-2	LPS conditioned Medium + antiMIP-2	6 h in NB-Medium containing 10 µg/ml LPS	Addition of anti-MIP-2 (4 µg/ml) for last 5 h

Table 2. Production of various conditioned media**.** The supernatants were removed, centrifuged, sterilized and stored at -20°C until use. The following drugs were used: LPS (10 µg/ml) (Sigma Aldrich); purified anti-mouse TNFα (4 µg/ml) (Biozol, Eching, Germany); monoclonal Anti-Macrophage Inflammatory protein-2 (4 µg/ml) (Sigma Aldrich).

3.1.7. Astrocyte cultures

1 h before preparation, culture flasks (T75) were precoated with poly-ornithin (100 µl in 10 ml HBSS$^{-/-}$) on table shaker and subsequently washed with HBSS$^{-/-}$. Shortly before plating the cells, flasks were washed with astrocyte medium.

Cultures of cortical astrocytes were prepared from P3 C57Bl/6 mice (**Figure 8 b**). The mice were decapitated and shortly dipped into 70% ethanol and medium. Scalp and skullcap were removed and hemispheres were placed in ice cold HBSS$^{-/-}$. Both hemispheres were isolated and the meninges and the bulbi olfactory were removed. The cortices were separated from the hippocampus, striatum and thalamic nuclei. The dissociation of the cortex was achieved by incubating the hemispheres in 0.05% trypsin/EDTA at a temperature of 37°C, 5% CO_2 and humidity of 95% for 20 min, after mechanical dissociation. Trypsinization was finally blocked by addition of HBSS$^{-/-}$ (Invitrogen) containing 10% horse serum. Cortices were further dissociated by repeated passages through a pipette blue tip cut to obtain a wider opening (3 mm) followed by a fire-polished Pasteur pipette. Cells were filtrated using an 80 µm pores size filter. Cells were centrifuged for 5 min at 1000 rpm and the cells were resuspended into astrocyte culture medium (MEM+10%HS) and transferred into T75 culture flasks. These cells are referred to as passage 0 ([P0] astrocytes. Cells are kept at 37°C, 5% CO_2 and humidity of 95% in the incubator. 24 h after preparation, cells were washed with HBSS$^{-/-}$ to remove cell debris and new media was added. Microglia and other small cells were removed through slight shaking of the culture flask. At a confluence of 80-90%, cells were trypsinized and seeded into new culture flasks. These cells are referred to as [P1] astrocytes. Cells were used at stadium [P3] for our experiments, were they have achieved 95% purity. Astrocytes were plated in 24 well plates (coated with poly-ornithin) at a density of 40,000 cells per well for immunostaining and Sholl analysis on cover slips. Fpr resazurin based *in vitro* toxicology assay kit (Alamar Blue assay) they were plated without cover slips.
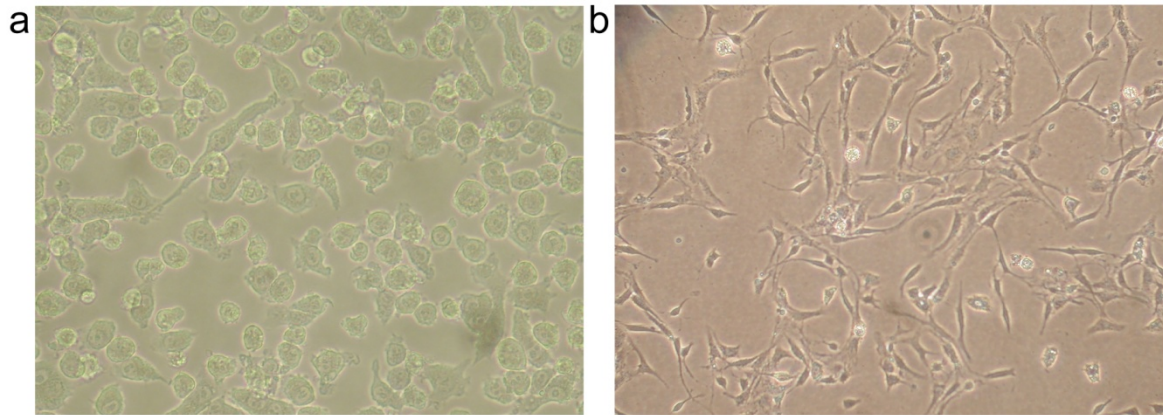
Figure 8. Light microscopic pictures of BV-2 cells and primary astrocytes. (**a**) BV-2 cells in culture medium reveal an amoeboid shape (**b**) Astrocytes of P3 mice direct after preparation.

3.1.8. Surgical preparation (***in cooperation with Jenq-Wei Yang and Shuming An***)

Extracellular recordings were performed in the barrel cortex of P3 to P5 rats using experimental protocols as described previously (Yang et al., 2009). Briefly, under deep ice-cooling anesthesia alone or combined with light intraperitoneal urethane injection (0.5-1 g/kg, Sigma-Aldrich, Taufkirchen, Germany), the head of a pup was fixed in a position that the dura was in parallel to the table. The bone, but not the dura mater, above the barrel cortex was removed carefully. Therefore, a 3 x 3 mm large part of the skull (S1, 0-3 mm posterior to bregma and 1.5-4.5 mm from the midline) was thinned using a driller and finally the residual bone was detached with the help of a very fine canula.

Afterwards, the body of the animals was surrounded by cotton and kept at a constant temperature of 37° C by placing it on a heating blanket. During recordings, urethane anesthesia (0.1-0.5x of original dose) was given when the pups showed any sign of distress. After 30-60 min recovery, Michigan-electrode (4x4, 16 channel electrode) were inserted perpendicularly into barrel cortex to obtain field potential (FP) recording (**Figure 9 a**). Neuropharmacological experiments were performed using a glass pipette (tip diameter: 30-40 µm) attached to a syringe. The tip of the pipette was positioned intracortically at a distance of 4-5 mm medial from the Michigan recording electrode (**Figure 9 b**). For intracortical drug injection LPS (10 µg in 2 µl PBS) or PBS was filled into glass pipette. After 40 min baseline control recording, 2 µl PBS or LPS was injected for 5-10 min. Spontaneous activity was recorded for 3 h following the injection of PBS or LPS. The activity recorded in the last 10 min of this 3 h

recording period was compared with the control activity recorded for 10 min before application of PBS or LPS.
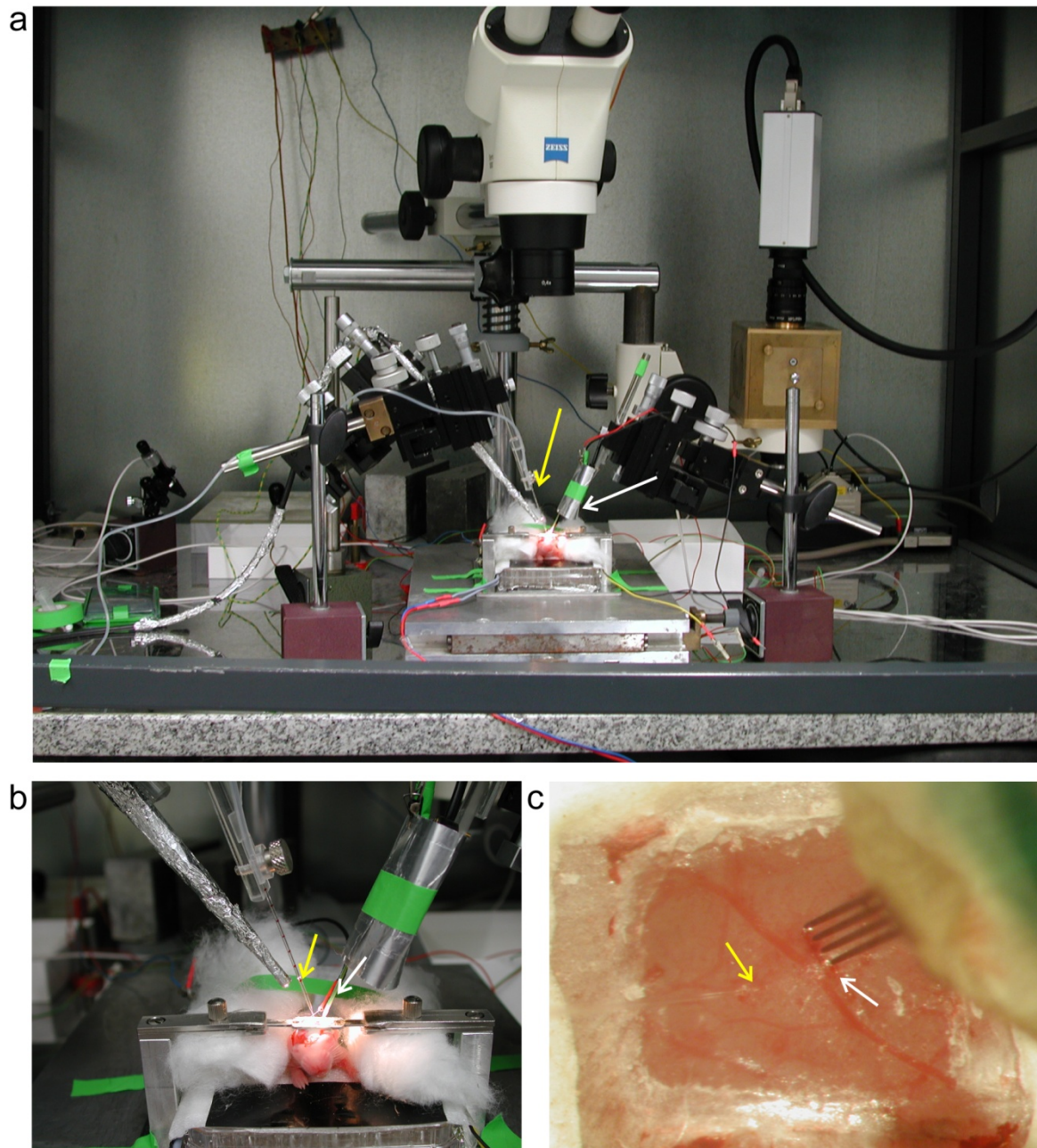
Figure 9. Experimental set up of an *in vivo* experiment. (**a**) Overview of the whole setup. White arrows in **a, b, c** indicate Michigan electrode (4x4, 16 channel electrode). Yellow arrows in **a, b, c** point at the fine glass pipette, used for applying LPS (10 μg in 2 μl PBS) or PBS, as control. (**b**) Rat pup surrounded by cotton and placed on a heating blanket after operation under urethane anesthesia. (**c**) Close-up view of an operated rat brain with Michigan electrode and glass pipette already inserted.

3.2. Staining and quantification

3.2.1. Immunostaining for activated caspase-3 and quantification of apoptotic cell death

An antibody directed against the cleaved active form of casp-3 was used (Asp175, Cell Signaling Technology Inc.) (Marin-Teva et al., 2004) to analyze the apoptosis rate of organotypic slices cultured with or without LPS application. After fixation of the organotypic slices with 4% paraformaldehyde (PFA), slices were rinsed in PBS, treated for 30 min with 0.1% Triton X-100 in PBS, and pre-incubated in 5% bovine serum albumin (BSA) in PBS for 2 h. Primary rabbit polyclonal antibody against activated casp-3 (Asp175, 1/400, Cell Signaling Technology Inc.) was incubated overnight at 4° C in 5% BSA + 0.1% Triton X-100 in PBS. Sections were washed in PBS and incubated with the secondary antibody (biotin-conjugated donkey polyclonal antibody directed against rabbit 1/400, Vector Laboratories) for 2 h at room temperature, then washed in PBS, and finally incubated with alexa488-conjugated streptavidin (Molecular Probes, Eugene, OR). After washing with PBS, sections were mounted on slides. For double staining with glial fibrillary acidic protein (GFAP), slices were immunostained for a-casp3 as described above and then fixed again with 4% PFA for 15 min. Immunostaining with rabbit polyclonal antibody directed against GFAP (1/400, Dako, A/S, Denmark) was then processed using the same protocol as for a-casp3.

Slices were analyzed using a confocal system (QLC100; Visitech, Sunderland, UK) attached to an upright Olympus microscope (BX 51 WI; Olympus, Tokyo, Japan). Immunostained whole cortex slices were observed at 600x (0.9 N.A., water immersion object, Olympus) magnification which corresponded to a field of view of 125 μm^2. Green and red fluorescence were excited through a mercury lamp at 488 nm (excitation filter: HQ 470/40) and at 568 nm (excitation filter: HQ 565/30). Apoptotic cells were counted in 18 fields (**Figure 10**) of view that were assigned to cover all cortical layers in 3 different regions of each slice. Because no significant differences between the regions and between the layers could be observed, the number of apoptotic cells from the 18 fields of view was averaged. For each field of view, the focus was manipulated to count cells in the whole depth of the slice. Permeabilization of the slice with Triton X-100 prior to immunostaining allowed the observation of positive cells in the depth of the slice. Using this standardized protocol, apoptotic cells were automatically counted with the Metamorph-program in

combination with ImageJ. Slices from at least 6 independent cultures were analyzed. The results are shown as percentage of the respective control condition (control is 100%).
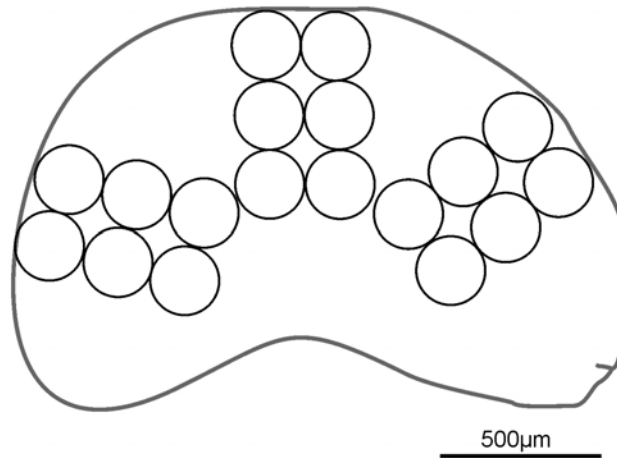
Figure 10. Template for analysis of a-casp-3 positive cells in organotypic slice cultures. Schematic representation of an organotypic slice cultures; circles indicate 18 areas of interest. These 18 fields were used to count the apoptotic cells and quantify them.

3.2.2. Immunostaining for GFAP-positive astrocytes - average intensity measurement

Organotypic neocortical slices were prepared from newborn (P0 and P1) C57Bl/6 mice and cultivated on membranes for 9 or 12 days, to analyze the amount of GFAP-positive astrocytes with or without LPS treatment.

Organotypic slice cultures were treated with LPS (10 µg/ml) or saline for 24 h before fixation (4% PFA) and GFAP staining (see above). GFAP positive astrocytes were counted in 18 fields of view that were assigned to cover all cortical layers in 3 different regions of each slice. Using this standardized protocol, average intensity was automatically counted with the Metamorph program. Slices from at least 6 independent cultures were analyzed. The results are shown as percentage of the respective control condition (control is set to 100%).

3.2.3. Immunostaining for GFAP and NeuN positive cells in dissociated neuronal culture

Antibodies directed against glial fibrillary acidic protein, GFAP and neuronal nuclei marker (NeuN) were used to quantify the number of astrocytes and neurons in dissociated neuronal cultures.

After fixation of the dissociated cells (14 DIV) with 4% PFA, cover slips were rinsed in PBS, treated for 30 min with 0.1% Triton X-100 in PBS, and preincubated in 5% bovine serum albumin (BSA) in PBS for 2 h. Primary rabbit polyclonal antibody against GFAP (1/400, Dako, A/S, Denmark) was incubated overnight at 4°C in 5% BSA + 0.1% Triton X-100 in PBS. Cells were washed in PBS and finally incubated with 1/800 Cy-2 (goat antibody directed against rabbit, 1/800, Dianova) for 2 h. For double staining with NeuN: Cells on cover slips were fixed again with 4% PFA for 15 min and afterwards washed again with PBS. Cover slips were preincubated in 3% BSA in PBS for 2 h. Primary antibody directed against NeuN (1/100, Chemicon) was incubated over night, washed 3 times in PBS and incubated with AlexaRed568 (goat antibody directed against mouse,1/400,Molecular Probes) for at least 2 h. After washing with PBS, sections were mounted on slides. Slices were analyzed by using a confocal system and the Metamorph program.

3.2.4. Immunostaining for CD14 receptor on various cell types

Antibodies directed against CD14, a receptor necessary for LPS recognition and propidium iodide (PI), a cell nucleus marker, were used, to distinguish on which cell types CD14 receptors are expressed in our experimental conditions.

Primary astrocytes, dissociated neurons and BV-2 cells were fixed with Aceton, rinsed in PBS, treated for 30 min with 0.1% Triton X-100 in PBS, and pre-incubated in 5% BSA in PBS for 2 h. Primary goat polyclonal antibody raised against a peptide mapping at the C-terminus of CD14 of mouse origin (1/50, Santa Cruz) was incubated over night at 4°C in 5% BSA + 0.1% Triton X-100 in PBS. Cells were washed and incubated with 1/200 anti-goat-biotin (Vector) for 2 h, washed 3 times with PBS and finally incubated with Streptavidin-Alexa488 1/400 (Molecular Probes) for an additional hour.

For double staining with PI, cells were washed with PBS 0.01 M after 15 min. fixation with PFA (4%). Cover slips were incubated with propidium iodide (1/400, Sigma Aldrich) for 10 min, washed 3 times with PBS and mounted on slides. Cover slips were analyzed as above using a confocal microscope system and the Metamorph program.

3.2.5. Live cell staining on various cell types, on which cells does LPS (conjugated with Alexa-488) bind?

Fluorescent conjugates of LPS coupled to AlexaFluor-488 were used (Molecular Probes), to find out onto which cell types LPS binds.

Neurons, astrocytes and microglia were mounted on cover slips and rinsed with HBSS$^{-/-}$ before experiments Medium containing the liposomes is pre-warmed to 37°C and cells are incubated for 1 h at 37°C with this solution (6 µg/ml). As control, all cell types were stained via Calcein red-orange (Acetoxymethyl and Acetate Esters, 1/200, Invitrogen) which is able to permeate the cell membranes and fluorescents at 568 nm. It was applied 30 min before samples were washed in appropriate medium. Cover slips were transferred into HBSS^{+++}, immobilized in an analysis chamber (Luigs and Neuman) and kept at 37°C via temperature control system (Luigs and Neuman) for the life cell analyzes. Cover slips were analyzed by using Metamorph program.

3.2.6. Immunostaining for GFAP-positive astrocytes - Sholl-analysis

P3 astrocytes were seeded at a density of 100,000 cells/ml on poly-ornithin coated cover slips in 24 well plates, to measure the number of processes with or without LPS application.

We let the cells attach for one day before they were treated for 24 h with LPS-CM (10 µg/ml) or C-CM. They were fixated with 4% PFA and stained with GFAP antibodies.

For analysis, pictures of single astrocytes were taken with the confocal microscope and converted into ImageJ files. Quantification of astrocytes was performed by counting the number of process intersections for concentric circles, centered at the centroid of the cell body, of gradually increasing radius. A specialist circle template with interspaces of 10 µm was used to count the intersections per circle and compare LPS treated astrocytes with control conditioned cells.

3.3. Molecular biology

3.3.1. Extraction of the mRNA

Per trial, two organotypic cortex slices of MEA experiments (see below) were used (control or LPS-treated for 1.5 h), to extract RNA. For extraction the High Pure Tissue Kit was utilized (Roche Applied Science). First the slices were homogenized by using a tissue ruptor, succeeded by mRNA extraction, following the company protocol.

The RNA purity was quantified photometrical, by calculating the absorption of the sample: $A_{260/280}$ and $A_{260/230}$.

3.3.2. Transcription of the RNA

The extracted RNA of the probes was purified with an RNeasy Mini Kit (Quiagen) following the company protocol. 1 µg of RNA was used for transcription. The high fidelity cDNA synthesis kit (Roche Applied Science) was used. We used random hexamer primer. The transcription reaction was carried out at 50°C for 30 min and the enzymes were inactivated through 85°C heating.

3.3.3. Realtime PCR (RT-PCR)

The cDNA was diluted 1:10 and the LightCylcer TaqMan Master kit (Roche) was used. This kit is based on the application of probes (Universal Probe Library (Roche Applied Science)). By using the probe library website, primers for each gene of interest were constructed (**Table 3**). The primers consist of a short DNA sequence, to which a fluorescent labeled probe can bind. Probe and primer accumulate to the degenerated DNA. The used polymerase contains a hydrolysis function - the probe is hydrolyzed during the elongation phase. The quencher is separated from the fluorophor and the probe fluoresces. This signal can be detected by the Light Cycler (Roche). The more DNA the stronger the signal is. The crossing point (Cp) is the cycle of the RT-PCR in which the fluorescence signal is stronger than the background signal. The relative gene expression was quantified by using the ΔΔCp method. Per reaction 2.0 µl cDNA were used. β–actin was chosen as reference.

Table 3

gen	forward primer	reverse primer	probe
IL-6	TCTAATTCATATCTTCAACCAAGAGG	TGGTCCTTAGCCACTCCTTC	78
IL-1β	TGTAATGAAAGACGGCACACC	TCTTCTTTGGGTATTGCTTG G	78
TNFα	CTGTAGCCCACGTCGTAGC	TTTGAGATCCATGCCGTT G	78
INF-γ	GGAGGAACTGGCAAAAGGAT	TTCAAGACTTCAAAGAGT CTGAGG	21
actin-β	TGACAGGATGCAGAAGGAGA	CGCTCAGGAGGAGCAATG	106

Table 3. Primer sequences. Primers used for the mentioned RT-PCR are listed here.

3.3.4. Western blot analysis after in vivo LPS application

Following the same surgical procedure as described above, without insertion of electrodes, barrel cortex was injected with either PBS or LPS (5 mg/ml). 6 hours later tissue was removed via a skin puncher (∅ 1 mm) and Western blot analysis was implemented. 3 control and LPS treated tissue samples were pooled and lysed in 125 µl extraction buffer (50 mM Tris-HCL pH7.4; 1% (v/v) Triton X-100; 150 mM NaCl; 1 mM EDTA) for 2 hours on ice. Nuclei and cellular debris were centrifuged at 5000g for 5 min at 4°C and the protein concentrations of the supernatants were determined using the BCA test (Pierce) according to the manufacturer's instructions. Organotypic slices (8 DIV) of P0 mouse brains, treated with staurosporin (100 nM for 24 h), were used as positive control. Slices were homogenized via a tissue ruptor and lysed in 300 µl extraction buffer for 1 hour on ice. Tissue was centrifuged at 9300 g for 10 min at 4°C and protein concentration of the supernatant was determined as described above. 20 µg of the samples were separated by SDS PAGE on precast 4-20% Ready gels (Biorad) and transferred to PVDF Blotting membranes over night. Membranes were blocked in TBS 0.01% (v/v) Tween 20 containing 4% (w/v) Milk. Antibodies directed against cleaved casp-3 (1:1000, Cell signaling) and GAPDH ((1:5000), Bethyl laboratories) were incubated at room temperature in blocking buffer for 4 hours or 1 hour, respectively, and detected with horseradish peroxidase-coupled secondary antibodies (Dianova) in an enhanced chemiluminesence reaction. Images were acquired with a ChemiDoc™ XRS+ System (Bio-Rad) and band intensities were quantified using Image lab software (Bio-Rad).

3.4. Electrophysiology

3.4.1. MEA electrophysiological recording in organotypic slice cultures

Electrophysiological recordings of neuronal network activity in 5-7 DIV organotypic slice cultures were performed with 3-D multi-electrode arrays (MEA, 200 μm inter-electrode spacing, electrode resistance 600-900 kOhm.; Ayanda Biosystems, Lausanne, Switzerland) (**Figure 11**) put on MEA 1060-INV-BC interface (Multi Channel System, Reutlingen, Germany), which was mounted on an inverted microscope (Optica, microscopes, Bergamo, Italy) equipped with a digital camera (Nikon Coolpix 4500, Tokyo, Japan). Slices were kept in artificial cerebrospinal fluid (ACSF) that resembled the ionic and molecular composition of the NB medium without B27 (Brewer et al., 1993) (in millimolar): 51.3 NaCl, 26 $NaHCO_3$, 0.9 NaH_2PO_4 H_2O, 0.812 $MgCl_2$ 6 H_2O, 1.8 $CaCl_2$, 5.36 KCl, 25 D-glucose, 10 (N-[2-hydroxyethyl]-piperazine-N´-[2-ethanesulfonicacid]) sodium salt, 0.23 sodium pyruvate, 0.5 L-glutamine, 0.4 glycine, 0.4 L-serine, 0.02 L-alanine, 0.028 choline chloride, and 0.2 μM $Fe(NO_3)_3$ H_2O equilibrated with 95% O_2/5% CO_2 (pH 7.4; osmolarity 205 mOsm). For a good contact between the slices and the electrodes, a 100 mg anchor, made by stainless steel and nylon lines, was used. Slices were continuously perfused at a rate of 2-3 ml/min at a temperature of 28°C. Spontaneous network activity was recorded in control slices and in LPS treated slices, which were exposed to 10 μg/ml LPS after recording network activity for 1.5 h under control conditions. Field potentials were recorded simultaneously with 60 extracellular electrodes at a sampling rate of 1 kHz using the MC_RACK software (Multi Channel Systems, Reutlingen, Germany). Data were imported to a custom program in Matlab version 7 (Mathworks, Natick, MA, USA) using the MC-Rack libraries (MC_Rack, Multi Channel Systems). Field potentials were plotted and the occurrence and duration of oscillations were calculated. Occurrence and duration were quantified by counting the number and duration of spontaneous network oscillations for 1.5 h at control conditions and comparing them to number and duration of oscillations following 1.5 h LPS application.
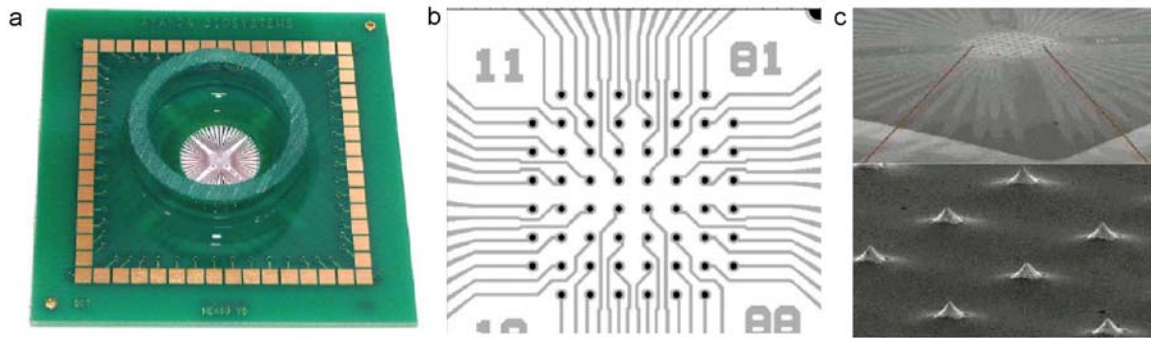
Figure 11. 3-D MEA chip. Every 3-D MEA has 60 micro-electrodes with an electrode spacing of 200 µm, electrode high of 50-70 µm and electrode dimension of 40 µm x 40 µm. (**a**) shows picture of whole 3-D MEA, (**b**) schematic illustration of the electrodes and connections to the motherboard, (**c**) triangle shaped electrodes (3-D). Picture adapted from http://www.ayanda-bioscy.com.

3.4.2. MEA recording of primary cell culture

The electrophysiological recordings of the dissociated neuronal cultures were performed after 14 DIV in NB/B27 medium using the 60 channel planar MEA (30 µm diameter with 200 µm spacing; MCS, Reutlingen, Germany) (**Figure 12 a**), with a sampling rate of 25 kHz and a 100 Hz high-pass filter. MC_RACK software (Multi Channel Systems) was used for data acquisition and online spike detection. Spikes were detected using a threshold-based detector set to a threshold of 7 times the standard deviation of noise level. After 1 h recording under control condition, 100 µl of the NB/B27 medium was exchanged with 100 µl of the conditioned medium (see **Table 1**) and the network activity was recorded for another hour. Dissociated cultures were perfused with 95% O_2/5% CO_2 during the whole experiment and kept at 28°C, which was monitored by a temperature control unit (TCO2, MCS). The MEA-chips were sealed during the experiment with a lid, to keep the pH value (**Figure 12 b**). Signals were obtained simultaneously from 59 electrodes with a sampling rate of 25 kHz and a 100Hz high-pass filter. Spike activity was recorded and network bursts and spike number were quantified.

Data were again imported to a custom program in Matlab version 7 (Mathworks, Natick, MA, USA) using the MC-Rack libraries (MC_Rack, Multi Channel Systems). When potentials exceeded a threshold of 7 times the standard deviation (SD) of noise levels, spike waveforms were taken into account.

For analysis we compared the burst index of various experimental setups. The burst index was defined as BI = (f_{15} − 0.15)/0.85 (Wagenaar et al., 2005) and normalized between 0 (no burst) and 1 (all spikes in burst). The binary data of the spike trains

were divided into bins of 2 s in size and summed up the number of spikes in each bin. f_{15} was derived from the total number of spikes by the number of spikes in the first 15% of sorted bins. When most spikes occurred in burst, this fraction, f_{15} was close to 1. If spikes were sparsely distributed in time, f_{15} was close to 0.15.

To detect synchronized bursting events we scanned the binary date in consecutive windows of 2 s. Each window was divided into bins of 200 ms in size. Only events with more than five active neurons, and a gap of 5 s between the previously found synchronized bursting event were taken in account (Raichman and Ben Jacob, 2008). Generally a burst is defined as a synchronized event, where several neurons fire in a relatively short time.
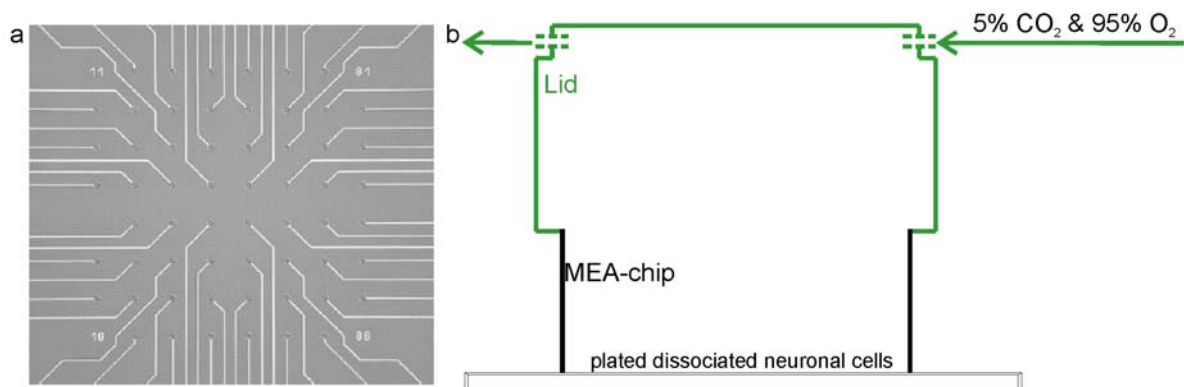
Figure 12. Planar MEA and chamber for long term recording. (**a**) The planar MEA (200/30iR-ITO-gr) has 59 recording electrodes and one internal grounding electrode. The electrode spacing is 200 μm and the electrode diameter is 30 μm. Picture adapted from http://www.ayanda-bioscy.com. (**b**) Chamber designed for long-term recording of cell culture on planar MEA. MEA chip (black color) is sealed with a lid (green color) for maintaining a constant pH value. 5% of CO2 and 95% of O2 was supplied.

3.4.3. In vivo *data analysis*

In vivo data were imported and analyzed offline using MATLAB software version 7.7 (Mathworks, Natick, MA). Spontaneous events were detected as FP deflections exceeding five times the baseline standard deviation (SD). Only events lasting >100 ms and containing more than 3 cycles were considered for analysis. The events were analyzed in their occurrence, duration, amplitude (voltage difference between the maximal positive and negative peak), maximal frequency within each event, and relative frequency fraction corresponding to the theta (4-8 Hz), alpha (8-13 Hz), beta (13-30 Hz) and gamma (30-80 Hz) frequency bands and analyzed in their occurrence, duration, amplitude and maximal frequency within each event. These

field potential oscillations were combined to spindle bursts and gamma oscillations. The dominant frequency of spindle bursts ranges in alpha. Gamma oscillations consisted of gamma bands (Yang et al., 2009). To detect the oscillatory events, the raw data were filtered between 5 to 30 Hz (spindle bursts) and 30 to 80 Hz (gamma oscillations) respectively using a Butterworth 3-order filter. Oscillatory events were detected as FP deflections exceeding five times the baseline SD. Only events lasting >100 ms and containing more than 3 cycles were considered for analysis.

3.5. Cell biological methods

3.5.1. Resazurin based in vitro toxicology assay kit (Alamar Blue assay)

To measure cell viability of dissociated neuronal cultures, BV-2 cells or astrocytes, culture medium was replaced by conditioned medium for 1, 2 or 6 h. After incubation time, medium was replaced with 200 µl Alamar Blue stock solution diluted 1:60 with HBSS^{+++}. Alamar Blue (AB) is a tetrazolium-based dye, incorporating resazurin and resorufin as oxidation–reduction indicators that yield colorimetric changes and a fluorescent signal in response to metabolic activity. The blue non-fluorescent oxidized form becomes pink and fluorescent upon reduction through metabolic active cells in the cultures. Alamar Blue and cultures were incubated for various periods at 37°C, 5% CO_2. Cell viability was measured 1, 3 and 6 h after Alamar Blue application in a Tecan plate reader (Tecan GmbH, Crailsheim, Germany) with excitation wavelength of 540 nm and the emission at 595 nm.

Cells were seeded into 24 or 96 well plates: DIV14 dissociated neuronal cultures, P3 astrocytes or BV-2 microglial cells. BV-2 cells at a density of 25,000 cells per well, astrocytes at a density of 40,000 cells per well and neurons at a density of 200,000 cells per well. 1, 2 or 6 h after conditioned medium treatment, media was exchanged for 400 / 200 µl Alamarblue solution (1:60). The plates were measured via Tecan plate reader. Plates were returned to the incubator after every measurement and the fluorescence was measured at 1, 3 and 6 h. Since the survival rate was not altered between 3 and 6 h, only data measured at 3 h are shown. The relative survival rate was normalized to control conditions.

3.5.2. Measurements of cytokine levels.

The release of cytokines in C-CM and LPS-CM was measured with a mouse cytokine array panel A array kit (R&D System, Minneapolis, USA). The assay was performed according to manufacturer´s protocol. Briefly capture antibodies directed against various cytokines are spotted in duplicate on nitrocellulose membranes. Cell culture supernatants are diluted and mixed with biotinylated detection antibodies. The sample/antibody mixture is then incubated with the Mouse Cytokine Array membrane. Any cytokine/detection antibody complex present is bound by its cognate immobilized capture antibody on the membrane. Following a wash to remove unbound material, Streptavidin-HRP and chemiluminescent detection reagents are added sequentially. Light is produced at each spot in proportion to the amount of cytokine bound.

3.5.3. Nitrite measurement in vitro (Griess reagent modified)

One possibility to investigate NO formation is to measure nitrite (NO_2^-), which is one of two primary, stable breakdown products of NO. The Griess assay is a colorimetric assay to measure the levels of nitrite in aqueous solutions. The assay relies on a diazotization reaction that was originally described by Griess in 1879 (Griess P., 1879). BV-2 cells were seeded into 24 well plates at a density of 20,000 cells per well and treated for 24 h with LPS (10 µg/ml) or saline. Nitrite release (µM) was measured via Griess reagent. Equal volume of 1x Griess reagent and sample are mixed and the absorbance is read in a plate reader at 540 nm after 15 min incubation time. By using a calibration curve values can be calculated (µM range).

3.5.4. ROS detection in vitro

For ROS detection BV-2 cells were seeded into 24 well plates at a density of 20,000 cells per well and incubated for 2 days in RPMI-media before use. For experiments media was exchanged to NB-Medium (without serum) containing LPS (10 µg/ml) or saline. After 6 h incubation time media was exchanged for HBSS^{+++} containing DCFH [(2´7´dichlorodihydrofluorescein), Sigma] and 1 µM Calcein red orange (Invitrogen). Calcein red orange was used to normalize DCF values to cell number. DCFH is oxidized by ROS to DCF, which is fluorescent. 10 µM DCFH are added to HBSS^{+++} and cells are incubated for 20 min at 37°C, supernatant is removed and plate is measured immediately on Tecan plate reader with an excitation of 485 nm and an

emission of 535 nm, for ROS detection and 540 nm and 595 nm for Calcein red orange detection.

3.5.5. Statistics.

For statistical analyses, we used Student´s t-test when distribution was Gaussian and Mann-Whitney test for non Gaussian distribution. For comparing different groups we used one-way ANOVA followed by Tukey-test when the distribution was Gaussian and Kruskal-Wallis followed by Dunns test when the distribution was not Gaussian. All data are expressed as mean $\pm$ standard error of the mean and statistically significant differences are indicated by * ($p<0.05$), ** ($p<0.01$) and *** ($p<0.001$).

4. Results

4.1. Microglia cell line BV-2 specifically binds LPS in vitro

In previous studies microglia were shown to be the only cells in the central nervous system to react on the inflammatory stimulus via lipopolysaccharide, while primary astrocytes and neurons don´t. To prove that in our model system, we prepared BV-2 cell cultures, purified cultures of astrocytes (both at a density of 40,000 cells/well) and neuronal dissociated cultures (density of 20,000 cells/well) on mounted cover slips and cultivated them for 2 days (BV-2 and astrocytes) and 14 days (neurons) respectively.

To study LPS binding in the CNS we used fluorescently tagged LPS (see Material and Methods: LPS conjugated with Alexa-488) to identify the LPS-binding cells. BV-2 cells, primary astrocytes ([P3]) and primary dissociated neuronal cultures were incubated with LPS-Alexa-488 at a concentration of 6 µg/ml for 1 h. As control, all cell types were stained with Calcein red-orange, which is able to permeate the cell membranes and emits light at 568nm. It was applied 30 min before the samples were washed in appropriate medium and immediately visualized by fluorescence microscopy. Microglia showed a strong double labeling with LPS-488 and Calcein red-orange, indicated with white arrows (**Figure 13 a**), while primary astrocytes (**Figure 13 b**) and dissociated neuronal cultures (**Figure 13 c**) showed only Calcein red orange labeling.
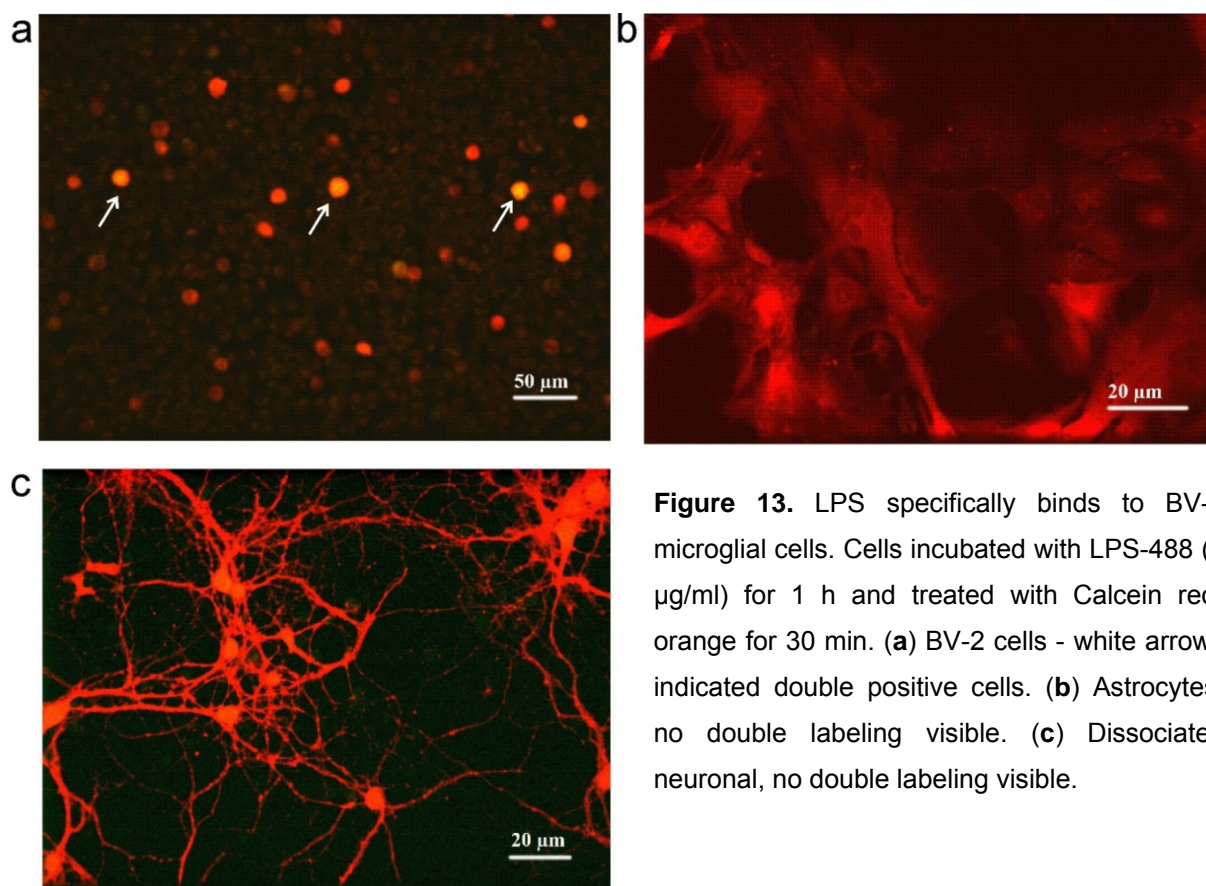
Figure 13. LPS specifically binds to BV-2 microglial cells. Cells incubated with LPS-488 (6 µg/ml) for 1 h and treated with Calcein red-orange for 30 min. (**a**) BV-2 cells - white arrows indicated double positive cells. (**b**) Astrocytes, no double labeling visible. (**c**) Dissociated neuronal, no double labeling visible.

4.2. BV-2 cells express the CD14 receptor

CD14 and TLR-4 receptors are required for the molecular and cellular effects of LPS on circulating monocytes (Means et al., 2000). It is also know that microglia cells express CD14 and TLR-4 (Becher et al., 1996;Lehnardt et al., 2002). We wanted to determine if CD14 receptors can be found on BV-2 cells or other CNS cells in our experimental set up. To demonstrate the distribution of CD14 receptors we used cells grown on cover slips and labeled them with CD14 receptor antibody and propidium iodide, which was used to visualize the nucleus of the cells. **Figure 14 a** shows that the microglia cell line BV-2 expresses CD14 receptors while on astrocytes and dissociated neuronal cultures we could not detect CD14 receptors.

Figure 14. CD14 receptors were only expressed on BV-2 cells. (**a**) Double labeling of microglial cell line BV-2, with CD14-receptor antibody (green) and PI (red). (**b**) Negative control without CD14-receptor staining.

4.3. Nitric oxide release following LPS stimulation
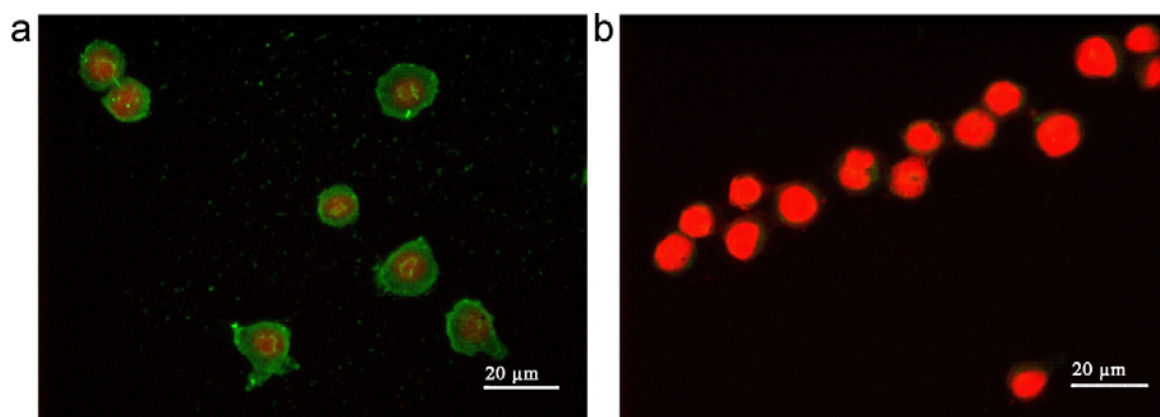
NO is released from the microglial cell line BV-2 and organotypic cultures following exposure to 10 µg/ml LPS (**Figure 15**). The nitrite release (NO_2^-), which is the terminal product of NO oxidation was measured in culture media via Griess assay. In these experiments BV-2 cell cultures or organotypic slice cultures (DIV12) were treated with 10 µg/ml LPS for 24 h. The media was removed and assessed for nitrite secretion. BV-2 cells increased nitrite release after 24 h LPS treatment from 0.59 ± 0.122 to 6.068 ± 0.337 (n=7, p<0.0001) (**Figure 15 a**). Similar to BV-2 cells, organotypic slice cultures also increased nitrite release into the culture media following 24 h LPS exposure from 1.16 ± 0.06 (n=7) to 1.88 ± 0.34 (n=6, p<0.05) (**Figure 15 b**).

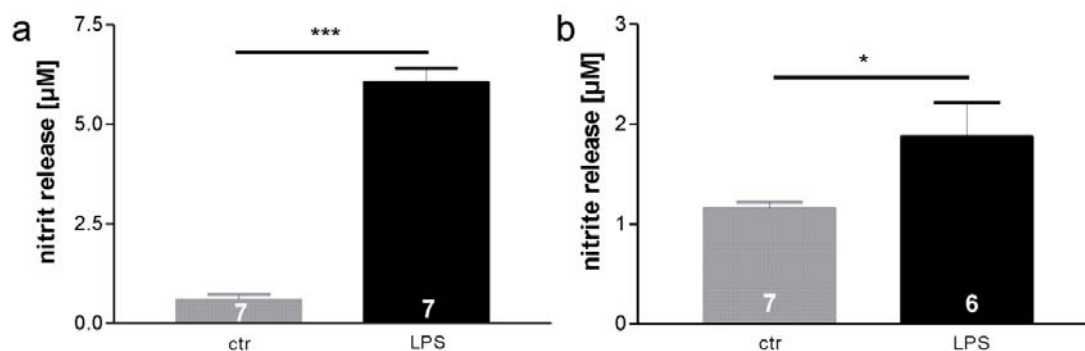**Figure 15.** Microglia and organotypic slice cultures release NO upon LPS treatment. (**a**) BV-2 cells (5 x 10^4 cells/ml) have an increased nitrite release after 24 h of LPS (10 µg/ml) treatment. (**b**) Organotypic culture (DIV12) treated for 24 h with LPS showed increased nitrite values. In this and the following figures data are presented as mean +/- SEM and the number of cultures is indicated in the bars.

4.4. Microglial activation leads to release of ROS

Microglial produced ROS is known to trigger the deleterious cascade of events in inflammation related processes (Gao et al., 2002). Therefore we wanted to characterize the LPS-induced microglial activation by measuring the levels of reactive oxygen species (ROS) released from activated microglia cell cultures. We used again the microglial cell line, BV-2 and seeded the cells into 24 well plates at a density of 20,000 cells per well. After attachment, cultures were treated 6 h or 24 h with LPS or saline. ROS was detected via DCFH oxidation and cell number was measured by using Calcein red orange. DCFH-DA enters cells passively and is deacetylated by esterase to non-fluorescent DCFH. DCFH reacts with ROS to form the fluorescent product DCF. The Calcein red orange signal was used to normalize DCF values to cell numbers. Values of control cultures were set to 100% and we could observe that LPS-induced a significant increase of ROS in BV-2 cells treated with 10 µg/ml LPS for 6 h (**Figure 16 a**) from 100 ± 7.02% to 124.4 ± 4.78% (n=9, p<0.01) and a significant increase from 100 ± 9.53% to 145.1 ± 7.30% (n=8, p<0.01) after 24 h LPS treatment (**Figure 16 b**).
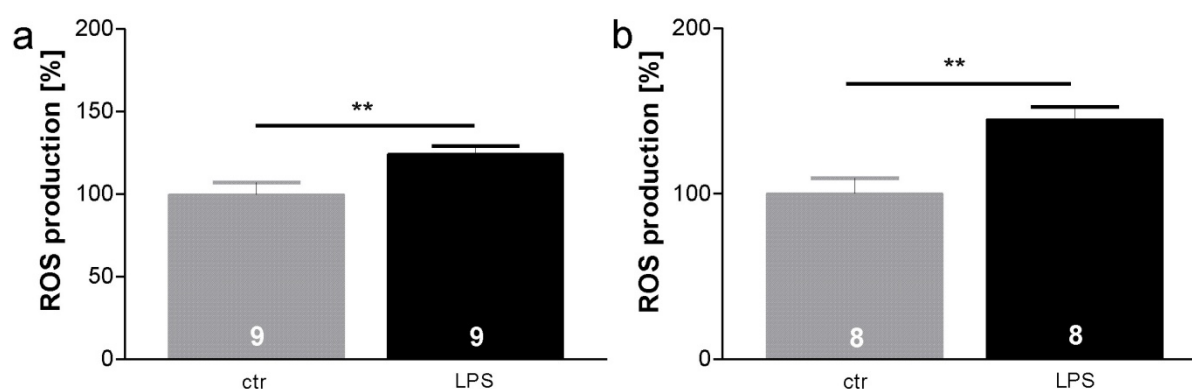
Figure 16. Microglial activation through LPS leads to increased ROS production. (**a**) ROS production of BV-2 cells after 6 h treatment with LPS (10 µg/ml). (**b**) ROS production of BV-2 cells after 24 h of LPS treatment.

4.5. No influence of LPS on the survival rate of BV-2 cells, HT-22 cells or astrocytes

To investigate the direct effect of LPS on the survival rate of different CNS cell types, we seeded the microglial cell line BV-2, the neuronal cell line HT-22 and primary astrocytes into 24 or 96 well plates and treated them with 10 µg/ml LPS for one to three hours. Control cultures were treated with saline for equal time (**Figure 17**).

Survival rate was quantified using a resazurin-based *in vitro* toxicology assay kit (Alamar Blue assay). Alamar Blue (AB) is a tetrazolium-based dye, incorporating resazurin and resorufin as oxidation-reduction indicators that yield colorimetric changes and a fluorescent signal in response to metabolic activity. Control experiments were set to 100% and differences to LPS treated cells were calculated.

After 1 or 3 hours LPS alone neither induce changes in the survival rate of BV-2 cells (n=4, p>0.05) (**Figure 17 a**) nor in the neuronal cell line HT-22 (n=12, p>0.05) (**Figure 17 b**). Primary astrocytes treated with 10 µg/ml LPS showed same results as BV-2 cells or HT-22 cells after 1 or 3 hours (n=3, p>0.05) (**Figure 17 c**). To see whether soluble factors, released from LPS-activated microglia cells, can influence survival of primary astrocytes we also tested conditioned medium of microglia (C-CM or LPS-CM; see Material and Methods). We observed a significant increase in the survival rate after 1 h, raising from 100 ± 1.32 to 106.0 ±1.65 (n=5, p<0.01) and a significant increase in the survival rate after 3 h LPS-CM treatment from 100 ± 1.1 to 105.2 ± 1.23 (n=5, p<0.01) (**Figure 17 d**).
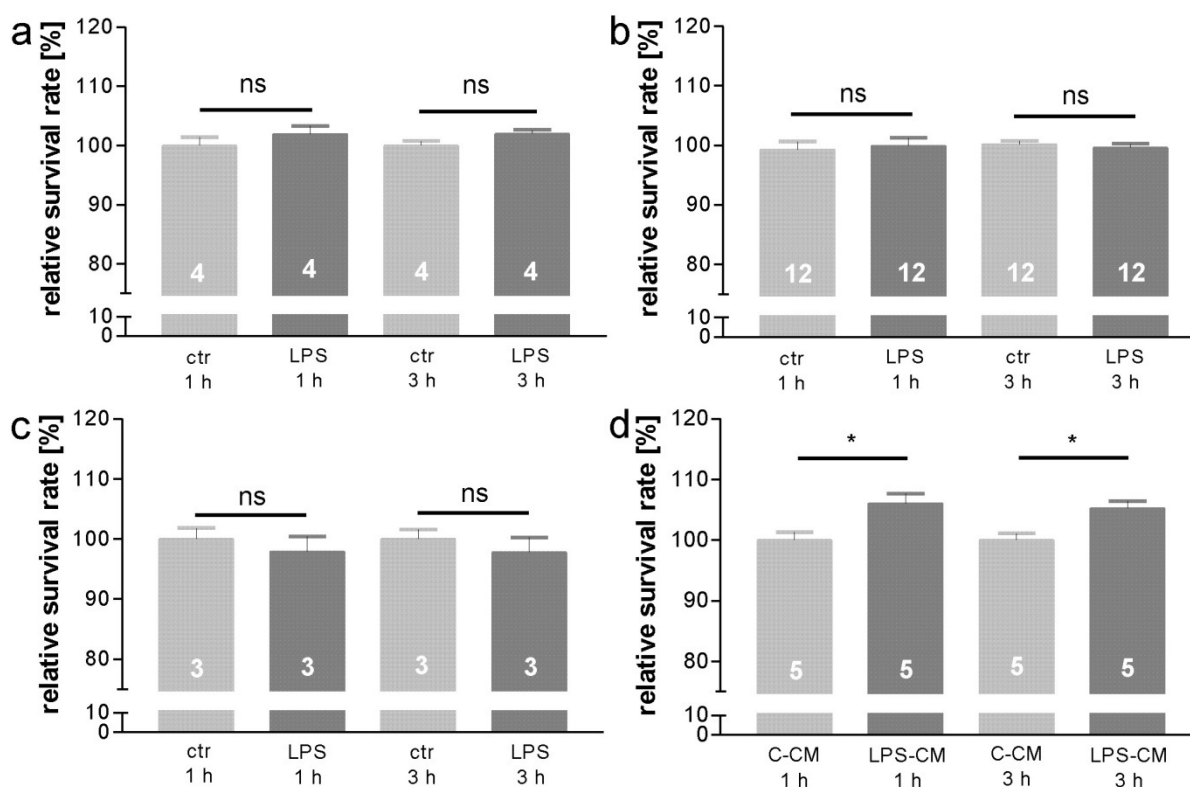
Figure 17. Influence of LPS-treatment on survival rate of various cell types. (**a**) BV-2 cells treated with LPS (10 µg/ml) for 1 or 3 h. (**b**) HT-22 cells treated with LPS (10 µg/ml) for 1 or 3 h. (**c**) Astrocytes treated with LPS (10 µg/ml) for 1 or 3 h. (**d**) Astrocytes treated with LPS-CM or C-CM medium for 1 or 3 h.

4.6. LPS conditioned microglia medium leads to astrogliosis

As we have observed an influence of LPS-conditioned microglia medium on survival rate of primary astrocytes (**Figure 17 d**) we also wanted to address the question if LPS-CM also leads to astrogliosis on primary astrocytes.

Reactive astrogliosis is a characteristic response of astrocytes to inflammation of the CNS and usually microglial activation is accompanied by astrogliosis (Sriram et al., 2006). To determine the increase in processes of astrocytes we used the Sholl-analysis method, which is normally used for morphometric neuronal studies (Milosevic and Ristanovic, 2007). Purified primary astrocytes were seeded at a density of 40,000 cells per well on poly-ornithin coated cover slips and treated with control conditioned medium (C-CM) or LPS-conditioned medium (LPS-CM) for 24 h. After immunostaining with GFAP antibody, confocal microscope pictures were taken and analyzed via Metamorph and ImageJ program. Quantification of astrocytes was performed by counting the number of process intersections with the concentric circles, centered at the centroid of the cell body, of gradually increasing radius. A circle template with interspaces of 10 μm was used to count the intersections per circle and C-CM and LPS-CM treated astrocytes were compared. Quantification of the various treatments shows a significant increase of processes at 30 μm (n=3, p<0.01) (**Figure 18 c**).
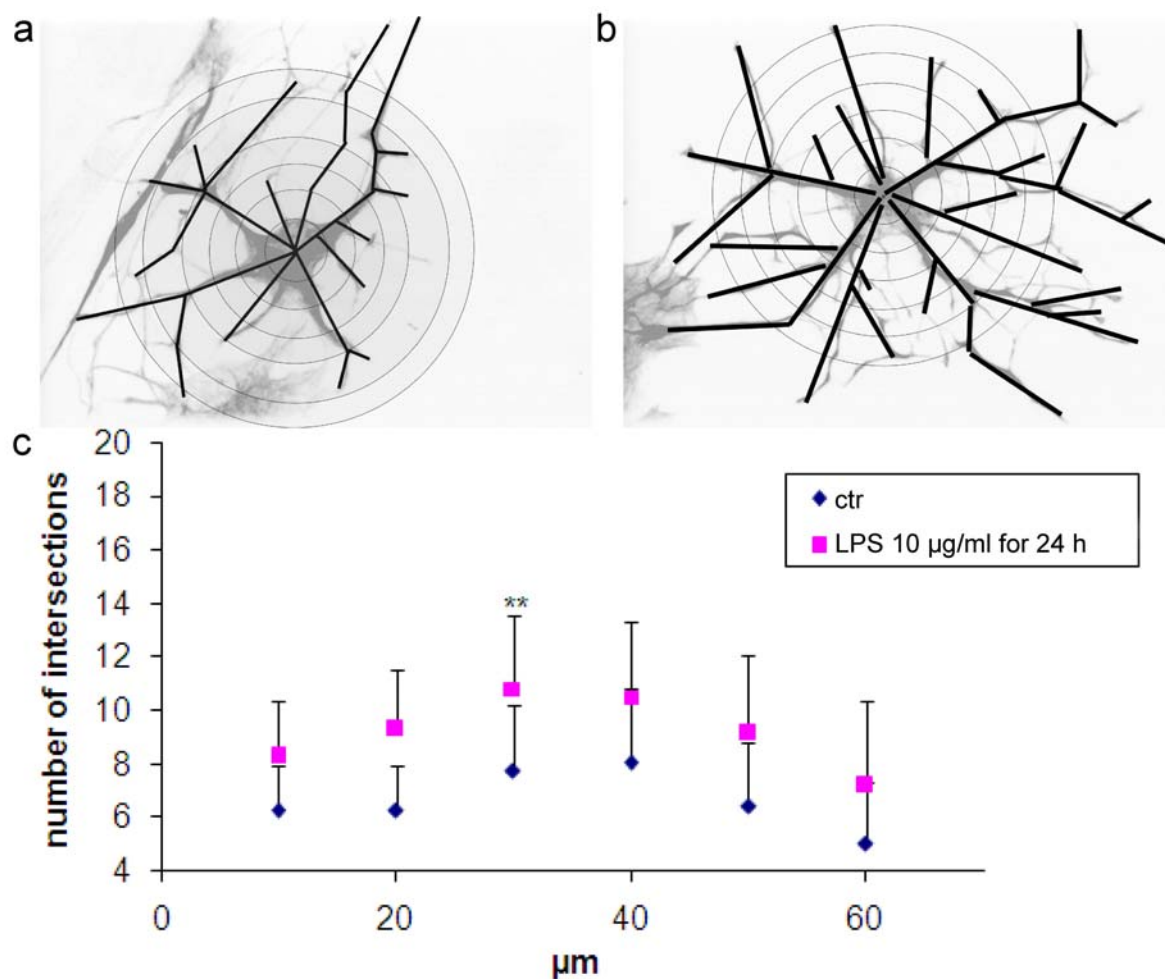
Figure 18. LPS treatment for 24 h leads to astrogliosis in primary astrocytes. (**a**) Picture of astrocyte with circles, taken for calculation of process intersections under control conditions. (**b**) Astrocytes processes 24 h after LPS application. (**c**) Quantitative calculation of intersections per µm.

4.7. LPS leads to astrogliosis in organotypic slice cultures

In order to study the astrogliosis effect under more physiological conditions we used organotypic slice cultures. Organotypic slices from P0-P1 mice were prepared and cultivated for 8 to 11 days. To investigate the influence of LPS on astrogliosis we treated the slices with saline or LPS (10 µg/ml) for 24 h. After immunostaining with GFAP antibody, confocal microscope pictures (600x magnification) were taken and average intensity was measured via Metamorph program at 18 fields of interest, following the schema for the analysis of a-casp-3 positive cells (see Material and Methods). **Figure 19 a** shows a control treated slice with low amount of average intensity. **Figure 19 b** shows an organotypic slice culture after 24 h LPS treatment and illustrates increased average intensity staining over the whole filed. Quantification of the average intensity in % revealed what was already observed in

Figure 19 a, b. LPS led to an increase of astrocytes branches and therefore an increase in the average intensity from 99.99 ± 1.08 to 124.3 ± 2.09 (n=10; 7, p<0.0001) at 9 DIV and 100 ± 1.57 to 137.5 ± 2.27 at 12 DIV (n=7/6, p<0.0001) (**Figure 19 c**).

Figure 19. LPS leads to increased astrogliosis in organotypic slice cultures. All cultures were stained via GFAP antibodies. (**a**) Organotypic culture treated for 24 h with saline. (**b**) Culture treated with LPS (10 µg/ml) for 24 h (bars = 20 µm). (**c**) Average intensity measurements show increased astrogliosis in DIV 9 and DIV 12 organotypic cultures, after LPS treatment.
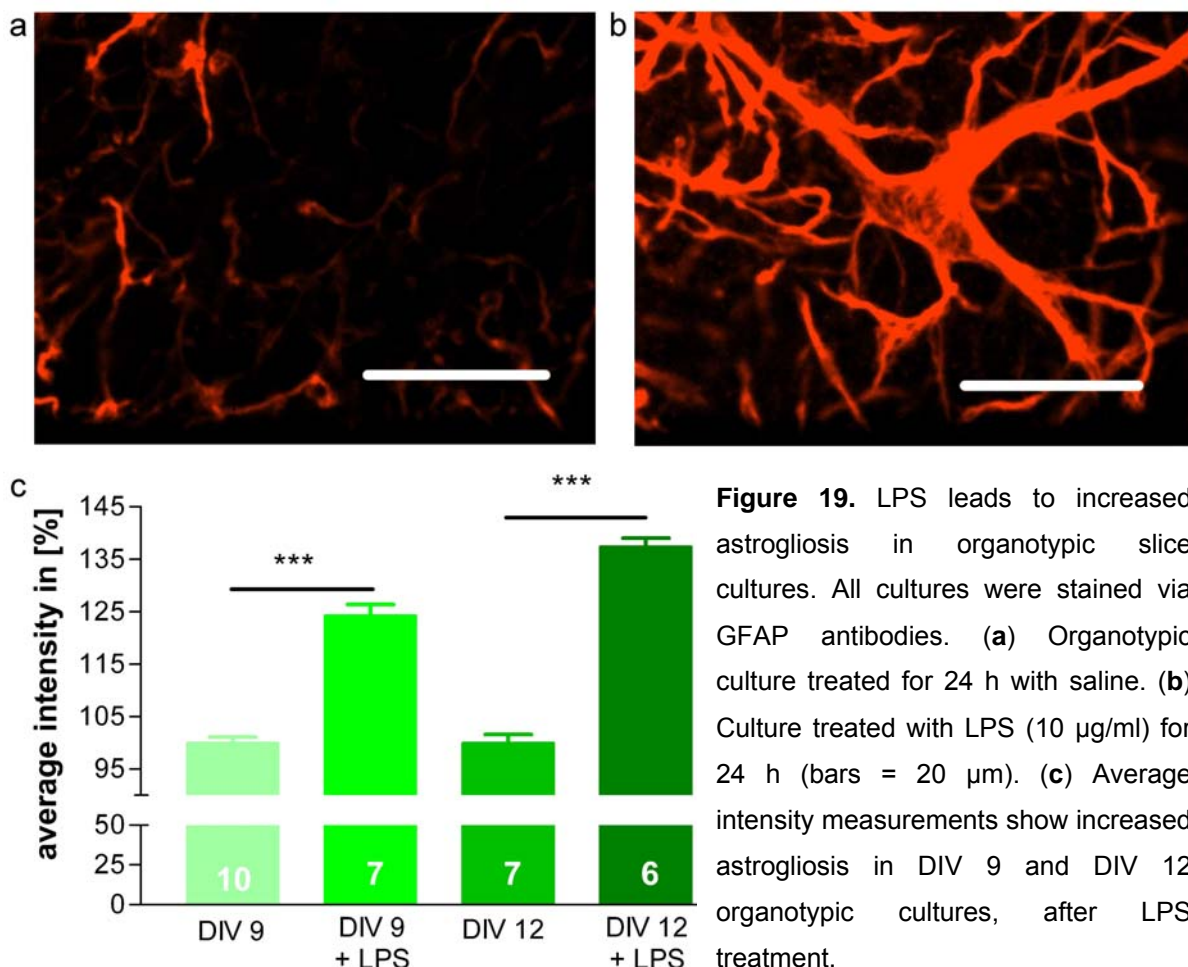
4.8. Organotypic slice cultures preserve their neocortical architecture and reveal caspase-3 dependent apoptosis.

We prepared organotypic slice cultures of the neocortex from newborn (P0-1) mice. Previous studies have demonstrated that organotypic slice cultures are well suited to investigate the molecular and cellular mechanisms underlying apoptosis during early cortical development (Haydar et al., 1999), as they preserve their neocortical architecture and reveal casp-3-dependent cell death (**Figure 20**). Nissl staining shows the preserved neocortical architecture in organotypic slice cultures, with the 6 layered cortex (**Figure 20 a**). To determine the casp-3-dependent apoptosis we used an antibody against cleaved-casp-3 (**Figure 20 b**). Under normal control conditions, casp-3-dependent apoptosis occurs in a low amount and neurons in all cortical layers

of the newborn mouse cerebral cortex undergo casp-3-dependent cell death. Activation of casp-3 is an early key event during apoptosis (Marin-Teva et al., 2004), cleaved-casp3-positive cells still showed a relatively normal morphology. In detail, analysis of the cells revealed a clear neuronal morphology (**Figure 20 c**). Following the first two days after preparation the amount of cleaved-casp-3 positive cells is high in all cortical layers. A stable baseline in the percentage of apoptotic cells could be observed after 3 DIV until 14 DIV (**Figure 20 d**). Therefore all the experiments with organotypic slice cultures were performed at slices starting at 4 days *in vitro*.
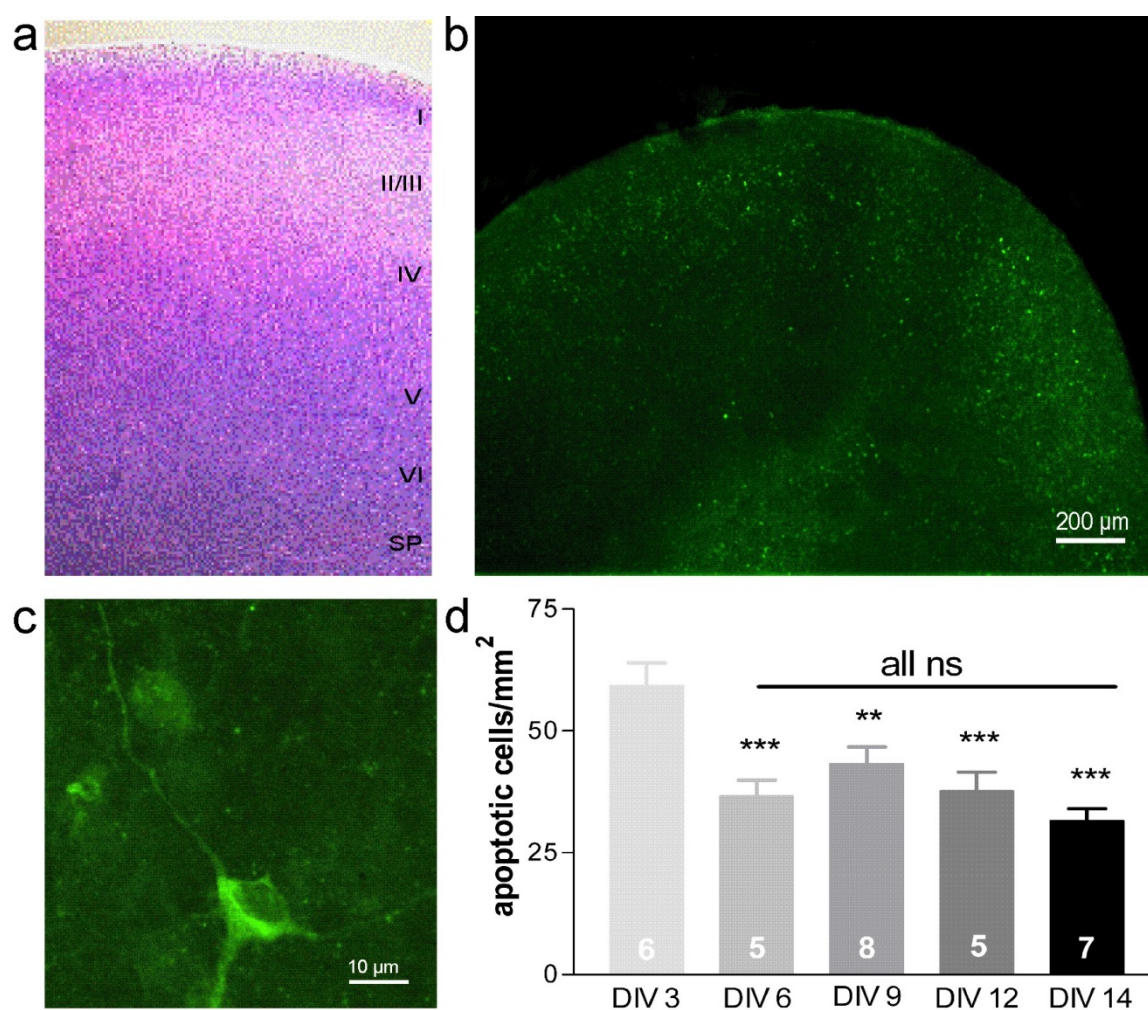
Figure 20. Organotypic slice preparations preserve their neocortical architecture and cellular morphology in culture. (**a**) Nissl staining shows the preserved neocortical architecture in organotypic slice cultures. (**b**) Fluorescence photograph of cleaved casp-3 stained slice culture at 3 DIV shows that cells stained for activated caspase 3 are distributed over the whole preparation. (**c**) High magnification fluorescence picture of a casp-3 positive cell morphologically identified as neuron. (**d**) Counting casp-3 positive cells after different days *in vitro* show that after 3 DIV a constant level of apoptosis is achieved.

4.9. LPS induces caspase-3 dependent cell death in organotypic neocortical slice cultures of the newborn mouse

The influence of inflammation on casp-3-dependent cell death was studied in neocortical organotypic slice cultures. In agreement with previous studies (Heck et al., 2008) developmentally regulated casp-3-dependent apoptosis could be detected under normal conditions in all cortical layers (**Figure 20 a**). We identified the casp-3 positive cells as neurons based on their clear neuronal morphology (**Figure 20 c**). After application of lipopolysaccharide (LPS, 10 µg/ml) for 24 h we observed in 6 DIV cultures a significant increase in the percentage of casp-3 positive cells to 273 ± 17% (n=10 cultures, p<0.0001) and in 12 DIV cultures an increase to 225 ± 17% (n=6, p<0.0001), both compared to the 6 DIV control condition of 100 ± 8% (**Figure 21 a**). This significant increase in the apoptosis rate could be already observed after 6 h treatment with LPS (n=10, p<0.0001) (**Figure 21 b**). LPS treated casp-3 positive cells were not double stained for GFAP, demonstrating that in our experimental conditions astrocytes were not affected by LPS. In addition we could not observe an effect of 3 h LPS application on the survival rate of BV-2 microglia cells or primary astrocytes (**Figure 17**). These data demonstrate that transient LPS application to organotypic neocortical slice cultures induces a prominent casp-3-dependent neuronal cell death, while microglial BV-2 cells and primary astrocytes are not affected, regarding apoptotic cell death.
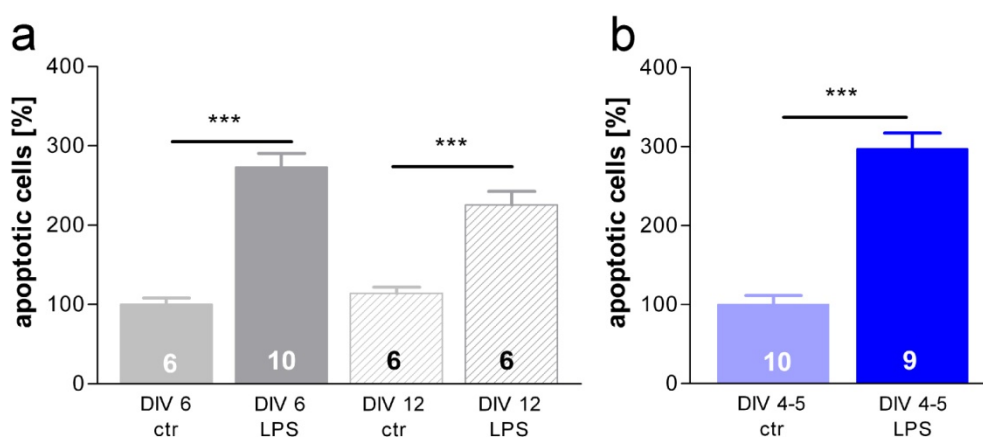
Figure 21. LPS leads to induced casp-3 activity in organotypic slice cultures. (**a**) Casp-3-dependent cell death in 6 and 12 DIV organotypic slice cultures treated for 24 h with 10 µg/ml LPS as compared to untreated controls. (**b**) Significant increase in percentage of apoptotic cells in 4-5 DIV cultures after 6 h LPS addition.

4.10. Expression of proinflammatory cytokines in LPS-treated organotypic slice cultures

The objective of this experiment was to investigate the extent of mRNA levels (using quantitative real-time PCR) for proinflammatory cytokines in the organotypic slice cultures of the neonatal mouse cortex. Organotypic slice cultures were exposed to LPS for 24 or 1.5 h which led to significant increase of various proinflammatory cytokines when compared to saline treated control slices (**Figure 22**). **Figure 22 a** shows a screen shot of RT-PCR. Black arrows indicate the different genes, for example TNFα as gene of interest and Actin-β as control. In organotypic slice cultures treated for 24 h with LPS TNFα, IL-6 and IL-1β expression was increased when compared to control. As shown in **Figure 22 b**, we found a 20.76 fold increase for TNFα, a 55.24 fold increase for IL-6 and a 62.43 fold increase for IL-1β. We could also observe that in organotypic slice cultures treated for 1.5 h with LPS, only TNFα was significantly increased 8.24 fold (**Figure 22 c**).
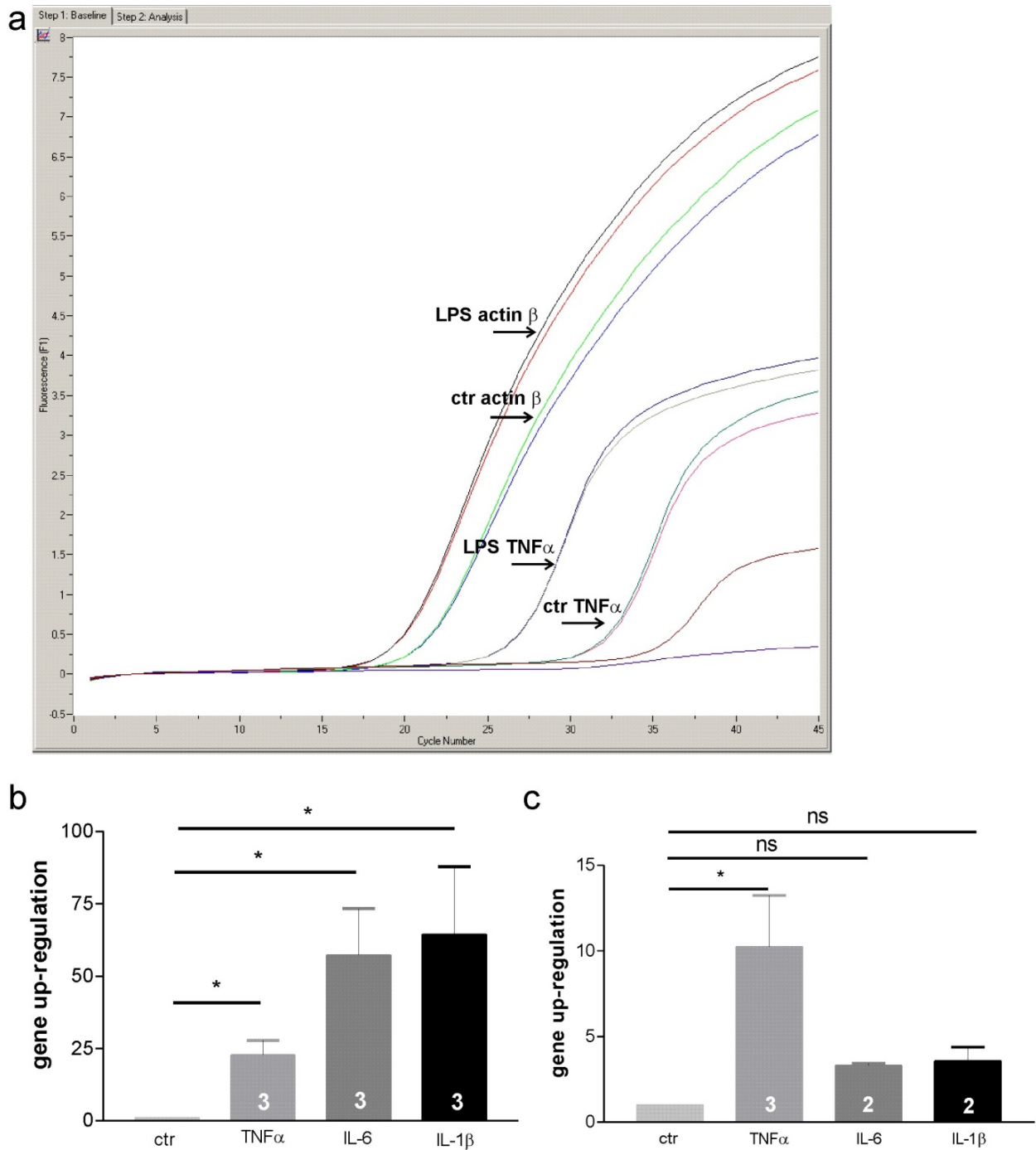
Figure 22. Genes of cytokines increase upon LPS treatment. (**a**) An example of RT-PCR curves. Organotypic cultures treated for 24 h with LPS (10 µg/ml). (**b**) 24 h treatment of organotypic slices with 10 µg/ml LPS. (**c**) 1.5 h treatment of organotypic slices on MEA and measurement of gene up-regulation.

4.11. LPS diminishes spontaneous synchronized network activity but increased duration of oscillations in organotypic slice cultures

We recorded in 5-7 DIV organotypic slice cultures spontaneous neuronal activity by using the multi electrode array system. This neuronal activity consists of network oscillations which occurred at an average rate of 18.3 ± 1.6 per hour (n=6 slices) (**Figure 23 a**), which is in agreement with previous observations (Heck et al., 2008). These oscillations had a duration of 10.4 ± 1.6 s (n=4), a frequency of 1.14 ± 0.3 Hz (n=3), amplitude of 473.2 ± 90.1 µV (n=4) and were synchronized over the whole organotypic neocortical slice (**Figure 23 b**). Organotypic slice cultures treated for 1.5 h with LPS (10 µg/ml) revealed, when compared to untreated control slice cultures, a significantly decrease in occurrence (10.1 ± 2.5 per hour, n=6; p<0.01) (**Figure 23 c**) and increased in duration of spontaneous network oscillations (from 100 ± 2.5 to 108.2 ± 2.23, n=6; p<0.05) (**Figure 23 d**). To further elucidate the molecular mechanisms underlying this LPS effect on synchronized network activity, we used primary dissociated neuronal cell cultures and recorded with MEAs the functional consequences of LPS application.
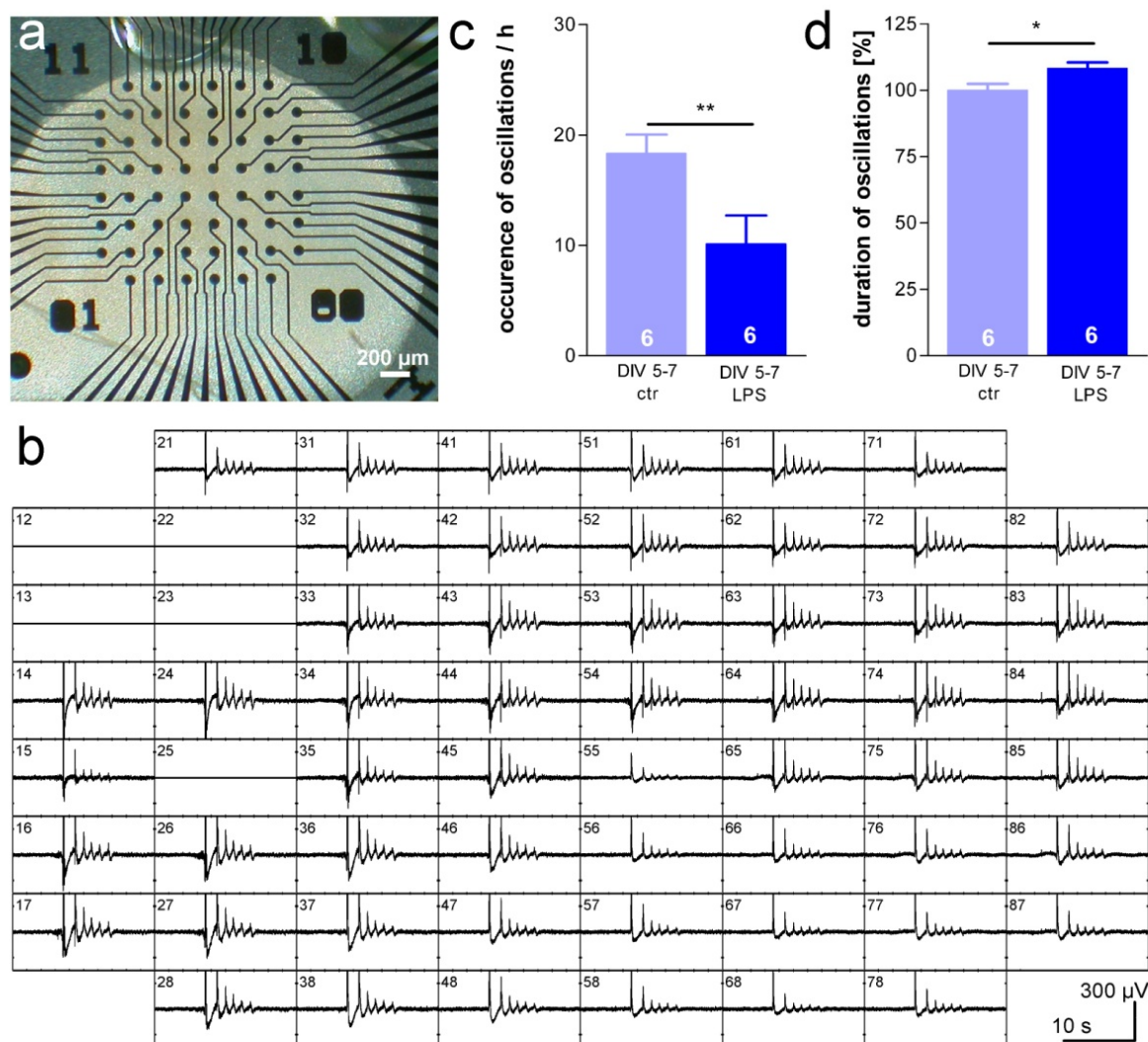
Figure 23. Effects of LPS on synchronized spontaneous network activity in neocortical slice cultures. (**a**) Image of a 5 DIV organotypic neocortical slice culture placed on a 60-channel MEA. Black dots represent extracellular recording electrodes separated by 200 µm. (**b**) Simultaneous 60-channel MEA recording of synchronized network oscillations in a control organotypic neocortical slice culture. Five channels are damaged and were switched off. (**c**) Spontaneous network oscillations recorded in 5-7 DIV organotypic cultures are significantly reduced while duration of oscillations increased (**d**) after LPS perfusion for 1.5 h as compared to untreated controls.

4.12. LPS-induced release of inflammatory factor(s) causes increase in firing rate, but disrupts neuronal network synchronization

To further elucidate the molecular mechanisms underlying the LPS effect on spontaneous network activity, we used primary dissociated neuronal cell cultures and recorded the functional consequences of LPS application with MEAs. Neuron

58

enriched cultures, containing little amounts of astrocytes (**Figure 24**) were plated at a density of 1,000,000 cells on poly-ornithin (Sigma) coated multi-electrode arrays (MEAs; Multi Channel Systems, Reutlingen, Germany). DIV14 dissociated cultures consist largely of neurons and few astrocytes (**Figure 24 a**), whereat neurons were 8.58 fold increased (**Figure 24 b**).
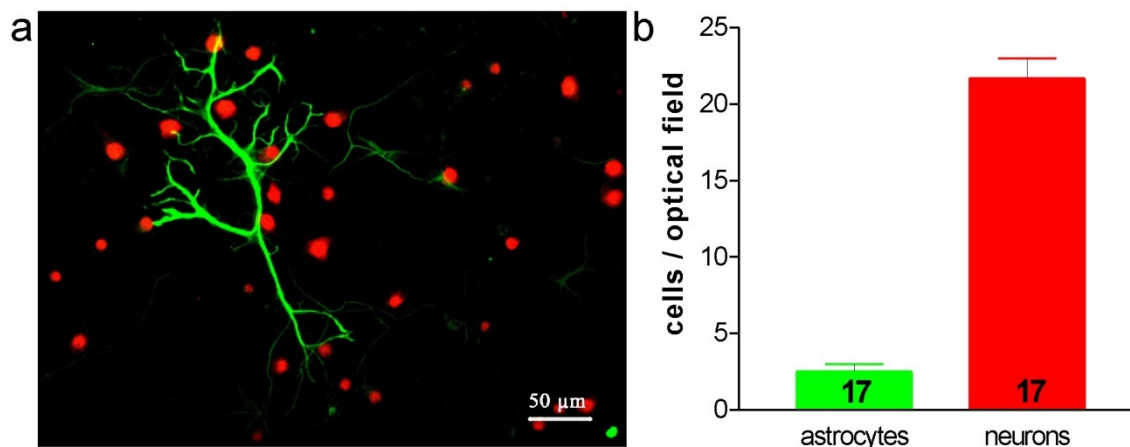
Figure 24. Purity of dissociated cultures. (**a**) DIV 14 dissociated cultures with astrocytes (GFAP, green) and neurons (NeuN, red). (**b**) Measurement of percentage of astrocytes per optical field.

Dissociated neuronal cultures also revealed a distinct pattern of spontaneous synchronized network activity (**Figure 25 a**) (Sun et al., 2010). These network bursts appeared on average 1.8 ± 0.5 times per minute (n=8 cultures) and single bursts had a duration of 4.6 ± 0.9 s. Dissociated cultures were treated with various conditioned media (see **Table 1 in Methods**). In cultures treated with C-CM (**Figure 25 a-(i)**) the average relative burst index amounted to 1.12 ± 0.13 (n=9) (**Figure 25 b**). In LPS-conditioned medium (LPS-CM) (**Figure 25 a-(ii)**) the burst index decreased significantly to 0.563 ± 0.055 (n=11, $p<0.001$) (**Figure 25 b**). In cultures treated with C-CM + LPS (**Figure 25 a-(iii)**) the burst index amounted to 0.937 ± 0.085 (n=5) and was not significantly different when compared to the C-CM control ($p>0.05$) (**Figure 25 b**). Similar results could be obtained with heat inactivated LPS-CM (1.127 ± 0.14, n=8, $p>0.05$) (**Figure 25 b**). As another parameter for the neuronal network activity the relative spike number was determined in these four experimental groups (**Figure 25 c**). In C-CM cultures this value amounted to 0.58 ± 0.11(n=9). Cultures in LPS-conditioned medium (LPS-CM) revealed a three-fold increase to 1.72 ± 0.5 (n=11), but this difference was not significant. In C-CM + LPS (1.022 ± 0.09, n=5) and LPS-CM heat (0.47 ± 0.19, n=5) treated cultures the spike number was close to the

control values of C-CM cultures. These results indicate that one or several soluble heat-sensitive factor(s), most likely proteins, are released from BV-2 cells after LPS treatment which induce an overall increase in firing rate, but a decrease in synchronized network activity.
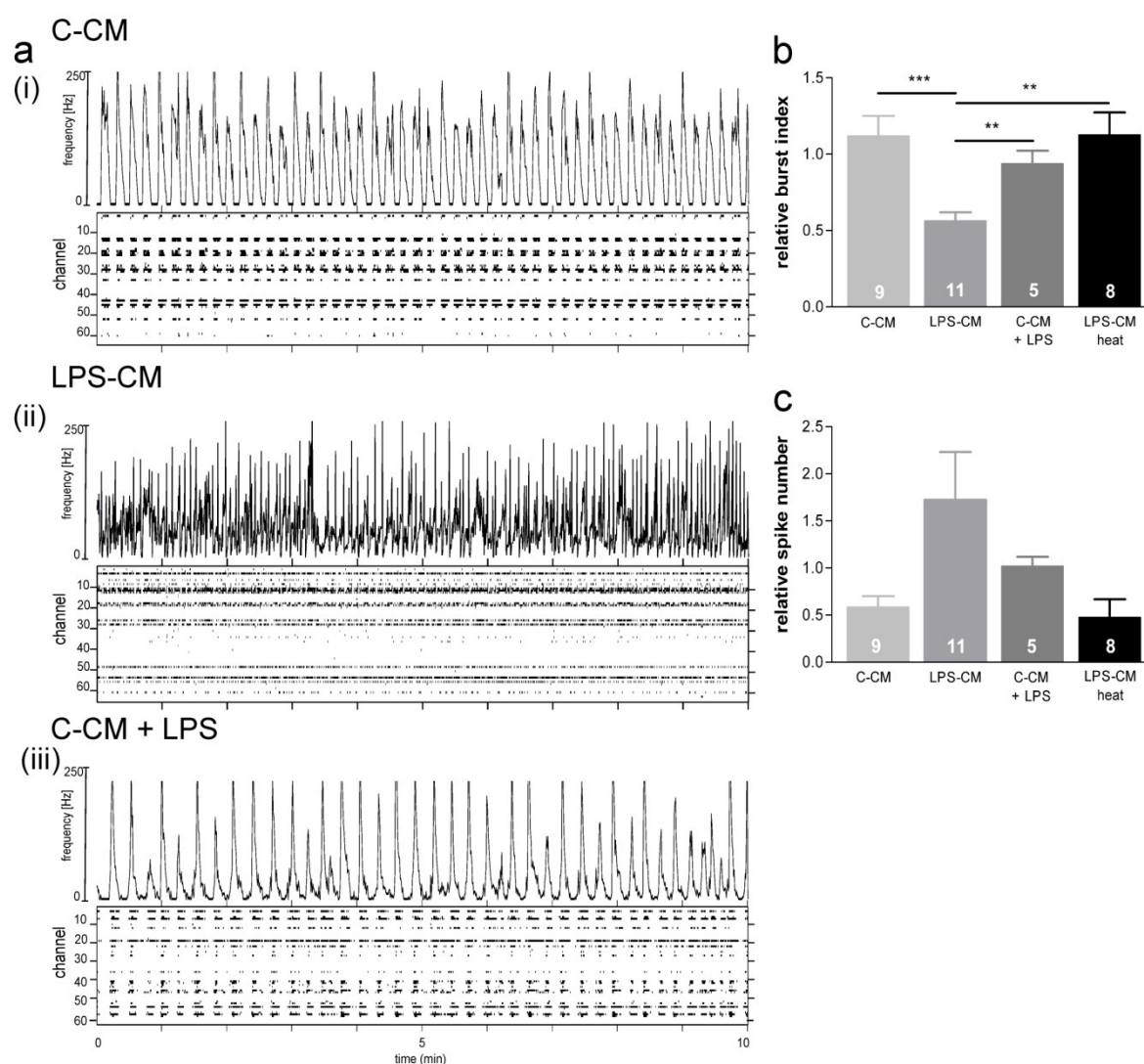
Figure 25. Desynchronization of neuronal network activity recorded in neuronal dissociated cultures following application of LPS conditioned medium. Representative MEA recording of 14 DIV dissociated neuronal culture (**a-(i)**) under control conditions (**a-(ii)**) after application of LPS-CM (**a-(iii)**) after application of C-CM + LPS. (**b**) Relative burst index in dissociated neuronal cultures under control conditions (C-CM), after 1 h application with the supernatant of LPS treated BV-2 cells (LPS-CM), after 1 h treatment with LPS only (C-CM + LPS) and after application of heat inactivated LPS-CM (LPS-CM heat). (**c**) Relative spike number in dissociated neuronal cultures under control conditions (C-CM), after 1 h application with the supernatant of LPS treated BV-2 cells (LPS-CM), after 1 treatment with LPS only (C-CM + LPS) and after application of heat inactivated LPS-CM (LPS-CM heat).

4.13. LPS induces fast release of rapidly acting inflammatory factor(s)

Dissociated cultures treated with LPS-CM revealed a significant decrease in the relative survival rate to 86.4 ± 1.2% (n=18, p<0.001) when compared to the relative survival rate of control C-CM cultures (100 ± 1.3%, n=18) (**Figure 26 a**). In agreement with our electrophysiological data, cultures treated with C-CM + LPS (99.4 ± 3.5%, n=4, p>0.05) or heat inactivated LPS-CM cultures (105 ± 2.6%, n=12, p>0.05) showed no significant difference in their survival rate when compared to C-CM control cultures (**Figure 26 a**). In order to estimate the time course of LPS-induced cell death, we treated the dissociated cultures for only 1 or 2 hours with conditioned medium (C-CM or LPS-CM). Whereas 1 h LPS-CM treatment had no significant effect on the survival rate (n=6, p>0.5), 2 h LPS-CM treatment induced a significant decrease in the survival rate to 80.3 ± 1.6% (n=5, p<0.001) compared to C-CM controls (100 ± 1.5%, n=5) (**Figure 26 b**). In order to study the question how fast LPS-activated BV-2 cells induce the release of inflammatory factor(s), LPS was applied for 2 h. Cultures treated for 6 h with this 2 h conditioned LPS-CM revealed a significant decrease in the survival rate to 81 ± 2.3% (n=3, p<0.001) when compared to C-CM controls (100 ± 2.6%, n=3) (**Figure 26 c**). These data indicate that heat-sensitive soluble factor(s) are released from BV-2 cells within less than 2 h after LPS addition, which caused a decrease in survival rate within 2 h.
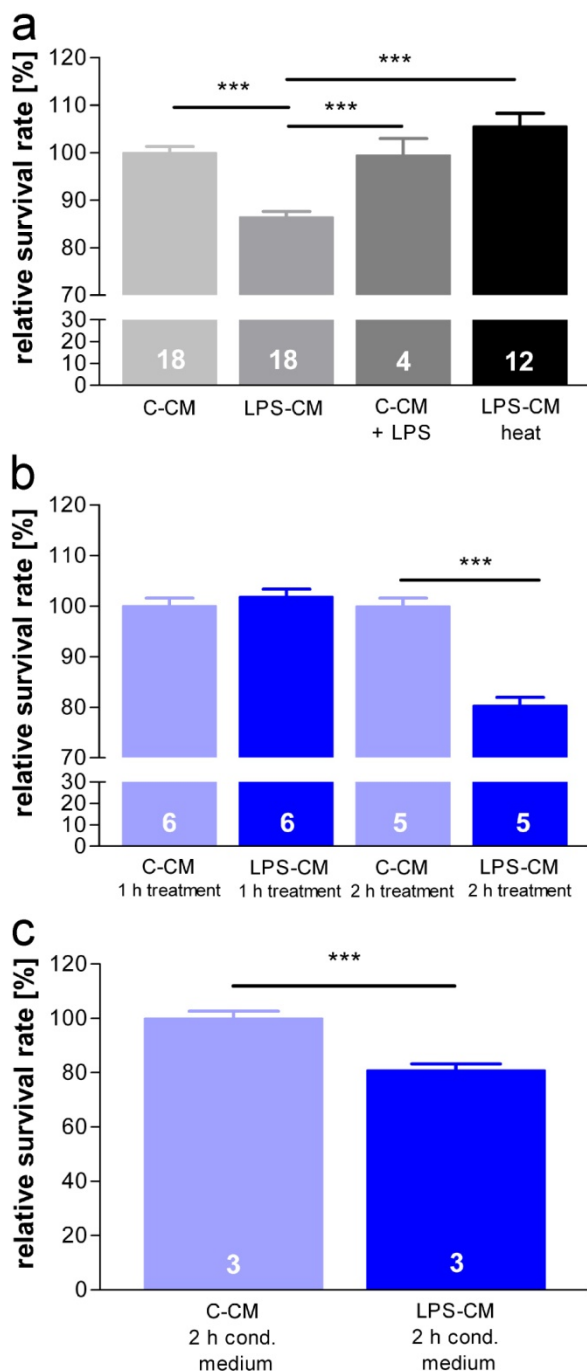
Figure 26. LPS conditioned medium induces rapid decrease in neuronal survival. (**a**) Relative survival rate in dissociated neuronal cultures under control conditions (C-CM), after 6 h application with the supernatant of LPS treated BV-2 cells (LPS-CM) and after 6 h treatment with LPS only (C-CM + LPS). No change in the survival rate of dissociated neurons when LPS-CM was heat inactivated before treatment (LPS-CM heat). (**b**) Treatment with LPS-CM (6 h conditioned medium) for 1h leads to no significant change in the survival rate while 2 h leads to decreased cell survival. (**c**) Conditioning of the medium for only 2 h already leads to decreased cell survival after 6 h application.

4.14. TNFα and MIP-2 are significantly up-regulated in LPS conditioned medium

LPS-CM treatment led to a decreased survival rate and decreased bursting activity and both effects were heat-sensitive. In order to identify the pro-inflammatory factors activated by LPS application, C-CM and LPS-CM were analyzed via protein array analysis. Various cytokines and chemokines revealed an increase in release upon

LPS treatment (**Figure 27 a-(i, ii)**). When compared to C-CM controls, the following factors were significantly up-regulated by LPS (**Figure 27 b**): G-CSF (from 0.02 ± 0.01 to 0.58 ± 0.04; $p<0.001$), KC (0.05 ± 0.01 to 0.79 ± 0.17; $p<0.05$), RANTES (0.02 ± 0.01 to 0.34 ± 0.07; $p<0.05$), GM-CSF (0.05 ± 0.01 to 1.06 ± 0.03; $p<0.001$), IL-1ra (0.08 ± 0.02 to 0.92 ± 0.15; $p<0.01$), TNFα (0.31 ± 0.054 to 1.76 ± 0.20; $p<0.01$), IL-6 (0.02 ± 0.01 to 1.12 ± 0.04; $p<0.001$) and MIP-2 (0.043 ± 0.013 to 2.24 ± 0.38, $p<0.01$) (all n=3). Only JE, a factor responding to mitogenic stimuli, was down-regulated (from 2.62 ± 0.19 to 0.81 ± 0.09; $p<0.001$). G-CSF is hypothesized to increase the activation of resident microglia and mobility of marrow-derived microglia (Sanchez-Ramos et al., 2009). KC (CXCL1) and RANTES are chemoattractants for a variety of inflammatory immune cells like neutrophils (van Rossum et al., 2008) and both can be excluded as potential factors in our model system. GM-CSF induces proliferation and activates microglia (Reddy et al., 2009) whereas IL-1ra inhibits IL-1 activity (Sims, 2002). TNFα, MIP-2 and IL-6 are important cytokines primarily involved in inflammation. It has been demonstrated that IL-6 causes reactive astrocytosis but no neuronal damage (Fattori et al., 1995;Raivich et al., 1999). Therefore the focus was on TNFα and MIP-2 as the most likely downstream candidates of LPS-induced neuronal desynchronization and cell death.
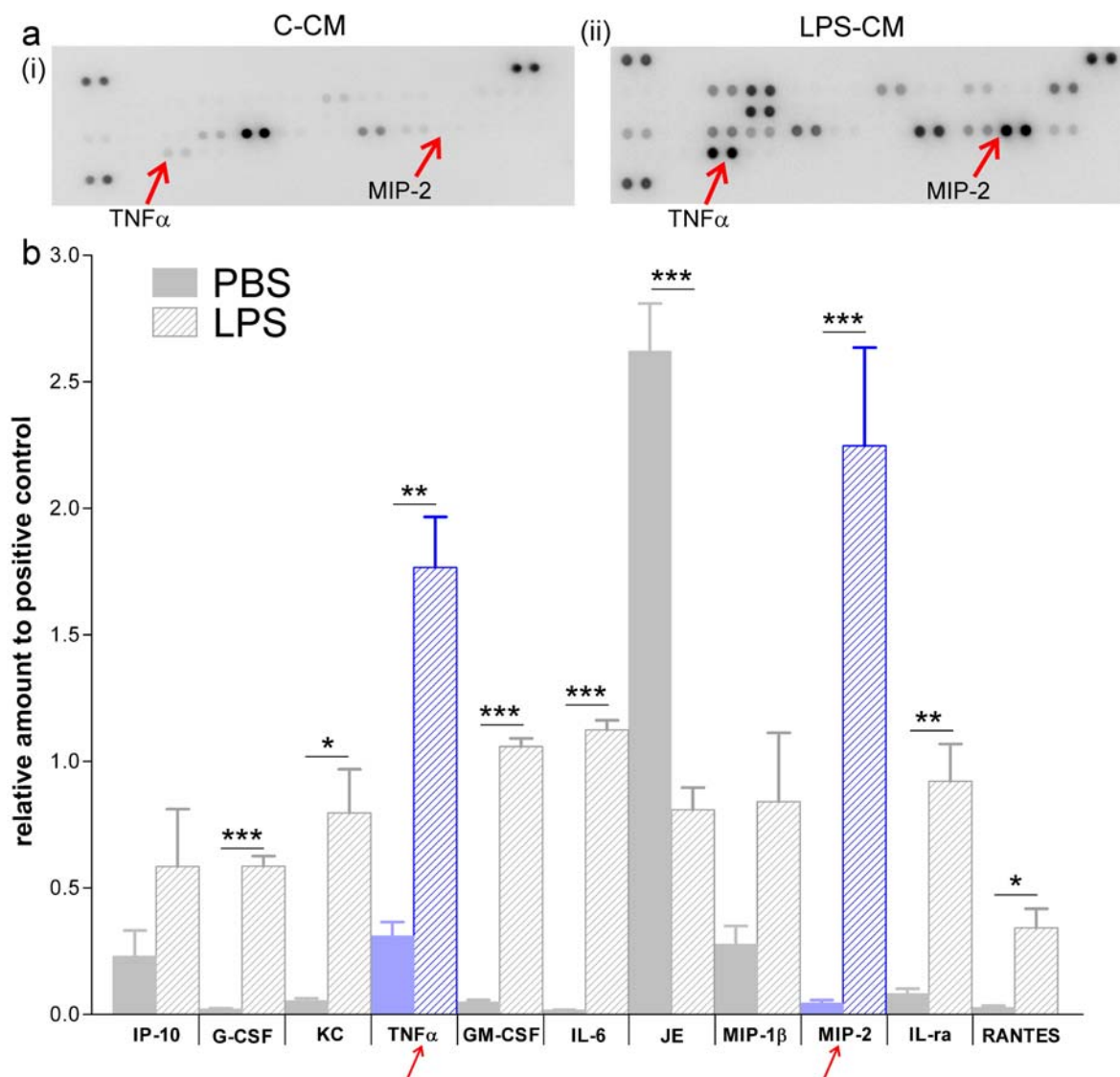
Figure 27. Microarray protein analysis demonstrates prominent LPS-induced up-regulation of various cytokines. (**a**) Cytokine-assay for control conditioned medium in (**i**) and LPS conditioned medium in (**ii**). (**b**) Quantitative analysis of up- and down-regulated cytokines. TNFα and MIP-2 were most significantly up-regulated in LPS conditioned.

4.15. Neutralization of TNFα or MIP-2 sustains cell survival and network synchronization

In order to study the consequences of TNFα and MIP-2 neutralization, anti-TNFα or anti-MIP-2 was added to the supernatant of the BV-2 cells and the effect on cell survival, neuronal network synchronization and relative spike number was analyzed (**Figure 28**). Treatment with anti-TNFα enhanced survival rate (**Figure 28 a**) and burst index (**Figure 28 c**) in LPS treated cultures and led to a normalization of the relative spike number (**Figure 28 d**), demonstrating that TNFα is critically involved in

the regulation of neuronal network activity and cell survival. Neither the survival rate, nor the burst index completely recovered in anti-TNFα conditions, suggesting the participation of additional factor(s) in both processes. Since our protein array analyses identified MIP-2 as another likely candidate, the effects of anti-MIP-2 were also studied. Application of anti-MIP-2 prevented the LPS-induced network desynchronization (**Figure 28 c**) and increase in relative spike number (**Figure 28 d**). However, in contrast to anti-TNFα the effect of anti-MIP-2 on cell survival rate was less clear and no significant effect could be observed when compared to the LPS-CM cultures (**Figure 28 b**). These data suggest that network synchronization recovers first or that MIP-2 has a strong impact on network synchronization with only minor effects on cell survival.
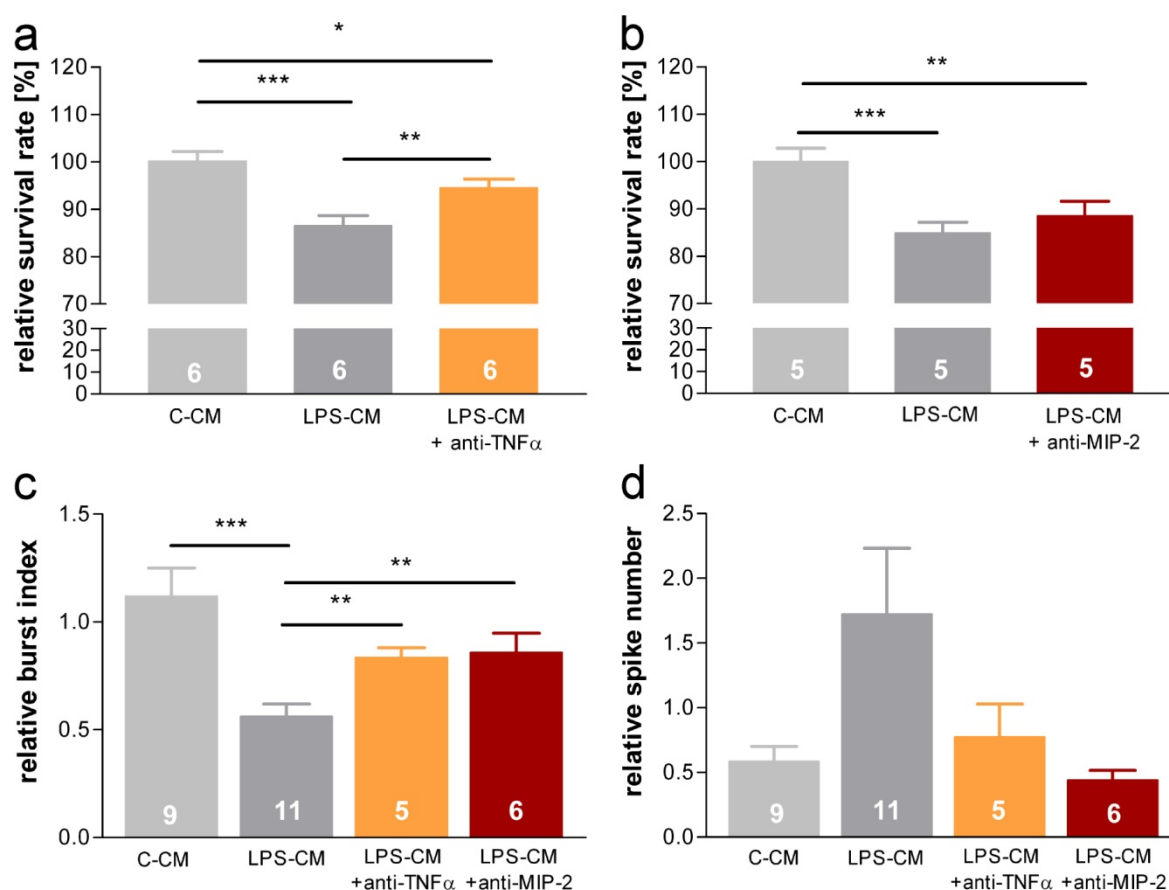
Figure 28. Neutralization of TNFα and MIP-2 leads to increased survival rate and burst index, as well as to a normalization of the spike number. Relative survival rate (**a** and **b**), relative burst index (**c**) and relative spike number (**d**) in C-CM, LPS-CM and LPS-CM+anti-TNFα (**a**,**c**,**d**) or LPS-CM+anti-MIP-2 (**b**,**c**,**d**) treated dissociated neuronal cultures. Note relatively normal survival rate, burst index and spike number after application of TNFα antibody or MIP-2 antibody treatment.

Our data indicate that LPS treatment leads to a release of TNFα which triggers the release of MIP-2 and causes an increase in spontaneous activity associated with a desynchronization of neuronal network activity. The lack of synchronized network bursts subsequently causes a decreased neuronal survival. As MIP-2 is released subsequent its effect is not as clear as the effect of TNFα on survival rate.

We next evaluated the relevance of these findings in an *in vivo* approach and analyzed the consequences of LPS-induced inflammation on the developing cerebral cortex in living rodents.

4.16. Decreased occurrence of oscillations in the γ-frequency and increased levels of cleaved caspase-3 after LPS injection in vivo *(in cooperation with Jenq-Wei Yang and Shuming An)*

The consequences of LPS-induced inflammation on neuronal activity in the developing cerebral cortex *in vivo* were studied with extracellular field potential recordings in the barrel cortex of P3-5 rats using 16-channel (4x4) Michigan-electrodes. In agreement with previous reports on somatosensory cortex of newborn rats and preterm human neonates, spontaneous network activity was characterized by distinct neuronal patterns (**Figure 29a-(i)**). In the newborn rat cortex *in vivo* spindle bursts had a duration of 1.1 ± 0.1 s, an amplitude of 831.3 ± 77.4 µV, frequency of 8.4 ± 0.2 Hz and occurred 5.5 ± 0.7 per min (see lower traces in **Figure 29a-(i)**). In contrast, gamma oscillations revealed a duration of 0.33 ± 0.04 s, an amplitude of 240.6 ± 26.1 µV, frequency of 38.8 ± 1.4 Hz and occurred 4.9 ± 0.7 per min (n=8 animals). Inflammation was induced by intracortical injection of lipopolysaccharide (LPS, 10 µg in 2 µl). Three hours after injection of LPS the occurrence of spindle bursts and gamma oscillations was reduced by 20-30% (**Figure 29a-(ii)**), but this effect reached significance only for the gamma oscillations, which were reduced by LPS treatment from 110.1 ± 4.8% to 77.6 ± 11.7% (n=8 animals, $p < 0.05$) (**Figure 29b-(i)**). Following intracortical LPS injection, the mean duration of spindle bursts increased significantly from 110.1 ± 5.6% to 169.9 ± 10.6% (n=8, $p < 0.001$) (**Figure 29b-(ii)**). Neither the amplitude nor the frequency of spindle bursts and gamma oscillations were changed by LPS application. These data demonstrate that LPS-induced inflammation causes rapid modifications in the properties of spontaneous network oscillations.
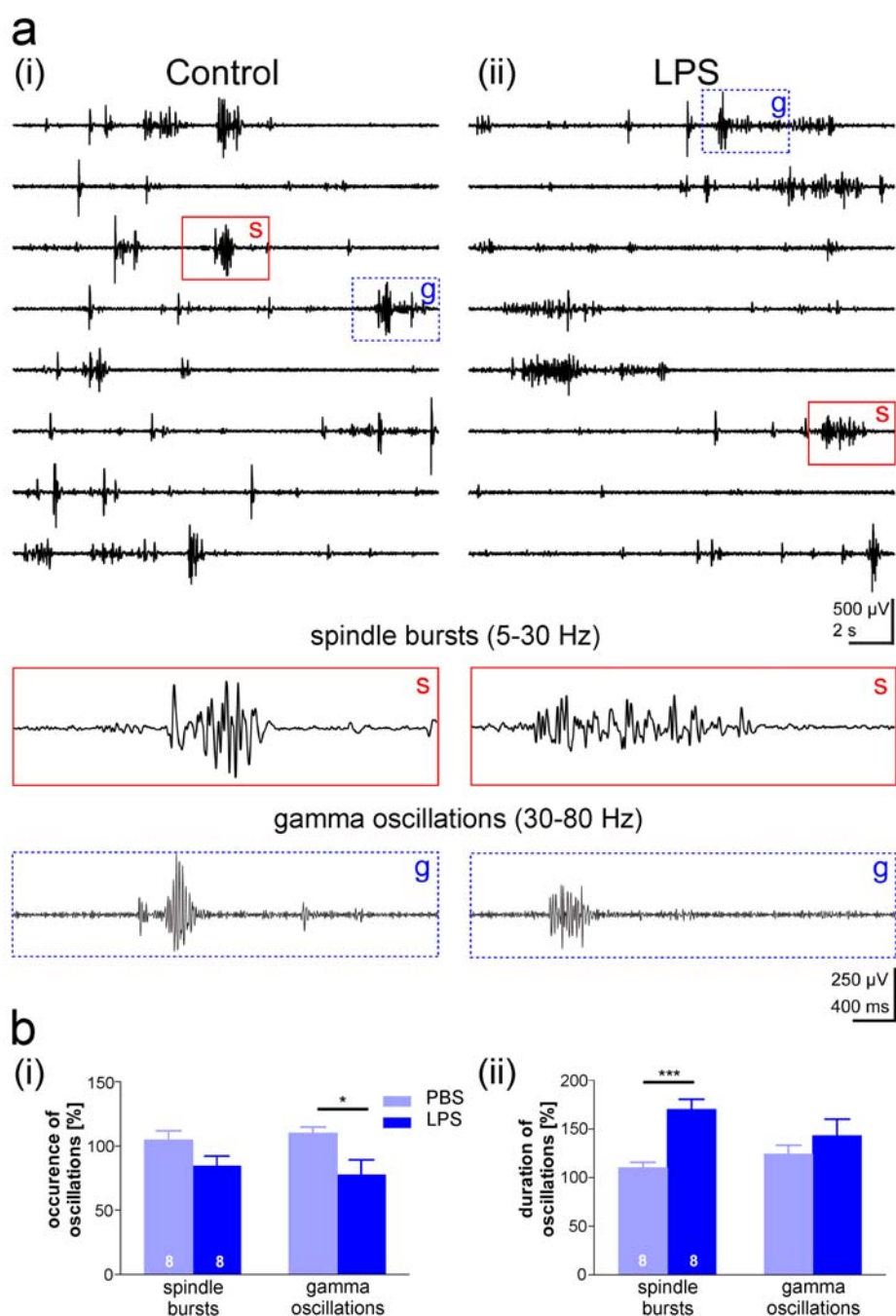
Figure 29. LPS injection *in vivo* leads to alterations in neuronal network activity. (**a**-(**i**)) 200 sec trace of a P4 rat shows several spontaneous oscillatory events. (**a**-(**ii**)) 200 sec continuous recording from the same P4 rat as in (i) after LPS injection shows fewer oscillatory events but the duration of events increased. In the newborn rat cortex *in vivo* spindle bursts had a duration of 1.1 ± 0.1 s, an amplitude of 831.3 ± 77.4 µV, frequency of 8.4 ± 0.2 Hz and occurred 5.5 ± 0.7 per min (see lower traces in **a**(**i**)). In contrast, gamma oscillations revealed a duration of 0.33 ± 0.04 s, an amplitude of 240.6 ± 26.1 µV, frequency of 38.8 ± 1.4 Hz and occurred 4.9 ± 0.7 per min (n=8 animals). (**b**-(**i**)) The average occurrence of gamma oscillations decreased significantly 3 h after LPS injection, while their duration remained relatively constant (**b**-(**ii**)). The occurrence of spindle bursts did not change after LPS injection (**b**-(**i**)) while the mean duration increased significantly (**b**-(**ii**)). The values are displayed normalized to their respective control.

Following the same surgical procedure as above, without insertion of electrodes, barrel cortex was injected with either PBS or LPS (5 mg/ml). 6 hours later the tissue was removed via a skin puncher and Western blot analysis was implemented. Western blot of 20µg total protein from pooled (n=3) barrel cortex samples (PBS control or 5 mg/ml LPS, n=3) detected a band at 17kD corresponding to cleaved casp-3. Mouse brain slice lysate, treated with staurosporin (100 nM for 24 h), was used as positive control and GAPDH served as a loading control (**Figure 30 a**). After LPS treatment, tissue shows a 3.3 fold increase in cleaved casp-3 protein levels compared to PBS control (**Figure 30 b**). The observed increase of cleaved casp-3 in LPS treated brain areas provides evidence that through fast occurring alterations in the electrical activity casp-3-dependent apoptosis rate is later on increased *in vivo*.
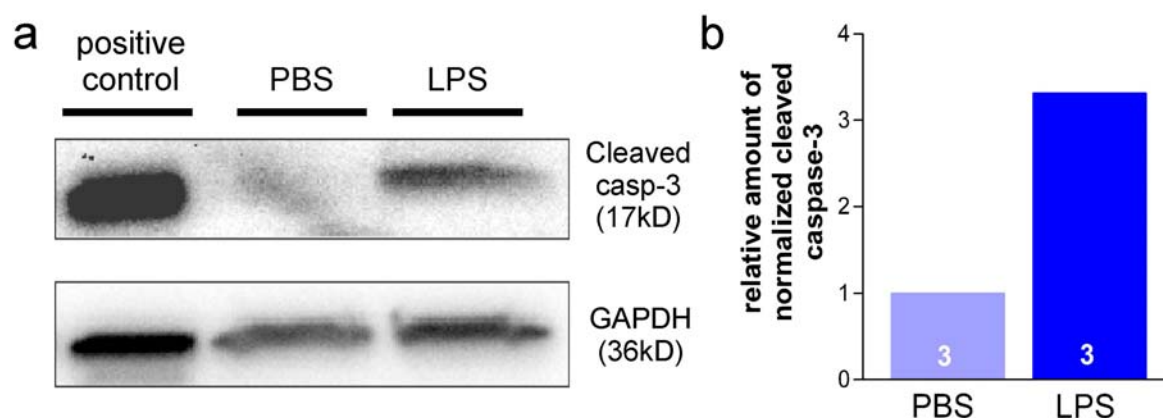
Figure 30. LPS injection *in vivo* leads to increased cleaved casp-3 level. Three P4-5 rats were injected with either LPS or PBS. 6 h later the tissue was removed. (**a**) Western blot of 20 µg total protein from pooled (n=3) barrel cortex samples (PBS control or 5 mg/ml LPS, n=3) detected a band at 17kD corresponding to cleaved casp-3. GAPDH served as a loading control and brain slices from mouse treated with staurosporin (100 nM) for 24 h were used as positive control. (**b**) The relative increase of cleaved casp-3 in LPS treated cells and in the presence of control PBS was blotted. Normalization revealed an increase of 3.3 fold of cleaved casp-3 after 6 hours LPS injection.

5. Discussion

I studied the role of inflammation-induced modifications in neuronal activity and the control of cell survival in a develoing neuronal network *in vivo* and *in vitro*.

The present data demonstrate that LPS-induced inflammation induces a rapid change in the pattern of spontaneous synchronized burst discharges and activated microglia are the initial mediators of this modifications. Spontaneous osciallatory activity patterns are disturbed, the release of survival factors is diminished and casp-3-dependent apoptic cell death increases. TNFα and MIP-2 were identified as the major pro-inflammatory factors causing activity-dependent neuronal cell death in the developing brain.

It was long believed that hypoxia is the major cause of perinatal brain injury and cerebral palsy but this view changed in the last decades and other risk factors like inflammation, as well as a combination of infection and birth asphyxia were postulated to lead to brain damage in preterm infants (Eklind et al., 2001). Since improved treatment in the first decade of life has led to increased survival rate, it is becoming more and more important to understand the mechanisms behind the disease as for example 8000 babies per year are born with cerebral palsy in the USA which is only one outcome of neonatal brain injury (Ferriero, 2004).

Intrauterine infection and fetal immune response are important pathogenic factors in a large subset of neurodevelopmental disorders which can lead to mental retardation in the early ontogenesis (Gilmore et al., 2003), cognitive impairment, learning deficits, perinatal brain damage and cerebral palsy (Deverman and Patterson, 2009;Folkerth, 2005;Volpe, 2001;Volpe, 2003).

The goal of this PhD thesis was to show that alterations in neuronal activity, after inflammatory stimuli, are important in the regulation of neuronal survival during early development. We studied the modifications in neuronal activity and apoptotic cell death, in response to LPS-induced inflammation. To address this question, we used dissociated neuronal cultures, organotypic slice cultures and *in vitro* / *in vivo* electrophysiological recordings of the somatosensory cortex in newborn rodents and analyzed inflammation-induced modifications in neuronal activity and apoptotic cell death. For further analyses we used cytokine arrays and antibodies directed against specific cytokines to identify factors responsible for our observed alterations and quantified cleaved-casp-3 protein levels in *in vivo* experiments. To induce

inflammation we used LPS, a cell wall component of gram-negative bacteria (Rietschel et al., 1994) which, by inducing a massive immune response, plays an important role in neurodegenerative disease (Hagberg and Mallard, 2005;Hanisch and Kettenmann, 2007). LPS leads to activation of microglia (Felts et al., 2005), which are the immune cells of the brain and form a network of resident macrophages, that monitor the well-being of their environment being able to react to any pathological change (Hanisch, 2002;Kreutzberg, 1996).

In detail we addressed the following questions: (i) Does LPS specifically bind to microglia in the CNS? (ii) How do astrocytes react to soluble factors released by activated microglia? (iii) What is the effect of LPS-induced inflammation on apoptotic cell death and spontaneous neuronal network activity in organotypic slice cultures? (iv) Which factors are released from LPS-treated microglia, influencing neuronal survival and network activity in dissociated neuronal cultures? (v) What is the time course of these actions of the pro-inflammatory factor(s)? (vi) Does neutralization of the identified cytokines lead to re-establishment of synchronized burst activity and cell survival? (vii) What are the consequences of LPS-induced inflammation on spontaneous network activity and apoptotic cell death in the neonatal cerebral cortex under *in vivo* conditions?

5.1. Microglia cells specifically bind and react to LPS in vitro

In this work it was shown that LPS, which is the major component of the outer membrane of gram-negative bacteria (Rietschel et al., 1994), is linked to the resident macrophage-like cell within the CNS, the microglia. LPS appliction is an accepted strategy to mimic an inflammatory response under experimental conditions (Barks et al., 2008;Hanisch, 2002;Sankar et al., 2007) and it is a potent activator of microglia (Liu and Hong, 2003). The activation already starts after applying 1 µg/ml LPS on microglial cells for 6 h (Kaur et al., 2006). In our experimental set-up, LPS only binds to BV-2 cells, a microglial cell line and not to dissociated primary cortical neurons or primary astrocytes (**Figure 13**). This specific binding of LPS on microglial cells was already shown in previous experiments (Lehnardt et al., 2002;Lehnardt et al., 2003). Further we observed that the CD14 receptor which is, among other receptors, necessary for the binding of LPS (Haziot et al., 1996), is only expressed by BV-2 cells (**Figure 14**). LPS binds to a complex on microglia cells consisting of the LPS-

binding protein (LBP) and the soluble or glycosylphosphatidylinositor-anchored CD14 (Wright et al., 1990). The so formed complex binds to TLR4 (Wright, 1999), and initiates an intracellular signaling pathway that regulates gene expression (Means et al., 2000) and leads later on for example to induction of apoptosis, astrogliosis or damage of myelin (Rousset et al., 2006) as well as to the production of NO (Gibbons and Dragunow, 2006;He et al., 2002) and ROS (Leviton et al., 2005;Wang et al., 2005). The latter two, effects could also be observed in our own experiments. To show the connection between NO production, ROS production and LPS treatment, we used BV-2 cells and organotypic slice cultures and applied LPS for 24 h or 6 and 24 h respectively. It was shown that the application of LPS on BV-2 cells or organotypic slice cultures lead to increased release of nitrite, a terminal product of NO oxidation (**Figure 15**). LPS treatment of BV-2 cells lead to release of ROS (**Figure 16**), which triggers the deleterious cascade of events in inflammation related processes (Gao et al., 2002).

To further investigate the direct effect of LPS on the survival of different CNS cell types, we generated primary astrocyte cultures from P3 mouse brains and used BV-2 cells and HT-22 cells, a neuronal cell line.

The BV-2 microglial cell line is well known to release various factors upon LPS treatment (Chao et al., 1993;Deng et al., 2008;Hanisch, 2002) but did not show any cell death after 1 or 3 h of LPS treatment (**Figure17 a**). As expected, we also did not see any changes in survival rate after applying LPS on HT-22 cells, since neurons do not express the receptors necessary for the binding of LPS as already shown on primary neuronal cell cultures (Lehnardt et al., 2003).

5.2. Astrogliosis is induced by soluble factors of activated microglia

Our astrocytes number was not altered by LPS toxicity, consistent with previous work (Lehnardt et al., 2003). Work of Lee et al., 1993 showed that cytokine induction lead to delayed response of astrocytes which suggests an indirect mechanism of activation (Lee et al., 1993) for example through released factors of activated microglia (Balasingam et al., 1994). We proved the results by applying conditioned media from LPS treated microglia onto astrocytes and could observe an increase in survival rate and enhanced astrogliosis of our primary astrocytes (**Figure 17d, 18**). This reactive astrogliosis is determined by hypertrophy and/or proliferation of astrocytes and is a characteristic response of astrocytes to inflammation and trauma

of the adult CNS (Balasingam et al., 1994). The presentation of astrogliosis following inflammation is a stereotypic occurrence which can be recognized in two ways, either by increased GFAP - immune response, a long-standing neuropathological hallmark (Hozumi et al., 1990;Moumdjian et al., 1991) or our method using the Sholl-analysis, which is normally used for analyzing dendrite branches of neurons (Milosevic and Ristanovic, 2007). In agreement with previous work (Lehnardt et al., 2003) our LPS-CM-treated astrocytes showed an increased number of branches and a hypertrophic shape compared with astrocytes under control conditions (**Figure 18, 19**). These results implicate immunoregulatory cytokines, released from microglia, as important factors contributing to the induction of astrogliosis following inflammation to the CNS.

5.3. Inflammation-induced alterations of neuronal activity in organotypic slice cultures of the neonatal mouse cortex

Previous work has demonstrated that organotypic slice cultures are well suited to investigate the molecular and cellular mechanisms underlying apoptosis during early cortical development. Their prime advantage is the maintenance of the architecture and the preservation of the zones of the neocortical wall, including physiological and morphological separation between the VZ and SVZ (Haydar et al., 1999). Slice cultures also reveal pronounced casp-3-dependent cell death during the first two days in vitro. Three days after preparation, the number of casp-3-positive cells markedly decreased and remained constant until 14 DIV, the latest developmental stage analyzed in our study. In a previous work (Heck et al., 2008) it was shown that casp-3-dependent apoptosis regulates the cell number in all layers of the early postnatal cerebral cortex and therefore we chose casp-3 as a marker for our experimental set-up. Casp-3 activation presents an early event in the apoptotic process and therefore these neurons still preserve their physiological morphology and can be easily recognized. Furthermore cleavage of specific cell components by casp-3 is essential for the morphological and biochemical changes that characterize apoptosis in developing neurons (Marin-Teva et al., 2004). We could show that application of LPS at 4 to 12 DIV revealed an increase in casp-3-dependent apoptosis in our organotypic slice cultures after 24 or 6 h treatment (**Figure 21**). To our knowledge these results showed for the first time that 6 h treatment with LPS already leads to measurable casp-3 mediated apoptosis in organotypic cortical cultures. The outcome is in agreement with similar *in vitro* observations

demonstrating that for example hippocampal slices treated with 10 µg/ml LPS showed strong propidium iodide uptake after 72 h in all regions of the hippocampus, which is an indicator for necrosis (Nam et al., 2008). Another study showed that in rat organotypic midbrain slices 100 ng/ml LPS applied for 72 h led to decreased slice viability (Ding and Li, 2008). The distribution of the cleaved-casp-3 positive cells in the control slices resemble more or less the *in vivo* situation (Heck et al., 2008) which suggests that our data might be also relevant for neuronal apoptosis during early cortical development *in vivo*. We propose that LPS activates resting microglia (Hanisch, 2002) which subsequently release cytokines and chemokines (Chao et al., 1992;Lee et al., 1993). To confirm these observations also in our organotypic slice cultures we investigated the extent of mRNA levels for proinflammatory cytokines in the organotypic slice cultures of the neonatal mouse cortex and could observe an increase of TNFα, IL-1 and IL-1β after 24 h as well as an increase of TNFα after 1.5 h. These data are supported by previous work which showed that cytokine genes like IL1-β and TNFα are upregulated in the fetal brain of mice after maternal administration of LPS and that these cytokines can be produced by microglia in the fetal brain (Dammann and Leviton, 1997).

As it was previously suggested that neuronal survival during the period of early development can be affected by blockade of normal excitation in the immature nervous system (Mennerick and Zorumski, 2000) we propose that cell loss following depression of electrical activity might explain a subset of neurodevelopmental disorders. As neuronal activity occurred in organotypic slice cultures spontaneously, as already shown in a previous work of our lab (Heck et al., 2008), we induced inflammation on organotypic slices while recording their electrical activity on MEA-set ups. By applying LPS we could observe a decrease of these spontaneous oscillations after 1.5 h. To our knowledge this was the first time to show a direct link between network activity in organotypic neocortical slice cultures and LPS addition. As our electrophysiological data recorded in slices resemble in many aspects the spontaneous activity patterns observed *in vivo*, our observations may also be relevant for the activity-dependent regulation of neuronal apoptosis during early cortical development *in vivo* (Khazipov and Luhmann, 2006)

5.4. Neuronal network alterations through induced inflammation in dissociated neuronal cultures of the neonatal mouse cortex

In order to gain more detailed information in respect to neuronal network alterations and inflammation we reduced our sytem to one that is easier to manipulate. We used dissociated neuronal cultures and BV-2 cells, a microglial cell line which responds similarly as primary microglia to LPS (Horvath et al., 2008). Dissociated neuronal cultures provide an easier insight into the complex network of cortical neurons and can be used to study CNS neuronal physiology, pathophysiology and drug action. These cultures are very useful to study neuronal function under conditions which are easier to control and to manipulate than intact brains or organotypic slice cultures (Dichter, 1978;Wagenaar et al., 2005). During earliest stages of development, neuronal networks in various brain regions generate spontaneous oscillatory activity patterns (Khazipov and Luhmann, 2006) and GABAergic interneurons play an important role in the generation of these synchronized discharges (Blankenship and Feller, 2010;Mann and Paulsen, 2007). Synchronized burst activity, rather than a steady rate of single action potentials, is most effective in triggering the release of neurotrophic survival factors, as BDNF (Lessmann et al., 2003). Spontaneous network bursts have been demonstrated in the cortex of newborn rats *in vivo* (Yang et al., 2009) and in preterm human babies (Milh et al., 2007), suggesting that this spontaneous activity may be required for the release of neurotrophic factors and the control of cell survival. It was recently shown using developing neocortical slice cultures that spontaneous burst activity supports neuronal survival by activation of the neurotrophin receptors TrkB and TrkC, which are both activated by BDNF (Heck et al., 2008). Our present data demonstrate that inflammation induces a change in the pattern of spontaneous activity from a synchronized burst discharge state to a non-synchronized high frequency single action potential firing state (**Figure 25**). The inflammation-induced switch in the spontaneous firing pattern is most likely mediated by the direct action of TNFα on synaptic function. TNFα causes an enhancement in the synaptic strength of glutamatergic synapses by a PI3 kinase-mediated increased surface expression of AMPA receptors (Beattie et al., 2002) and also induces a decrease in inhibitory synaptic strength (Stellwagen et al., 2005). This inflammation-induced imbalance in excitatory-inhibitory synaptic function causes an increase in the overall firing rate of the neuronal network activity. The decrease in GABAergic function also induces a desynchronization of the network, since an intact inhibition is

required for the generation of synchronized burst activity (Mann and Paulsen, 2007). Our data suggests that these inflammation-induced modifications in neuronal network activity and cell death occur within less than 2 h, as our experiments revealed no change of relative survival rate 1 h after applying LPS-CM but a significant decrease of survival 2 h after treating dissociated neurons with LPS-CM (**Figure 26**). This indicates that inflammation may induce a rapid and strong neuronal response.

It is well known that activated microglia release various cytokines like TNFα, MIP-2 (Dammann and Leviton, 1997;Hausler et al., 2002), IL-1α (Dammann and Leviton, 1997;Hausler et al., 2002) IL-6, (Dammann and Leviton, 1997;Hausler et al., 2002;Lee et al., 1993) and MIP-1α (Hausler et al., 2002) *in vitro*. To investigate which cytokines released from stimulated microglia play an important role in our model system we determined the various factors released by BV-2 cells after 6 h LPS treatment and could determine the following factors to be up-regulated: G-CSF, KC, RANTES, GM-CSF, IL-1ra, TNFα, IL-6 and MIP-2 (**Figure 28**).

G-CSF is believed to increase the activation of resident microglia and mobilization of marrow-derived microglia (Sanchez-Ramos et al., 2009). KC, also called CXCL1, and RANTES are chemoattractants for a variety of inflammatory immune cells like neutrophils (van Rossum et al., 2008) and thus can be excluded as potential factors in our model system. GM-CSF induces proliferation and activates microglia (Reddy et al., 2009) and IL-1ra inhibits IL-1 activity (Sims, 2002). TNFα, MIP-2 and IL-6 are important cytokines primarily involved in inflammation. It has been demonstrated that IL-6 causes reactive astrocytosis but no neuronal damage (Fattori et al., 1995;Raivich et al., 1999). Therefore, we focused on TNFα and MIP-2 as the most likely downstream molecules mediating LPS-induced modifications in spontaneous neuronal activity and cell death.

5.5. Cytokine-dependent regulation of apoptosis and neuronal network activity

Our data further indicate that the chemokine TNFα has a direct influence on neuronal cell survival and electrical activity as capturing antibodies, added to LPS-CM lead to an increased survival rate, which was not totally restored, compared to normal levels (**Figure 28**). The network activity of neurons seems to be affected first by the released factors and thereafter decreased cell survival follows. TNFα has an impact

on both electrical activity and cell survival in our experimental set up, while MIP-2 has only a slight effect on cell survival. This result is not surprising since it has been demonstrated in different cell types that TNFα induces the expression of MIP-2 (Matejuk et al., 2002;Otto et al., 2001;Sakai et al., 1997). Further it was shown in TNFα knockout mice that TNFα triggers the release of MIP-2 (Matejuk et al., 2002;Otto et al., 2001). Even though MIP-2 antibody application does not lead to a significant difference compared to LPS-CM alone in our dissociated neuronal cell cultures, we could observe a slight increase in the survival rate and burst index compared to C-CM. However, MIP-2 might be also induced by a direct effect of LPS and may be produced in microglia following LPS stimulation (Hanisch, 2002;Sakai et al., 1997).

Since blockade of TNFα is sufficient to reestablish synchronized network activity and to rescue neuronal survival, we propose that it is the major factor released from activated microglia which is critically involved in, electrical activity and survival. To a lesser extent MIP-2 might represent another inflammatory factor causing activity-dependent neuronal cell death in the developing brain.

In this work we further wanted to demonstrate that induced inflammation altered not only the mechanisms of coordinated activity patterns and survival rate *in vitro* but also *in vivo*. It is clear that in many CNS regions, there is an important connection between neuronal activity and neuronal survival. This idea may be of huge importance as neuronal cell death is most prominent during the period of brain growth and synaptogenesis, which occurs in late gestation and the first post-natal months in the human and the first post-natal week in the rat (Mennerick and Zorumski, 2000). For the *in vivo* approach we used multi-electrode recording techniques, more specifically Michigan-electrodes inserted into the S1 region of newborn somatosensory cortex of rats and for determining apoptosis rates we performed Western-blot analysis of the extracted tissue area. As previously shown in our lab (Yang et al., 2009), three distinct oscillatory activity patterns can be recorded spontaneously: spindle bursts, gamma oscillations and long oscillations.

Spindle bursts have been already observed in the somatosensory cortex and reflect the major pattern of neocortical activity in newborn rats *in vivo* (Khazipov et al., 2004;Minlebaev et al., 2007). Gamma oscillations which have been represented in cerebral cortices of infants (Csibra et al., 2000) and in rat hippocampi *in vivo* (Palva et al., 2000) are the second pattern altered in our experimental set up (**Figure 28**).

Disorganization of neuronal network activity patterns, induced by inflammatory processes, during early development (Gilmore et al., 2003) may cause long-term alterations in cortical network activities. Therefore it might lead to cognitive impairment, learning deficits and various other neurological diseases like perinatal brain damage and cerebral palsy (Deverman and Patterson, 2009;Folkerth, 2005;Volpe, 2001;Volpe, 2003). Hints for this hypothesis, that alteration of specific patterns of electrical activity lead to casp-3-dependent cell death, are supported by our own data (**Figure 29**).

Our data provide new experimental evidence for the physiological role of spontaneous synchronized burst activity, which is transiently expressed in the developing cortex (Khazipov and Luhmann, 2006). EEG recordings from the somatosensory cortex of human preterm babies have demonstrated spontaneous and stimulus-evoked network activity classified as spontaneous activity transients (Tolonen et al., 2007) or delta-brush oscillations (Colonnese et al., 2010;Milh et al., 2007) with a frequency up to 25-30 Hz. Similar spontaneous activity patterns can be found in the cerebral cortex of newborn rodents (Khazipov and Luhmann, 2006) and it has been postulated that these early network oscillations play an important role in the formation of topographic maps (Khazipov et al., 2004) and in coupling developing neocortical networks to functional columns (Dupont et al., 2006). Early networks bursts may not only mediate activity-dependent changes in synaptic strength, but as shown in the present study also control neuronal survival during early stages of neuronal development. This leaves us with our following model which is shown in **Figure 31**.

During earliest stages of development, neuronal networks in various brain regions generate spontaneous oscillatory activity patterns (Khazipov and Luhmann, 2006) and GABAergic interneurons play an important role in the generation of these synchronized discharges by activating GABA-A receptors on pyramidal cells (Blankenship and Feller, 2010;Mann and Paulsen, 2007) (**Figure 31a**). Our present data demonstrate that inflammation induces a rapid change in the pattern of spontaneous synchronized burst discharges (**Figure 31b**). Since LPS selectively activates microglial cells via the TLR-4 receptor (see **(1)** in **Figure 31b**) and because astrocytes and neurons do not express TLR-4 receptors (Block and Hong, 2005;Lehnardt et al., 2002;Lehnardt et al., 2003;Wright et al., 1990), we suggest that

activated microglia are the initial players in inflammation-induced modifications of spontaneous network activity. Activated microglia releases TNFα (Hanisch, 2002) (**2**), which subsequently induces the expression of MIP-2 (Glabinski et al., 2003;Kobayashi, 2008;Otto et al., 2001). Stimulation with LPS may also cause a direct production and release of MIP-2 in microglia (**3**) (Hanisch, 2002). TNFα released from activated microglia has a direct effect on glutamatergic (**4**) and GABAergic synaptic (**5**) function. TNFα causes an enhancement in the synaptic strength of glutamatergic synapses by a PI3 kinase-mediated increased surface expression of AMPA receptors (**6**) (Beattie et al., 2002) and also an endocytosis of GABA-A receptors (**5**), resulting in a decrease in inhibitory synaptic strength (Stellwagen et al., 2005). This inflammation-induced imbalance in excitatory-inhibitory synaptic function may cause an increase in the overall firing rate of the neuronal network activity (**Figure 25a-(ii), c**). The decrease in GABAergic function may also induce a desynchronization of the network associated with a decrease of the burst index (**Figure 25a-(ii), b**) (**7**), since an intact inhibition is required for the generation of synchronized burst activity (Mann and Paulsen, 2007). Both, our *in vitro* data on organotypic slice cultures and our *in vivo* recordings, demonstrated a fast LPS-induced reduction in the occurrence of spontaneous oscillatory activity (**Figure 23c, 29c**). *In vivo*, a significant decrease could be observed only for the gamma oscillations. Both, *in vitro* and *in vivo* recordings demonstrated a prolongation of spontaneous activity (**Figure 23d, 29d**) and *in vivo* this effect was highly significant for the spindle bursts. Our data indicate that LPS-induced inflammation causes fast (in less than 2 h) modifications in neuronal network activity. Spontaneous oscillatory activity patterns, predominantly gamma oscillations, are disturbed (**7**), the release of survival factors is diminished (**8**) and casp-3-dependent apoptotic cell death increases (**9**). As our experiments with specific antibodies demonstrate (**Figure 28a-d**), TNFα and to a lesser extent the chemokine MIP-2 represent the main inflammatory factors causing activity-dependent neuronal cell death in the developing brain.

Here we provide evidence that inflammation induces rapid alterations in the pattern of spontaneous spindle bursts and gamma oscillations, which subsequently leads to increased apoptotic cell death in the developing cerebral cortex *in vivo* and *in vitro*. Since the immature human brain is most vulnerable to inflammation (Hagberg H., 2005), prenatal infection or exposure to inflammatory factors may modify

spontaneous neocortical activity. We provide evidence that programmed cell death may be disturbed during these critical, early developmental stages and it might be that conventional EEG recordings and analyses may not detect or underestimate these inflammation-induced modifications in neocortical network activity.

Figure 31. Model of inflammation-induced modifications in neuronal network activity and control of cell survival. (**a**) Developing neuronal network consisting of interconnected pyramidal neurons (blue) and GABAergic interneurons (red) generates spontaneous synchronized burst activity (blue bars), which leads to the release of survival factors and sustains cell survival. (**b**) LPS activates via the TLR4 receptor microglial cells (green), which then release various cytokines including TNFα and MIP-2. TNFα activates TNF receptor-1 on pyramidal neurons, which via the PI3K pathway leads to increased surface expression of AMPA receptors and strengthening of glutamatergic synapses (Beattie et al., 2002). TNFα also acts on GABAergic interneurons causing an endocytosis of GABA-A receptors and a decrease in synaptic inhibition (Stellwagen et al., 2005). The increase in glutamatergic excitation and the decrease in GABAergic inhibition leads to an increased firing rate, but also to a desynchronization of the network. The decrease in burst activity leads to a reduction in the release of survival factors and to enhanced apoptosis.

6. Summary

During the perinatal period the developing brain is most vulnerable to inflammation. Prenatal infection or exposure to inflammatory factors can have a profound impact on fetal neurodevelopment with long-term neurological deficits, such as cognitive impairment, learning deficits, perinatal brain damage and cerebral palsy.

Inflammation in the brain is characterized by activation of resident immune cells, especially microglia and astrocytes whose activation is associated with a variety of neurodegenerative disorders like Alzheimer´s disease and Multiple sclerosis. These cell types express, release and respond to pro-inflammatory mediators such as cytokines, which are critically involved in the immune response to infection. It has been demonstrated recently that cytokines also directly influence neuronal function. Glial cells are capable of releaseing the pro-inflammatory cytokines MIP-2, which is involved in cell death, and tumor necrosis factor α (TNFα), which enhances excitatory synaptic function by increasing the surface expression of AMPA receptors. Thus constitutively released TNFα homeostatically regulates the balance between neuronal excitation and inhibition in an activity-dependent manner. Since TNFα is also involved in neuronal cell death, the interplay between neuronal activity MIP-2 and TNFα may control the process of cell death and cell survival in developing neuronal networks.

An increasing body of evidence suggests that neuronal activity is important in the regulation of neuronal survival during early development, e.g. programmed cell death (apoptosis) is augmented when neuronal activity is blocked.

In our study we were interested on the impact of inflammation on neuronal activity and cell survival during early cortical development. To address this question, we investigated the impact of inflammation on neuronal activity and cell survival during early cortical development *in vivo* and *in vitro*.

Inflammation was experimentally induced by application of the endotoxin lipopolysaccharide (LPS), which initiates a rapid and well-characterized immune response. I studied the consequences of inflammation on spontaneous neuronal network activity and cell death by combining electrophysiological recordings with multi-electrode arrays and quantitative analyses of apoptosis. In addition, I used a cytokine array and antibodies directed against specific cytokines allowing the identification of the pro-inflammatory factors, which are critically involved in these
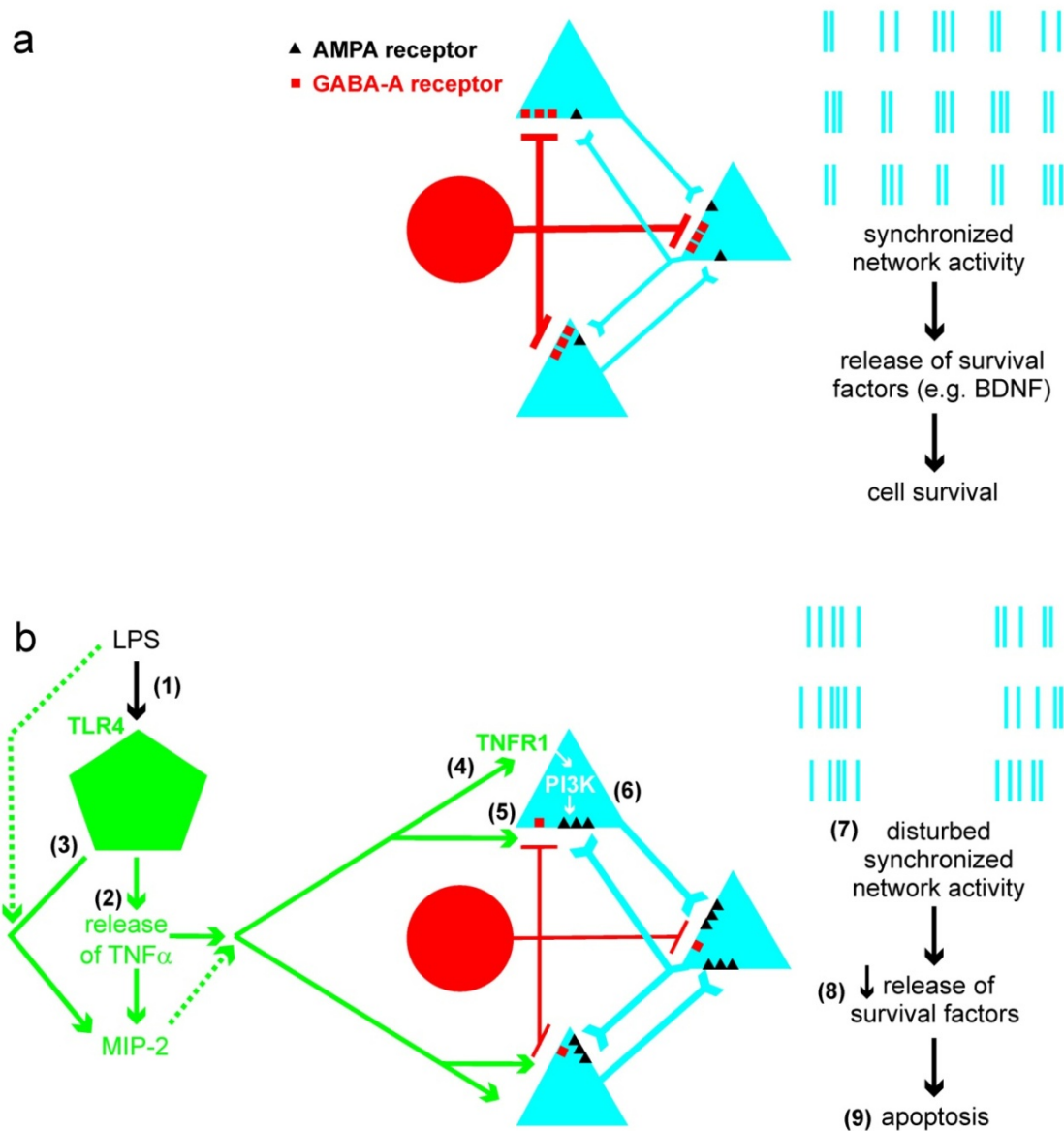
processes. In this study I demonstrated a direct link between inflammation-induced modifications in neuronal network activity and the control of cell survival in a developing neuronal network for the first time.

Our *in vivo* and *in vitro* recordings showed a fast LPS-induced reduction in occurrence of spontaneous oscillatory activity. It is indicated that LPS-induced inflammation causes fast release of proinflammatory factors which modify neuronal network activity. My experiments with specific antibodies demonstrate that TNFα and to a lesser extent MIP-2 seem to be the key mediators causing activity-dependent neuronal cell death in developing brain.

These data may be of important clinical relevance, since spontaneous synchronized activity is also a hallmark of the developing human brain and inflammation-induced alterations in this early network activity may have a critical impact on the survival of immature neurons.

7. Zusammenfassung

Intrauterine Infektionen und die fötale Immunantwort sind wichtige pathogene Faktoren bei Frühgeburten. Während der frühen Ontogenese können sie Störungen des Gehirnaufbaus und Langzeitschäden induzieren, wie beispielsweise kognitive Störungen, Lerndefizite und zerebrale Lähmungen. Entzündungsreaktionen im Gehirn sind charakterisiert über die Aktivierung von ortsansässigen Immunzellen, wie Astrozyten und Mikroglia. Deren Aktivierung wird mit einigen neurodegenerativen Erkrankungen, wie Alzheimer und Multipler Sklerose in Verbindung gebracht. Die beiden Zelltypen haben die Fähigkeit nach Ihrer Aktivierung pro-inflammatorische Zytokine auszuschütten und ebenso auf diese zu reagieren. Diese Zyotkine spielen eine wichtige Rolle bei der Immunantwort und es wurde erst kürzlich gezeigt, dass sie auch Einfluss auf neuronal Funktionen haben können.

Besonderes Augenmerk wurde in meiner Arbeit auf die beiden Zytokine TNFα und MIP-2 gelegt. Es wurde bereits gezeigt, dass sowohl MIP-2 als auch TNFα im neuronalen Zelltod involviert sind. Im Bezug auf TNFα ist ebenso bekannt, dass es zu erhöhter Erregung und zu einer Erhöhung der Anzahl der AMPA Rezeptoren auf der Zelloberfläche von Neuronen führt. Daraus lässt sich schließen, dass kontinuierlich freigesetztes TNFα wichtig für ein Gleichgewicht zwischen Erregung und Inhibierung in Neuronen ist. Ich vertrete die These, dass ein Zusammenspiel zwischen neuronaler Aktivität, TNFα und MIP-2 wichtig für die Regulation des Zelltodes während der frühen Entwicklung ist.

In meiner Dissertation wurde der Einfluss von Entzündungsmechanismen auf die neuronale Aktivität und das neuronale Überleben während der frühen Entwicklung *in vivo* sowie auch *in vitro* untersucht. Dazu wurden elektrophysiologische Aufnahmen mit Hilfe eines Mulit-Electrode Array Systems und quantitative Analysen des Zelltods verwendet. Die Immunantwort wurde mit Hilfe von Lipopolysaccarid (LPS), einer strukturellen Komponente der Zellwand von gram negativen Bakterien, induzierte. Zusätzlich wurden Zytokin-Arrays und Antikörper gegen spezifische Zytokine zur genaueren Identifizierung der involvierten Faktoren verwendet. In dieser Studie wird zum ersten Mal eine direkte Verbindung zwischen der Veränderung in der neuronalen Netzwerkaktivität nach Entzündung und dem Zellüberleben im sich entwickelnden Kortex gezeigt.

Neben *in vitro* wurden auch *in vivo* Experimente durchgeführt. Die elektrophysiologischen Aufzeichnungen zeigen eine durch LPS induzierte Reduktion von spontan auftretender oszillatorischer Netzwerkaktivität. Meine Ergebnisse lassen darauf schließen, dass es durch eine LPS induzierte Entzündung in der frühen Entwicklung zur Freisetzung von proinflammatorischen Faktoren kommt, die zu einer Veränderung der spontanen Netzwerkaktivität und darauf folgend zum neuronalen Zelltod führen. Vor allem TNFα und MIP-2 spielen eine Schlüsselrolle im aktivitäts-abhängigen neuronalen Zelltod im neonatalen Gehirn.

Da spontane Netzwerkaktivität auch im sich entwickelnden menschlichen Gehirn nachweisbar ist, könnten diese Daten zudem von großer klinischer Relevanz sein. Entzündungsreaktionen in diesem frühen Stadium der Entwicklung können zu Veränderungen der Netzwerkaktivität und damit zum Tod von Neuronen führen.

__Reference List__

Abbott NJ, Ronnback L, Hansson E (2006) Astrocyte-endothelial interactions at the blood-brain barrier. Nat Rev Neurosci 7: 41-53.

Allen NJ, Barres BA (2009) NEUROSCIENCE Glia - more than just brain glue. Nature 457: 675-677.

Angevine JB, Sidman RL (1961) Autoradiographic Study of Cell Migration During Histogenesis of Cerebral Cortex in Mouse. Nature 192: 766-&.

Balasingam V, Tejadaberges T, Wright E, Bouckova R, Yong VW (1994) Reactive Astrogliosis in the Neonatal Mouse-Brain and Its Modulation by Cytokines. J Neurosci 14: 846-856.

Barks JDE, Liu YQ, Shangguan Y, Li J, Pfau J, Silverstein FS (2008) Impact of indolent inflammation on neonatal hypoxic-ischemic brain injury in mice. International Journal of Developmental Neuroscience 26: 57-65.

Beattie EC, Stellwagen D, Morishita W, Bresnahan JC, Ha BK, Von Zastrow M, Beattie MS, Malenka RC (2002) Control of synaptic strength by glial TNF alpha. Science 295: 2282-2285.

Becher B, Fedorowicz V, Antel JP (1996) Regulation of CD14 expression on human adult central nervous system-derived microglia. Journal of Neuroscience Research 45: 375-381.

Ben Ari Y (2001) Developing networks play a similar melody. Trends in Neurosciences 24: 353-360.

Ben-Ari Y, Gaiarsa JL, Tyzio R, Khazipov R (2007) GABA: a pioneer transmitter that excites immature neurons and generates primitive oscillations. Physiol Rev 87: 1215-1284.

Berens P, Keliris GA, Ecker AS, Logothetis NK, Tolias AS (2008) Comparing the feature selectivity of the gamma-band of the local field potential and the underlying spiking activity in primate visual cortex. Front Syst Neurosci 2: 1-11.

Blankenship AG, Feller MB (2010) Mechanisms underlying spontaneous patterned activity in developing neural circuits. Nat Rev Neurosci 11: 18-29.

Blasi E, Barluzzi R, Bocchini V, Mazzolla R, Bistoni F (1990) Immortalization of Murine Microglial Cells by A V-Raf/V-Myc Carrying Retrovirus. Journal of Neuroimmunology 27: 229-237.

Block ML, Hong JS (2005) Microglia and inflammation-mediated neurodegeneration: Multiple triggers with a common mechanism. Prog Neurobiol 76: 77-98.

Brewer GJ, Torricelli JR, Evege EK, Price PJ (1993) Optimized Survival of Hippocampal-Neurons in B27-Supplemented Neurobasal(Tm), A New Serum-Free Medium Combination. Journal of Neuroscience Research 35: 567-576.

Chao CC, Hu SX, Close K, Choi CS, Molitor TW, Novick WJ, Peterson PK (1992) Cytokine Release from Microglia - Differential Inhibition by Pentoxifylline and Dexamethasone. Journal of Infectious Diseases 166: 847-853.

Chao CC, Molitor TW, Hu SX (1993) Neuroprotective Role of Il-4 Against Activated Microglia. Journal of Immunology 151: 1473-1481.

Chaparro-Huerta V, Flores-Soto ME, Gudino-Cabrera G, Rivera-Cervantes MC, Bitzer-Quintero OK, Beas-Zarate C (2008) Role of p38 MAPK and pro-inflammatory cytokines expression in glutamate-induced neuronal death of neonatal rats. International Journal of Developmental Neuroscience 26: 487-495.

Colonnese MT, Kaminska A, Minlebaev M, Milh M, Bloem B, Lescure S, Moriette G, Chiron C, Ben Ari Y, Khazipov R (2010) A Conserved Switch in Sensory Processing Prepares Developing Neocortex for Vision. Neuron 67: 480-498.

Csibra G, Davis G, Spratling MW, Johnson MH (2000) Gamma oscillations and object processing in the infant brain. Science 290: 1582-1585.

Dammann O, Leviton A (1997) Intrauterine infection, cytokines, and brain damage in the preterm newborn. Pediatric Research 42: 1-8.

De Paola M, Buanne P, Biordi L, Bertini R, Ghezzi P, Mennini T (2008) Chemokine MIP-2/CXCL2, acting on CXCR2, induces motor neuron death in primary cultures. Neuroimmunomodulation 14: 310-316.

Deng YY, Lu J, Sivakumar V, Ling EA, Kaur C (2008) Amoeboid microglia in the periventricular white matter induce oligodendrocyte damage through expression of proinflammatory cytokines via MAP kinase signaling pathway in hypoxic neonatal rats. Brain Pathology 18: 387-400.

Deverman BE, Patterson PH (2009) Cytokines and CNS Development. Neuron 64: 61-78.

Dichter MA (1978) Rat Cortical-Neurons in Cell-Culture - Culture Methods, Cell Morphology, Electrophysiology, and Synapse Formation. Brain Res 149: 279-293.

Ding Y, Li L (2008) Lipopolysaccaride preconditioning induces protection against lipopolysaccaride-induced neurotoxicity in organotpyic midbrain slice culture. Neuroscience Bulletin 24: 209-218.

Dolmetsch RE, Pajvani U, Fife K, Spotts JM, Greenberg ME (2001) Signaling to the nucleus by an L-type calcium channel - Calmodulin complex through the MAP kinase pathway. Science 294: 333-339.

Dupont E, Hanganu IL, Kilb W, Hirsch S, Luhmann HJ (2006) Rapid developmental switch in the mechanisms driving early cortical columnar networks. Nature 439: 79-83.

Eklind S, Mallard C, Leverin AL, Gilland E, Blomgren K, Mattsby-Baltzer I, Hagberg H (2001) Bacterial endotoxin sensitizes the immature brain to hypoxic-ischaemic injury. European Journal of Neuroscience 13: 1101-1106.

Engel AK, Fries P, Singer W (2001) Dynamic predictions: Oscillations and synchrony in top-down processing. Nat Rev Neurosci 2: 704-716.

Fattori E, Lazzaro D, Musiani P, Modesti A, Alonzi T, Ciliberto G (1995) IL-6 expression in neurons of transgenic mice causes reactive astrocytosis and increase in ramified microglial cells but no neuronal damage. European Journal of Neuroscience 7: 2441-2449.

Felts PA, Woolston AM, Fernando HB, Asquith S, Gregson NA, Mizzi OJ, Smith KJ (2005) Inflammation and primary demyelination induced by the intraspinal injection of lipopolysaccharide. Brain 128: 1649-1666.

Ferriero DM (2004) Medical progress - Neonatal brain injury. New England Journal of Medicine 351: 1985-1995.

Fields RD, Lee PR, Cohen JE (2005) Temporal integration of intracellular Ca2+ signaling networks in regulating gene expression by action potentials. Cell Calcium 37: 433-442.

Folkerth RD (2005) Neuropathologic substrate of cerebral palsy. Journal of Child Neurology 20: 940-949.

Gao HM, Jiang J, Wilson B, Zhang W, Hong JS, Liu B (2002) Microglial activation-mediated delayed and progressive degeneration of rat nigral dopaminergic neurons: relevance to Parkinson's disease. Journal of Neurochemistry 81: 1285-1297.

Garden GA, Moller T (2006) Microglia Biology in Health and Disease. Journal of Neuroimmune Pharmacology 1: 127-137.

Gibbons HM, Dragunow M (2006) Microglia induce neural cell death via a proximity-dependent mechanism involving nitric oxide. Brain Res 1084: 1-15.

Gilmore JH, Jarskog LF, Vadlamudi S (2003) Maternal infection regulates BDNF and NGF expression in fetal and neonatal brain and maternal-fetal unit of the rat. Journal of Neuroimmunology 138: 49-55.

Glabinski AR, Bielecki B, Kolodziejski P, Han YL, Selmaj K, Ransohoff RM (2003) TNF-alpha microinjection upregulates chemokines and chemokine receptors in the central nervous system without inducing leukocyte infiltration. Journal of Interferon and Cytokine Research 23: 457-466.

Golbs A, Nimmervoll B, Sun JJ, Sava IE, Luhmann HJ (2010) Control of programmed cell death by distinct electrical activity patterns. Cereb Cortex.

Gomes FCA, Spohr TCLS, Martinez R, Neto VM (2001) Cross-talk between neurons and glia: highlights on soluble factors. Brazilian Journal of Medical and Biological Research 34: 611-620.

Gotz M, Sommer L (2005) Cortical development: the art of generating cell diversity. Development 132: 3327-3332.

Griess P. (1879) Bemerkungen zu der Abhandlung der h.H. Weselsky und Benedikt "über einige Azoverbindungen". Chemical Berlin 12: 426-428.

Gupta A, Tsai LH, Wynshaw-Boris A (2002) Life is a journey: A genetic look at neocortical development. Nature Reviews Genetics 3: 342-355.

Hagberg H. Role of cytokines in preterm labour and brain injury. Mallard C. and Jacobsson B. 112 (1), 16-18. 2005. B.
Ref Type: Generic

Hagberg H, Mallard C (2005) Effect of inflammation on central nervous system development and vulnerability. Current Opinion in Neurology 18: 117-123.

Hanganu IL, Ben Ari Y, Khazipov R (2006) Retinal waves trigger spindle bursts in the neonatal rat visual cortex. J Neurosci 26: 6728-6736.

Hanisch UK (2002) Microglia as a source and target of cytokines. Glia 40: 140-155.

Hanisch UK, Kettenmann H (2007) Microglia: active sensor and versatile effector cells in the normal and pathologic brain. Nat Neurosci 10: 1387-1394.

Hara MR, Snyder SH (2007) Cell signaling and neuronal death. Annual Review of Pharmacology and Toxicology 47: 117-141.

Harry GJ, d'Hellencourt CL, McPherson CA, Funk JA, Aoyama M, Wine RN (2008) Tumor necrosis factor p55 and p75 receptors are involved in chemical-induced apoptosis of dentate granule neurons. Journal of Neurochemistry 106: 281-298.

Hausler KG, Prinz M, Nolte C, Weber JR, Schumann RR, Kettenmann H, Hanisch UK (2002) Interferon-gamma differentially modulates the release of cytokines and chemokines in lipopolysaccharide- and pneumococcal cell wall-stimulated mouse microglia and macrophages. European Journal of Neuroscience 16: 2113-2122.

Hauwel M, Furon E, Canova C, Griffiths M, Neal J, Gasque P (2005) Innate (inherent) control of brain infection, brain inflammation and brain repair: the role of microglia, astrocytes, "protective" glial stem cells and stromal ependymal cells. Brain Res Rev 48: 220-233.

Haydar TF, Bambrick LL, Krueger BK, Rakic P (1999) Organotypic slice cultures for analysis of proliferation, cell death, and migration in the embryonic neocortex. Brain Research Protocols 4: 425-437.

Haziot A, Ferrero E, Kontgen F, Hijiya N, Yamamoto S, Silver J, Stewart CL, Goyert SM (1996) Resistance to endotoxin shock and reduced dissemination of gram-negative bacteria in CD14-deficient mice. Immunity 4: 407-414.

He BP, Wen WY, Strong MJ (2002) Activated microglia (BV-2) facilitation of TNF-alpha-mediated motor neuron death in vitro. Journal of Neuroimmunology 128: 31-38.

Heck N, Golbs A, Riedemann T, Sun JJ, Lessmann V, Luhmann HJ (2008) Activity-dependent regulation of neuronal apoptosis in neonatal mouse cerebral cortex. Cereb Cortex 18: 1335-1349.

Hetier E, Ayala J, Mallat M, Denefle P, Bousseau A, Prochiantz A (1988) Microglial Cells and Not Astrocytes Synthesize Interleukin-1 Invitro. Lymphokine Research 7: 263.

Horvath RJ, Nutile-McMenemy N, Alkaitis MS, Deleo JA (2008) Differential migration, LPS-induced cytokine, chemokine, and NO expression in immortalized BV-2 and HAPI cell lines and primary microglial cultures. Journal of Neurochemistry 107: 557-569.

Hozumi I, Chiu FC, Norton WT (1990) Biochemical and Immunocytochemical Changes in Glial Fibrillary Acidic Protein After Stab Wounds. Brain Res 524: 64-71.

Hughes SW, Lorincz M, Cope DW, Blethyn KL, Kekesi KA, Parri HR, Juhasz G, Crunelli V (2004) Synchronized oscillations at alpha and theta frequencies in the lateral geniculate nucleus. Neuron 42: 253-268.

John ER (2002) The neurophysics of consciousness. Brain Res Rev 39: 1-28.

Johnson HA, Erner S (1972) Neuron Survival in Aging Mouse. Experimental Gerontology 7: 111-&.

Kalehua AN, Nagel JE, Whelchel LM, Gides JJ, Pyle RS, Smith RJ, Kusiak JW, Taub DD (2004) Monocyte chemoattractant protein-1 and macrophage inflammatory protein-2 are involved in both excitotoxin-induced neurodegeneration and regeneration. Experimental Cell Research 297: 197-211.

Katz LC, Crowley JC (2002) Development of cortical circuits: Lessons from ocular dominance columns. Nat Rev Neurosci 3: 34-42.

Katz LC, Shatz CJ (1996) Synaptic activity and the construction of cortical circuits. Science 274: 1133-1138.

Kaur C, Sivakumar V, Dheen ST, Ling EA (2006) Insulin-like growth factor I and II expression and modulation in amoeboid microglial cells by lipopolysaccharide and retinoic acid. Neuroscience 138: 1233-1244.

Kerr JFR, Wyllie AH, Currie AR (1972) Apoptosis - Basic Biological Phenomenon with Wide-Ranging Implications in Tissue Kinetics. British Journal of Cancer 26: 239-&.

Khazipov R, Luhmann HJ (2006) Early patterns of electrical activity in the developing cerebral cortex of humans and rodents. Trends in Neurosciences 29: 414-418.

Khazipov R, Sirota A, Leinekugel X, Holmes GL, Ben Arf Y, Buzsaki G (2004) Early motor activity drives spindle bursts in the developing somatosensory cortex. Nature 432: 758-761.

Kobayashi Y (2008) The role of chemokines in neutrophil biology. Frontiers in Bioscience 13: 2400-2407.

Kreutzberg GW (1996) Microglia: A sensor for pathological events in the CNS. Trends in Neurosciences 19: 312-318.

Kriegstein AR, Noctor SC (2004) Patterns of neuronal migration in the embryonic cortex. Trends in Neurosciences 27: 392-399.

Laurenzi MA, Arcuri C, Rossi R, Marconi P, Bocchini V (2001) Effects of microenvironment on morphology and function of the microglial cell line BV-2. Neurochemical Research 26: 1209-1216.

Le Van Quyen M., Khalilov I, Ben-Ari Y (2006) The dark side of high-frequency oscillations in the developing brain. Trends Neurosci 29: 419-427.

Lee SC, Liu W, Dickson DW, Brosnan CF, Berman JW (1993) Cytokine Production by Human Fetal Microglia and Astrocytes - Differential Induction by Lipopolysaccharide and Il-1-Beta. Journal of Immunology 150: 2659-2667.

Lehnardt S, Lachance C, Patrizi S, Lefebvre S, Follett PL, Jensen FE, Rosenberg PA, Volpe JJ, Vartanian T (2002) The toll-like receptor TLR4 is necessary for lipopolysaccharide-induced oligodendrocyte injury in the CNS. J Neurosci 22: 2478-2486.

Lehnardt S, Massillon L, Follett P, Jensen FE, Ratan R, Rosenberg PA, Volpe JJ, Vartanian T (2003) Activation of innate immunity in the CNS triggers neurodegeneration through a Toll-like receptor 4-dependent pathway. Proceedings of the National Academy of Sciences of the United States of America 100: 8514-8519.

Lessmann V, Gottmann K, Malcangio M (2003) Neurotrophin secretion: current facts and future prospects. Prog Neurobiol 69: 341-374.

Leviton A, Dammann O, Durum SK (2005) The adaptive immune response in neonatal cerebral white matter damage. Annals of Neurology 58: 821-828.

Levitt P, Eagleson KL, Powell EM (2004) Regulation of neocortical interneuron development and the implications for neurodevelopmental disorders. Trends Neurosci 27: 400-406.

Lewis DA (2004) Structure of the human prefrontal cortex. American Journal of Psychiatry 161: 1366.

Lipton SA (2006) NMDA receptors, glial cells, and clinical medicine. Neuron 50: 9-11.

Liu B, Hong JS (2003) Role of microglia in inflammation-mediated neurodegenerative diseases: Mechanisms and strategies for therapeutic intervention. Journal of Pharmacology and Experimental Therapeutics 304: 1-7.

Mann EO, Paulsen O (2007) Role of GABAergic inhibition in hippocampal network oscillations. Trends Neurosci 30: 343-349.

Marin-Teva JL, Dusart I, Colin C, Gervais A, van Rooijen N, Mallat M (2004) Microglia promote the death of developing Purkinje cells. Neuron 41: 535-547.

Matejuk A, Dwyer J, Ito A, Bruender Z, Vandenbark AA, Offner H (2002) Effects of cytokine deficiency on chemokine expression in CNS of mice with EAE. Journal of Neuroscience Research 67: 680-688.

Means TK, Golenbock DT, Fenton MJ (2000) The biology of Toll-like receptors. Cytokine & Growth Factor Reviews 11: 219-232.

Mennerick S, Zorumski CF (2000) Neural activity and survival in the developing nervous system. Molecular Neurobiology 22: 41-54.

Milh M, Kaminska A, Huon C, Lapillonne A, Ben-Ari Y, Khazipov R (2007) Rapid cortical oscillations and early motor activity in premature human neonate. Cereb Cortex 17: 1582-1594.

Milosevic NT, Ristanovic D (2007) The Sholl analysis of neuronal cell images: Semi-log or log-log method? Journal of Theoretical Biology 245: 130-140.

Minlebaev M, Ben-Ari Y, Khazipov R (2007) Network mechanisms of spindle-burst oscillations in the neonatal rat barrel cortex in vivo. J Neurophysiol 97: 692-700.

Moumdjian RA, Antel JP, Yong VW (1991) Origin of Contralateral Reactive Gliosis in Surgically Injured Rat Cerebral-Cortex. Brain Res 547: 223-228.

Nam KN, Son MS, Park JH, Lee EH (2008) Shikonins attenuate microglial inflammatory responses by inhibition of ERK, Akt, and NF-kappa B: neuroprotective implications. Neuropharmacology 55: 819-825.

Nguyen L, Besson A, Roberts JM, Guillemot F (2006) Coupling cell cycle exit, neuronal differentiation and migration in cortical neurogenesis. Cell Cycle 5: 2314-2318.

Nimmerjahn A, Kirchhoff F, Helmchen F (2005) Resting microglial cells are highly dynamic surveillants of brain parenchyma in vivo. Science 308: 1314-1318.

O'Leary DDM, Chou SJ, Sahara S (2007) Area patterning of the mammalian cortex. Neuron 56: 252-269.

Olson JK, Miller SD (2004) Microglia initiate central nervous system innate and adaptive immune responses through multiple TLRs. Journal of Immunology 173: 3916-3924.

Opitz T, De Lima AD, Voigt T (2002) Spontaneous development of synchronous oscillatory activity during maturation of cortical networks in vitro. J Neurophysiol 88: 2196-2206.

Oppenheim RW, Flavell RA, Vinsant S, Prevette D, Kuan CY, Rakic P (2001) Programmed cell death of developing mammalian neurons after genetic deletion of caspases. J Neurosci 21: 4752-4760.

Otto VI, Stahel PF, Rancan M, Kariya K, Shohami E, Yatsiv I, Eugster HP, Kossmann T, Trentz O, Moreganti-Kossmann MC (2001) Regulation of chemokines and chemokine receptors after experimental closed head injury. Neuroreport 12: 2059-2064.

Palva JM, Lamsa K, Lauri SE, Rauvala H, Kaila K, Taira T (2000) Fast network oscillations in the newborn rat hippocampus *in vitro*. J Neurosci 20: 1170-1178.

Purves D, Augustine GJ, Fitzpatrick D, Katz LC, LaMantia A-S, McNamara J.O. (1997) Neuroscience. Sinauer Associates Inc.

Raffray M, Cohen GM (1997) Apoptosis and necrosis in toxicology: A continuum or distinct modes of cell death? Pharmacology & Therapeutics 75: 153-177.

Raichman N, Ben Jacob E (2008) Identifying repeating motifs in the activation of synchronized bursts in cultured neuronal networks. J Neurosci Methods 170: 96-110.

Raivich G, Bohatschek M, Kloss CUA, Werner A, Jones LL, Kreutzberg GW (1999) Neuroglial activation repertoire in the injured brain: graded response, molecular mechanisms and cues to physiological function. Brain Res Rev 30: 77-105.

Rakic P, Komuro H (1995) The Role of Receptor/Channel Activity in Neuronal Cell-Migration. Journal of Neurobiology 26: 299-315.

Reddy PH, Manczak M, Zhao W, Nakamura K, Bebbington C, Yarranton G, Mao PZ (2009) Granulocyte-macrophage colony-stimulating factor antibody suppresses microglial activity: implications for anti-inflammatory effects in Alzheimer's Disease and multiple sclerosis. Journal of Neurochemistry 111: 1514-1528.

Rietschel ET, Kirikae T, Schade FU, Mamat U, Schmidt G, Loppnow H, Ulmer AJ, Zahringer U, Seydel U, Dipadova F, Schreier M, Brade H (1994) Bacterial, Endotoxin - Molecular Relationships of Structure to Activity and Function. Faseb Journal 8: 217-225.

Rivest S (2003) Molecular insights on the cerebral innate immune system. Brain Behavior and Immunity 17: 13-19.

Rock RB, Gekker G, Hu SX, Sheng WS, Cheeran M, Lokensgard JR, Peterson PK (2004) Role of microglia in central nervous system infections. Clinical Microbiology Reviews 17: 942-+.

Rousset CI, Chalon S, Cantagrel S, Bodard S, Andres C, Gressens P, Saliba E (2006) Maternal exposure to LPS induces hypomyelination in the internal capsule and programmed cell death in the deep gray matter in newborn rats. Pediatric Research 59: 428-433.

Sakai S, Ochiai H, Nakajima K, Terasawa K (1997) Inhibitory effect of ferulic acid on macrophage inflammatory protein-2 production in a murine macrophage cell line, RAW264.7. Cytokine 9: 242-248.

Sanchez-Ramos J, Song S, Sava V, Catlow B, Lin X, Mori T, Cao C, Arendash GW (2009) Granulocyte Colony Stimulating Factor Decreases Brain Amyloid Burden and Reverses Cognitive Impairment in Alzheimer'S Mice. Neuroscience 163: 55-72.

Sankar R, Auvin S, Mazarati A, Shin D (2007) Inflammation contributes to seizure-induced hippocampal injury in the neonatal rat brain. Acta Neurologica Scandinavica 115: 16-20.

Schmitz T, Chew LJ (2008) Cytokines and Myelination in the Central Nervous System. Thescientificworldjournal 8: 1119-1147.

Sejnowski TJ, Destexhe A (2000) Why do we sleep? Brain Res 886: 208-223.

Sheng HZ, Fields RD, Nelson PG (1993) Specific Regulation of Immediate-Early Genes by Patterned Neuronal-Activity. Journal of Neuroscience Research 35: 459-467.

Sims JE (2002) IL-1 and IL-18 receptors, and their extended family. Current Opinion in Immunology 14: 117-122.

Spitzer NC, Root CM, Borodinsky LN (2004) Orchestrating neuronal differentiation: patterns of Ca2+ spikes specify transmitter choice. Trends in Neurosciences 27: 415-421.

Sriram K, Matheson JM, Benkovic SA, Miller DB, Luster MI, O'Callaghan JP (2006) Deficiency of TNF receptors suppresses microglial activation and alters the susceptibility of brain regions to MPTP-induced neurotoxicity: role of TNF-alpha. Faseb Journal 20: 670-682.

Stellwagen D, Beattie EC, Seo JY, Malenka RC (2005) Differential regulation of AMPA receptor and GABA receptor trafficking by tumor necrosis factor-alpha. J Neurosci 25: 3219-3228.

Stellwagen D, Malenka RC (2006) Synaptic scaling mediated by glial TNF-alpha. Nature 440: 1054-1059.

Stoppini L, Buchs PA, Muller D (1991) A simple method for organotypic cultures of nervous tissue. J Neurosci Methods 37: 173-182.

Streit WJ (2002) Microglia as neuroprotective, immunocompetent cells of the CNS. Glia 40: 133-139.

Taylor RC, Cullen SP, Martin SJ (2008) Apoptosis: controlled demolition at the cellular level. Nature Reviews Molecular Cell Biology 9: 231-241.

Tolonen M, Palva JM, Andersson S, Vanhatalo S (2007) Development of the spontaneous activity transients and ongoing cortical activity in human preterm babies. Neuroscience 145: 997-1006.

van Rossum D, Hanisch UK (2004) Microglia. Metabolic Brain Disease 19: 393-411.

van Rossum D, Hilbert S, Strassenburg S, Hanisch UK, Bruck W (2008) Myelin-phagocytosing macrophages in isolated sciatic and optic nerves reveal a unique reactive phenotype. Glia 56: 271-283.

Voigt T, Baier H, deLima AD (1997) Synchronization of neuronal activity promotes survival of individual rat neocortical neurons in early development. European Journal of Neuroscience 9: 990-999.

Volpe JJ (2001) Neurobiology of periventricular leukomalacia in the premature infant. Pediatric Research 50: 553-562.

Volpe JJ (2003) Cerebral white matter injury of the premature infant - More common than you think. Pediatrics 112: 176-180.

Wagenaar DA, Madhavan R, Pine J, Potter SM (2005) Controlling bursting in cortical cultures with closed-loop multi-electrode stimulation. J Neurosci 25: 680-688.

Wagenaar DA, Pine J, Potter SM (2006) An extremely rich repertoire of bursting patterns during the development of cortical cultures. Bmc Neuroscience 7.

Wang XJ, Chen SD, Ma GZ, Ye M, Lu GQ (2005) Involvement of proinflammatory factors, apoptosis, caspase-3 activation and Ca2+ disturbance in microglia activation-mediated dopaminergic cell degeneration. Mechanisms of Ageing and Development 126: 1241-1254.

Wonders CP, Anderson SA (2006) The origin and specification of cortical interneurons. Nat Rev Neurosci 7: 687-696.

Wright SD (1999) Toll, a new piece in the puzzle of innate immunity. Journal of Experimental Medicine 189: 605-609.

Wright SD, Ramos RA, Tobias PS, Ulevitch RJ, Mathison JC (1990) Cd14, A Receptor for Complexes of Lipopolysaccharide (Lps) and Lps Binding-Protein. Science 249: 1431-1433.

Yang JW, Hanganu-Opatz IL, Sun JJ, Luhmann HJ (2009) Three patterns of oscillatory activity differentially synchronize developing neocortical networks *in vivo*. J Neurosci 29: 9011-9025.

Yuste R, Nelson DA, Rubin WW, Katz LC (1995) Neuronal Domains in Developing Neocortex - Mechanisms of Coactivation. Neuron 14: 7-17.

Yuste R, Peinado A, Katz LC (1992) Neuronal Domains in Developing Neocortex. Science 257: 666-669.

Zhou Q, Poo MM (2004) Reversal and consolidation of activity-induced synaptic modifications. Trends in Neurosciences 27: 378-383.

Zierler S, Klein B, Furtner T, Bresgen N, Lutz-Meindl U, Kerschbaum HH (2006) Ultraviolet irradiation-induced apoptosis does not trigger nuclear fragmentation but translocation of chromatin from nucleus into cytoplasm in the microglial cell-line, BV-2. Brain Res 1121: 12-21.

Zujovic V, Benavides J, Vige X, Carter C, Taupin V (2000) Fractalkine modulates TNF-alpha secretion and neurotoxicity induced by microglial activation. Glia 29: 305-315.

Acknowledgments

At this point I want to thank all persons who supported these studies.

Curriculum vitae
MA. rer. nat. Birgit Nimmervoll

Personal information

Name:	<u>Birgit</u> Verena Nimmervoll
Adresse:	Rheinalle 8, 55118 Mainz, Germany
e-mail:	nimmervo@uni-mainz.de
Nationality:	Austria
Date of birth:	12.4.1984
Place of birth:	Linz, Upper Austria

Education

2007 – 2011	Johannes Gutenberg University Mainz (Germany) PhD-thesis, Institute of Physiology and Pathophysiology Universal Medical Center „LPS-induced modification in spontaneous network activity causes neuronal apoptosis in neonatal cerebral cortex" Supervisor Prof. Dr. H.J. Luhmann
2005 – 2007	Paris Lodron University Salzburg (Austria) Master degree in Zoology (passed with distinction) Diploma-thesis, Institute for Cell Biology, Salzburg: „Does cGMP mediate ammonia-induced programmed cell death in the microglial cell line, BV-2?" Supervisor Prof. Dr. H.H. Kerschbaum
10.2002 – 07.2005	Paris Lodron University Salzburg Studies Bakk. biol. (Bachelor) Physiology and Cell Biology
10.1997 – 6.2002	BORG Honauerstraße Linz (secondary school)

Scholarships

01. 2009	Election as the speaker of the Neuroscience-graduate school
11.2007	Ph.D. scholarship of the DFG in the Neuroscience-graduate school
2007	Scholarship of the University of Salzburg

Publications

- Nimmervoll B, Svoboda N, Sacha B, Kerschbaum HH (2009) Sustained elevation of cyclic guanosine monophosphate induces apoptosis in microglia. Brain Research Bulletin 80: 428-432.
- Golbs A, Nimmervoll B, Sun J-J, Sava IE, Luhmann HJ (2010) Control of programmed cell death by distinct electrical activity patterns. Cerebral Cortex. epub ahead of print, doi: 10.1093/cercor/bhq200.

- Nimmervoll B, Yang J-W, An S, White R, Sun J-J, Luhmann HJ (2010) LPS-induced microglial secretion of TNFα increases activity-dependent neuronal apoptosis in neonatal cerebral cortex. Submitted.

Poster presentations

Consequences and protection of inflammatory neurodegeneration in the perinatal mouse cortex
Nimmervoll B., Luhmann H.J.
DFG presentation, 2008, Mainz, Germany

Nimmervoll B., Sun J.J., White R., Luhmann H.J.
Influence of induced inflammation on survival rate and spontaneous network activity of immature cortical neurons.
7th FENS meeting, 2010, Amsterdam, Netherlands

Nimmervoll B., Sun J.J., White R., Luhmann H.J.
Influence of induced inflammation on survival rate and spontaneous network activity of immature cortical neurons
EMBO meeting 2010, Barcelona, Spain

Nimmervoll B., Sun J.J., White R., Luhmann H.J.
Influence of induced inflammation on survival rate and spontaneous network activity of immature cortical neurons
Rhine-Main Neuroscience Network (rmn^2) meeting, 2010, Oberwesel, Germany